

New Boron–Hydrogen Insertion Reactions of Ligated Boranes

by

Thomas H. Allen

B.S. Chemistry, Magna Cum Laude, Ohio Northern University, 2012

Submitted to the Graduate Faculty of the
Kenneth P. Dietrich School of Arts and Sciences in partial fulfillment
of the requirements for the degree of
Doctor of Philosophy

University of Pittsburgh

2018

UNIVERSITY OF PITTSBURGH
KENNETH P. DIETRICH SCHOOL OF ARTS AND SCIENCES

This dissertation was presented

by

Thomas H. Allen

It was defended on

July 17, 2018

and approved by

Sruti Shiva, Associate Professor, Department of Pharmacology and Chemical Biology

W. Seth Horne, Associate Professor, Department of Chemistry

Kay M. Brummond, Professor, Department of Chemistry

Committee Chair: Dennis P. Curran, Distinguished Service Professor and Bayer Professor,

Department of Chemistry

Copyright © by Thomas H. Allen

2018

New Boron–Hydrogen Insertion Reactions of Ligated Boranes

Thomas H. Allen, PhD

University of Pittsburgh, 2018

Chemical transformations of ligated borane complexes, including *N*-heterocyclic carbene boranes, are demonstrated. Chapter 1 begins with an introduction of Lewis base borane complexes, rhodium carbene chemistry, and B–H insertion of ligated boranes. The second part of Chapter 1 describes the insertion of rhodium carbenes, previously demonstrated with NHC-boranes, into the B–H bonds of other ligated boranes. Stable ligated α -boryl esters were isolated. A series of competitive B–H insertion experiments are described that were used to develop a relative reactivity profile of ligated boranes toward rhodium-catalyzed B–H insertion. The enantioselective B–H insertion of NHC-boranes with chiral dirhodium catalysts was also investigated. Finally, the synthesis and application of two chiral bridged dirhodium catalysts is described.

Chapter 2 describes the discovery and isolation of NHC-boryl hydrazones by non-chain radical recombinations of NHC-boranes, diazomalones, and azo initiators. Thermal 1,1-hydroborations of a diazo dione and a diazonium salt to give boryl hydrazone and boryl diazene products are demonstrated. Chapter 3 explores the use of electrophilic NHC-borane complexes to catalyze B–H insertion reactions with diazoesters. The boryl iodide catalyzed method is adept at producing α -substituted- α -NHC-boryl esters. A small family of NHC-boryl esters with amino acid side chains was synthesized. Chapter 4 describes the basic hydrolyses of ligated α -boryl esters to yield ligated α -boryl acetic acids. The boryl acetic acid derivatives were characterized by X-ray crystallography and acidity constant measurements. They are among the least acidic

carboxylic acids known. The electron-donating ability of ligated borane substituents was further quantified by using derived Hammett constants from ^{13}C NMR chemical shift correlation experiments.

TABLE OF CONTENTS

PREFACE.....	XX
1.0 RHODIUM(II)-CATALYZED B–H INSERTION CHEMISTRY & SYNTHESIS OF CHIRAL BRIDGED RHODIUM(II) CATALYSTS	1
1.1 INTRODUCTION	1
1.1.1 Lewis Base Borane Adducts.....	1
1.1.2 Rhodium(II)-Catalyzed Carbene Insertion into C–H Bonds	4
1.1.2.1 Rhodium-catalyzed C–H Insertion Mechanism.....	5
1.1.2.2 Donor/Acceptor Diazo Compounds.....	7
1.1.2.3 Bridged Rh(II) Tetracarboxylate Catalysts.....	8
1.1.2.4 Chiral Rh(II) Catalysts with Bridging Ligands	10
1.1.3 Catalytic Carbene Insertion into B–H Bonds	11
1.2 RESULTS AND DISCUSSION.....	17
1.2.1 Rhodium-catalyzed B–H Bond Insertions with Lewis Base Adducts of Borane.	17
1.2.1.1 Synthesis of Stable Lewis Base Complexes of α-Boryl Carbonyl Compounds.....	17

1.2.1.2	Determination of Relative Rates of Ligated Boranes and a Borohydride Salt in Rhodium(II)-Catalyzed Competitive B–H Insertion Experiments.....	26
1.2.1.3	Enantioselective NHC B-H Insertions with Donor/Acceptor Rhodium Carbenes	31
1.2.1.4	Enantioselective NHC B–H Insertion with Rhodium Carbenes (Boron Stereocenter)	34
1.2.2	Exploring the Synthesis and Application of a Chiral Rh ₂ (esp) ₂ Analog...	38
1.2.2.1	Synthesis of Methyl and Benzyl Chiral Rh ₂ (esp) ₂ Analogs	38
1.2.2.2	Application of Methyl and Benzyl Chiral Rh ₂ (esp) ₂ Analogs	46
1.3	CONCLUSIONS	48
2.0	RADICAL AND THERMAL REACTIONS OF N-HETEROCYCLIC CARBENE BORANES WITH ELECTROPHILIC DIAZO COMPOUNDS	50
2.1	INTRODUCTION	50
2.1.1	Radical Initiators	50
2.1.1.1	Azo initiators	50
2.1.2	Radical chemistry of NHC-boranes	51
2.1.3	Radical chemistry of diazo compounds	52
2.2	RESULTS AND DISCUSSION	53
2.2.1	Reaction of NHC-boranes and Diazo Compounds with Radical Initiators.....	53
2.2.2	Synthesis of an NHC-boryl Hydrazone via 1,1-Hydroboration	60
2.2.3	Thermal Reaction of an NHC-borane with a Diazonium Salt.....	65

2.3	CONCLUSIONS	69
3.0	BORENIUM ION EQUIVALENT CATALYZED B–H INSERTION REACTIONS OF N-HETEROCYCLIC CARBENE BORANES	71
3.1	INTRODUCTION	71
3.1.1	Borenum ion chemistry of NHC-boranes.....	71
3.2	RESULTS AND DISCUSSION	73
3.2.1	Optimization of B–H Insertion Reaction Conditions with Excess Diazo Component.....	73
3.2.2	Preparative B–H Insertion Reactions of NHC-boranes with Ethyl Diazoacetate	77
3.2.3	Diiodine-Catalyzed B–H Insertion Screening with other Ligated Boranes.....	79
3.2.4	Preparative Reactions of 1,3-Dimethylimidazol-2-ylidene Borane with Substituted Diazoacetates.....	80
3.2.5	Optimization of B–H Insertion Reaction Condition with Excess Borane Component.....	83
3.2.6	Structure and Stability of α -NHC-Boryl Esters.....	85
3.2.7	Mechanistic Experiments.....	86
3.3	CONCLUSIONS	89
4.0	SYNTHESIS AND CHARACTERIZATION OF LIGATED BORYL ACETIC ACIDS.....	91
4.1	INTRODUCTION	91
4.1.1	α -Boryl Carboxylic Acids.....	91

4.2	RESULTS AND DISCUSSION	93
4.2.1	Hydrolysis of Ligated α -Boryl Esters.....	93
4.2.2	X-ray Structures of Ligated α -Boryl Acetic Acids	97
4.2.3	Acidity Constant Measurements	100
4.2.4	NHC-borane Hammett Values Derived from ^{13}C NMR Chemical Shift Correlation.....	104
4.3	CONCLUSIONS	108
5.0	EXPERIMENTAL	109
5.1	GENERAL INFORMATION.....	109
5.2	EXPERIMENTAL DATA FOR CHAPTER 1	110
5.3	EXPERIMENTAL DATA FOR CHAPTER 2	124
5.4	EXPERIMENTAL DATA FOR CHAPTER 3	131
5.5	EXPERIMENTAL DATA FOR CHAPTER 4	143
	BIBLIOGRAPHY	151

LIST OF TABLES

Table 1. Solvent effect of rhodium-catalyzed asymmetric cyclopropanation	11
Table 2. Enantioselective C–H insertion of dimethylphosphine-borane 34 with Zhou ligand 35	14
Table 3. B–H insertion of Lewis base borane adducts.....	20
Table 4. Lewis base additives in Rh(II) B–H insertion system	26
Table 5. Competitive B–H insertion experiments.....	29
Table 6. Relative rates toward B–H insertion, BDE values, and Mayr N values for various boranes	30
Table 7. Relative rate of boranes toward B–H insertion.....	31
Table 8. Synthesis of racemic standard NHC-borane insertion products	32
Table 9. Chiral rhodium(II) catalyst screening with NHC B–H insertion (α -carbon stereocenter)	34
Table 10. Chiral rhodium(II) catalyst screening with NHC B–H insertion (boron stereocenter).	36
Table 11. Complexation of methyl diacid 72 with Rh ₂ (tfa) ₄	43
Table 12. Enantioselective NHC B–H insertion (α -carbon stereocenter).....	47
Table 13. Enantioselective styrene cyclopropanation.....	48
Table 14. Radical initiator screening	54
Table 15. Screening substituted diazo compounds.....	57

Table 16. Screening differentially substituted NHC-boranes	58
Table 17. Formation of NHC B–N and B–C adducts with dione diazo 100	63
Table 18. Initial discovery of B–H reaction with NHC-boranes and activators	74
Table 19. Reaction conditions screening with diazo compound in excess	76
Table 20. Isolated yields in preparative reaction of NHC-boranes with ethyl diazoacetate	79
Table 21. Diiodine-catalyzed B–H insertion of ligated boranes	80
Table 22. Isolated yields in preparative reactions of NHC-borane 5 with substituted diazoacetates	82
Table 23. Reaction conditions screening with NHC-borane in excess	84
Table 24. Hydrolysis of NHC-boryl ester 114	94
Table 25. Synthesis of ligated boryl acetic acids	97
Table 26. Acidity constant measurements of ligated boryl acetic acids	102
Table 27. Electrophilic Hammett constants for ligated borane substituents	107

LIST OF FIGURES

Figure 1. Representative Lewis base borane adducts	2
Figure 2. Examples of NHC-boranes	3
Figure 3. (a) Dirhodium tetracarboxylate, $\text{Rh}_2(\text{OAc})_4$, and (b) Rh(II)-catalyzed C–H insertion of 2-methylbutane	5
Figure 4. Diazo decomposition and carbene insertion mechanism.....	6
Figure 5. Metastable carbenoid intermediate 13.....	6
Figure 6. Retention of stereoconfiguration during cyclization ¹⁷ and Doyle's three-centered transition state	7
Figure 7. Transition state model of Nakamura's intermediate Rh(II) carbene/alkane complex	7
Figure 8. Structures of diazoacetate and two donor/acceptor diazo compounds	8
Figure 9. Davies' chiral bridged dirhodium catalysts	11
Figure 10. Examples of carbene insertion into B–H bonds, (a) alkynylcarbene insertion, (b) samarium carbene insertion, (c) dichlorocarbene insertion	12
Figure 11. B–H insertion using Rh(I) catalysts	15
Figure 12. Borane isomer equilibria	18
Figure 13. Phosphonium ylide 56	22

Figure 14. ^{13}C NMR spectra of crude reaction mixture containing cyanoborohydride product	54
.....	25
Figure 15. D_2 , C_2 and C_4 symmetric chiral Rh(II) catalysts	33
Figure 16. Tributyltin hydride radical addition to diazomalonate	85
Figure 17. X-ray structure of NHC-boryl hydrazone	91
Figure 18. Structure of NHC-boryl hydrazone	101
Figure 19. Proposed mechanism for the 1,1-hydroboration of	100
Figure 20. ^{11}B NMR spectra of isolated boryl salt intermediate	66
Figure 21. ^1H NMR spectrum of isolated boryl salt intermediate	67
Figure 22. Proposed structures of dicationic boryl salt intermediate	68
Figure 23. X-ray structure of NHC boryl diazene oxide	108
Figure 24. X-ray structure of NHC-boryl ester	144
Figure 25. Proposed catalytic cycle	86
Figure 26. (Top) ^{11}B NMR spectrum NHC-boryl iodide 155; (Bottom) Regeneration of NHC-boryl ester 114	88
Figure 27. α -Boryl acetic acids with carborane substituents (CH vertex indicated by black dot)	92
Figure 28. Unknown compound boroacetic acid and its ligated derivative	93
Figure 29. X-ray structure of imidazole-boryl acid 163 dimer	98
Figure 30. X-ray structure of benzimidazole-boryl acid 164 dimer	98
Figure 31. X-ray structure of trimethylamine-boryl acid 167 dimer	99
Figure 32. X-ray structure of pyridine-boryl acid 170 dimer	99
Figure 33. Hydrogen bonding network of benzimidazole-boryl diacids	100
Figure 34. Acidity constant measurements of comparable acids	103

Figure 35. Correlation of $\delta(C_p)$ of monosubstituted benzenes with σ_p^+	104
Figure 36. Hammett correlation equation applied to NHC-boryl arene 171	104

LIST OF SCHEMES

Scheme 1. Synthesis of NHC-borane 6.....	3
Scheme 2. Preparation of monochelated bridged dimer 15	9
Scheme 3. Cyclization of α -diazo β -keto ester 16	9
Scheme 4. Preparation of Rh ₂ (esp) ₂ 19	10
Scheme 5. Rhodium-catalyzed B–H insertion of NHC-borane 5	12
Scheme 6. Copper-catalyzed B–H insertion of triphenylphosphine-borane 3.....	13
Scheme 7. Enantioselective B–H insertion synthesis of boryl furan 37	14
Scheme 8. Enzyme catalyzed enantioselective B–H insertion of NHC-borane 5	16
Scheme 9. Triphenylphosphine scavenging with Merrifield resin	21
Scheme 10. Competition experiment between NHC-borane 5 and pyridine-borane 4.....	28
Scheme 11. B–H insertion of benzimidazole aryl borane 67.....	35
Scheme 12. Boron stereocenter racemization study with mixed starting material	37
Scheme 13. Proposed synthetic pathway to a chiral Rh ₂ (esp) ₂ analog	39
Scheme 14. Finkelstein reaction of bis(bromoethyl)benzene 70	40
Scheme 15. Double alkylation of bis(iodomethyl)benzene 74	40
Scheme 16. Hydrolysis of bis alkylated benzene 71.....	41
Scheme 17. Reduction of diacid 72 with LAH.....	41
Scheme 18. Mosher's acid esterification of 75	42

Scheme 19. Synthesis of hydrocinnamoyloxazolidinone 79	45
Scheme 20. Synthesis of chiral benzyl diacid 81	45
Scheme 21. Complexation of benzyl diacid 81 with Rh ₂ (tfa) ₂	46
Scheme 22. Radical fragmentation of AIBN	51
Scheme 23. Preparative scale synthesis of NHC-boryl hydrazone 91	56
Scheme 24. Synthesis of azo initiator NHC-boryl hydrazone analogs	59
Scheme 25. Proposed mechanism for the formation of NHC-boryl hydrazone 91	60
Scheme 26. Reaction of NHC-borane 5 with diazo dione 100 (AIBN present)	61
Scheme 27. Reaction of NHC-borane 5 and diazo dione 100 without AIBN	64
Scheme 28. Pathway to proposed NHC boryl diazene 104	65
Scheme 29. Synthesis of NHC boryl diazene oxide 108	68
Scheme 30. Electrophilic halogenation of NHC-borane 6.....	72
Scheme 31. Nucleophilic substitutions of NHC-boryl iodide 109 with NaN ₃ or NaCN	72
Scheme 32. Hydroboration of 2,3-dimethyl-2-butene by NHC-borane 5	73
Scheme 33. Preparation of α-NHC boryl ester 114	77
Scheme 34. Experimental confirmation of turnover step	87
Scheme 35. Yudin's synthesis of α-MIDA-boryl acid 157	91
Scheme 36. Synthesis of NHC-boryl acetic acid 163	95

LIST OF ABBREVIATIONS

Ac	acetyl
ACN	acetonitrile
Ad	1-adamantyl
AHCN	1,1'-azobis(cyclohexanecarbonitrile)
AIBN	2,2'-azobis(2-methylpropionitrile)
BA _{rF}	tetrakis[3,5-bis(trifluoromethyl)phenyl]borate
BDE	bond dissociation energy
Bn	benzyl
BTF	(trifluoromethyl)benzene (benzotrifluoride)
Bu	butyl
CBS	Corey–Bakshi–Shibata
CHD	1,4-cyclohexadiene
Cy	cyclohexyl
DBU	1,8-diazabicyclo[5.4.0]undec-7-ene
DCC	<i>N,N'</i> -dicyclohexylcarbodiimide
DCE	dichloroethane
DCM	dichloromethane
DMAP	4-dimethylaminopyridine

DMSO	dimethyl sulfoxide
DTBP	di- <i>tert</i> -butyl peroxide
dipp	1,3-bis(2,6-diisopropylphenyl)
dr	diastereomeric ratio
ee	enantiomeric excess
EPR	electron paramagnetic resonance
er	enantiomeric ratio
Et	ethyl
HMDS	bis(trimethylsilyl)amine
HPLC	high performance liquid chromatography
HRMS	high resolution mass spectrometry
HSQC	heteronuclear single quantum coherence
<i>i</i> Pr	<i>iso</i> -propyl
LAH	lithium aluminum hydride
LB	Lewis base
LDA	lithium diisopropylamide
LFP	laser flash photolysis
Me	methyl
MIDA	<i>N</i> -methyliminodiacetic acid
MTPA	α -methoxy- α -(trifluoromethyl)phenylacetyl chloride
<i>N</i>	Mayr nucleophilicity parameter
NHC	<i>N</i> -heterocyclic carbene
NMR	nuclear magnetic resonance

<i>p</i> -ABSA	4-acetamidobenzenesulfonyl azide
Ph	phenyl
ppm	parts per million
pyr	pyridine
R_f	retention factor
rt	room temperature
σ_p^+	electrophilic substituent constant
<i>t</i> Bu	<i>tert</i> -butyl
10-CSA	camphor sulfonic acid
TEP	Tolman electronic parameter
Tf	triflate
TFA	trifluoroacetic acid
THF	tetrahydrofuran
TLC	thin layer chromatography
TS	transition state
t_R	retention time
V-65	2,2'-azobis(2,4-dimethylvaleronitrile)
UV	ultraviolet

PREFACE

The completion of my dissertation represents a capstone on a six-year journey nearing its conclusion. A cast of individuals from my youth, my studies at ONU, and my time at University of Pittsburgh has led me to this point. I would like to take this opportunity to thank many of these individuals who have had a positive impact on my graduate studies.

Foremost, I would like to express my sincere gratitude to my advisor, Professor Dennis Curran, for his outstanding mentorship over the last six years. His professionalism was instrumental toward fostering an atmosphere of mutual respect that made working in his group a first-rate experience. Learning from his research philosophy and collaborative spirit has allowed me to mature as a chemist, in both my research and my writing. I am truly honored to have had the opportunity be a part of such a storied career, and I will always owe him a great deal.

I am appreciative toward my dissertation committee members Professors Kay Brummond, Seth Horne, and Sruti Shiva, for their attention and valued input on my comprehensive exam, research proposal, and dissertation writing. Professor Peng Liu is also acknowledged for his expedient guidance through the proposal writing process.

The NHC-borane project has been successful in part to the collaborations that have taken place with colleagues within the Curran group. Hanmo Zhang's positive mentorship during my first summer was a wonderful introduction to the Curran group. I am grateful for the excellent research conducted by Xiben Li that laid the foundation for many of my eventual contributions

to the project. I would also like to express thanks to the following researchers involved with the NHC-borane project: Tsuyoshi Taniguchi, Xiangcheng Pan, Everett Merling, Swapnil Nerkar, Timothy McFadden, Wen (David) Dai, and Daniel Bolt. Their many contributions and cherished friendship are hopefully well-reflected in my work, and I wish them well.

I would like to thank the following co-authors on my publications: Takuji Kawamoto and Sean Gardner for initiating the NHC-boryl iodide catalysis project; and Anthony Horner and Prof. Stephen Weber whose acidity constant measurements and analytical chemistry expertise were critical for the completion of the NHC-boryl acid project.

My thanks also go to Dr. Damodaran Krishnan and Dr. Bhaskar Godugu for maintaining the excellent NMR and HRMS facilities. Dr. Steve Geib was always a pleasure to work with during the process of solving X-ray crystal structures.

Special thanks to Prof. Brian Myers whose hands-on mentorship at ONU set me on the path toward organic chemistry research, and his recommendation to apply to Pitt no doubt changed the course of my life. Also thanks to Mrs. Judy Johnston whose stern tutelage in my first chemistry classes imparted discipline on my studies carried through to this day.

I have been able achieve much in life due to the unconditional love and support from my family, especially my parents, Dave and Melinda. Their sacrifices through the years are not forgotten.

My six years in Pittsburgh would have been a duller experience without the friendship of James, Miles, Erin, Eric, Tyler, Halina, Andreas, Greg, Chad and Nadine. Best wishes to them all. Finally, I would like to thank Hannah. She has been an inspiration for the last two and a half years. I am truly grateful that she is a part of my life.

I dedicate this dissertation to John Harmon and Nancy Allen.

1.0 RHODIUM(II)-CATALYZED B–H INSERTION CHEMISTRY & SYNTHESIS OF CHIRAL BRIDGED RHODIUM(II) CATALYSTS

1.1 INTRODUCTION

1.1.1 Lewis Base Borane Adducts

Trivalent borane species are rare. Neutral Lewis bases complex with borane (BH_3) to produce tetravalent, neutral borane adducts. Borane exists as a dimer (B_2H_6) when a Lewis base is absent. Trimethylamine-borane **2**, triphenylphosphine-borane **3** and pyridine-borane **4** are representative examples of ligated tetravalent boranes (**Figure 1**). These compounds have a formal negative charge on boron and a formal positive charge on the Lewis base. The 2-electron, 2-center bond is variously depicted as a covalent bond ($\text{R}_3\text{N}-\text{BH}_3$), a dative bond ($\text{R}_3\text{N}\cdots\text{BH}_3$ or $\text{R}_3\text{N}\rightarrow\text{BH}_3$), or as a bullet ($\text{R}_3\text{N}\bullet\text{BH}_3$).¹ Here we use the common covalent bond depiction because Lewis base adducts with non-labile bonds are the predominant borane species tested in the following experiments.

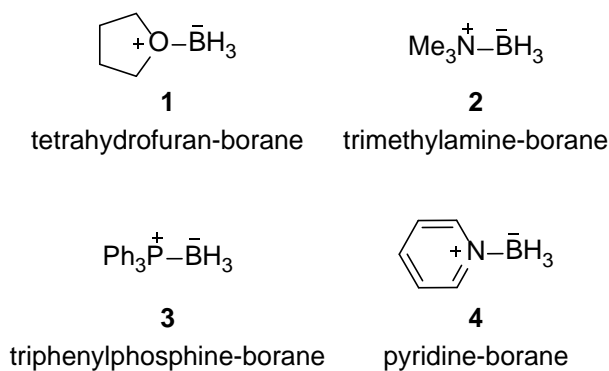


Figure 1. Representative Lewis base borane adducts

Borane complexes with THF ($\text{BH}_3\text{-THF}$ **1**) or dimethyl sulfide ($\text{BH}_3\text{-SMe}_2$) undergo rapid Lewis base exchange with alkenes and alkynes. Following exchange, reaction of borane (BH_3) with an alkene results in the *syn*-addition of $\text{H}_2\text{B-H}$ across a π -bond through a 4-center transition state. In contrast, borane adducts **2**, **3**, and **4** resist Lewis base exchange at ambient temperature, thereby allowing for additional synthetic applications beyond hydroboration. Amine-boranes have been used as hydrogen-storage reagents,² organocatalysts (for example, the CBS reagent³), and as amine protecting groups.¹ Secondary phosphine-boranes undergo hydrophosphinylation with alkenes and alkynes rather than hydroboration.⁴ Pyridine-boranes are weak hydride donors that have higher solubility in aprotic organic solvents than borohydride.⁵

Related to amine- and phosphine-boranes, NHC-boranes are complexes of an N-heterocyclic carbene (Lewis base) with a borane (Lewis acid).⁶ Several typical NHC-boranes are shown in **Figure 2**.

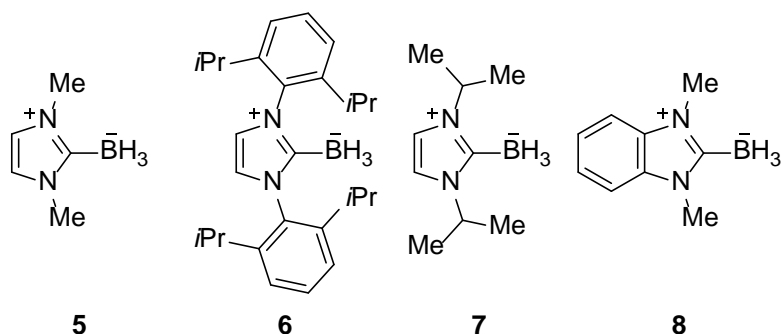
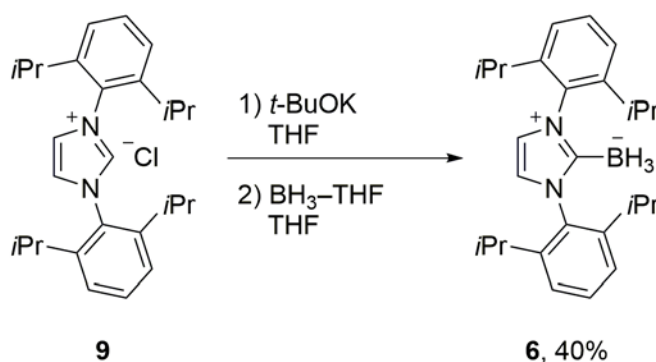


Figure 2. Examples of NHC-boranes

NHC-boranes can be prepared on gram scale by deprotonation of an imidazolium salt followed by complexation with a borane source. For example, NHC-borane **6** is synthesized by deprotonation of imidazolium salt **7** with the strong base *t*-BuOK to generate an *in situ* carbene (Scheme 1). Addition of BH₃–THF **1** as a borane source gives NHC-borane **6** in 40% yield as a stable solid.⁷ NHC-boranes resist dissociation even under heating,⁶ which allows for access to borenium, boryl radical and anion reactive intermediates. Applications of NHC-boranes as reagents have included radical reductions of alkyl and aryl halides,⁸ and ionic reductions of halides, sulfonates and ketones.⁹



Scheme 1. Synthesis of NHC-borane **6**

1.1.2 Rhodium(II)-Catalyzed Carbene Insertion into C–H Bonds

An efficient strategy for formation of heteroatom–carbon (C–X) bonds is the insertion of transient carbenes into an X–H bond (X = N, S, O, Si). Thermally or photochemically generated free carbenes (:CH₂ or :CCl₂) have limited utility due to poor selectivity in insertion reactions. The reactivity of metal carbenes generated from diazoalkanes by transition metals (Cu or Rh) can be fine-tuned to allow for greater synthetic utility in selective intra- and intermolecular functionalizations.¹⁰

The dirhodium tetracarboxylate complexes (Rh₂L₄, L = CO₂R) are constructed from a dinuclear core surrounded by four equatorial carboxylate ligands. The core is held together by a rhodium–rhodium single bond.¹¹ Dirhodium tetraacetate **10** [Rh₂(OAc)₄] is a representative example of rhodium carboxylates, exhibiting *D*_{4h} symmetry (**Figure 3**).

The Teyssie group first reported the intermolecular C–H insertion of ethyl diazoacetate into various alkanes, catalyzed by dirhodium tetraacetate.¹² For example, Rh₂(OAc)₄ catalyzed C–H insertion of ethyl diazoacetate **11** with 2-methylbutane gave the insertion product **12** in 90% yield.

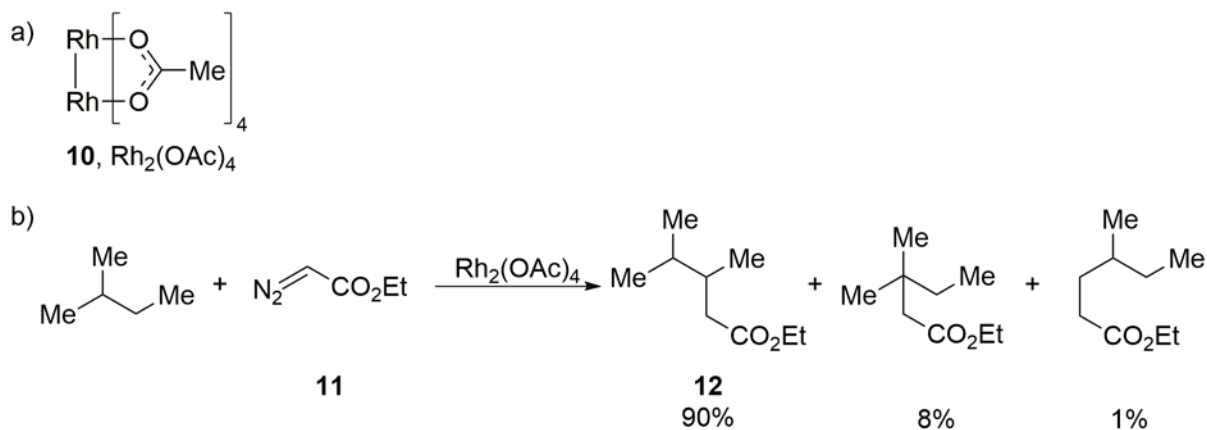


Figure 3. (a) Dirhodium tetracarboxylate, Rh₂(OAc)₄, and (b) Rh(II)-catalyzed C–H insertion of 2-methylbutane

1.1.2.1 Rhodium-catalyzed C–H Insertion Mechanism

A simplified catalytic cycle for a diazo decomposition/carbene insertion reaction involving dirhodium tetracarboxylate (Rh₂L₄) is pictured in **Figure 4**. First, the negatively-polarized carbon of diazoester complexes at the axial site of the coordinately-unsaturated dirhodium tetracarboxylate to form Rh/diazoester species **I** (step i).¹³ According to Doyle,¹⁴ nitrogen extrusion from the diazoester generates the metastable rhodium–carbene complex **II** (step ii). Step II is thought to be rate-limiting. Davies and coworkers recently reported the direct characterization of metastable dirhodium–carbene intermediate **13** by vibrational and NMR spectroscopy, and X-ray absorption analysis (**Figure 5**).¹⁵

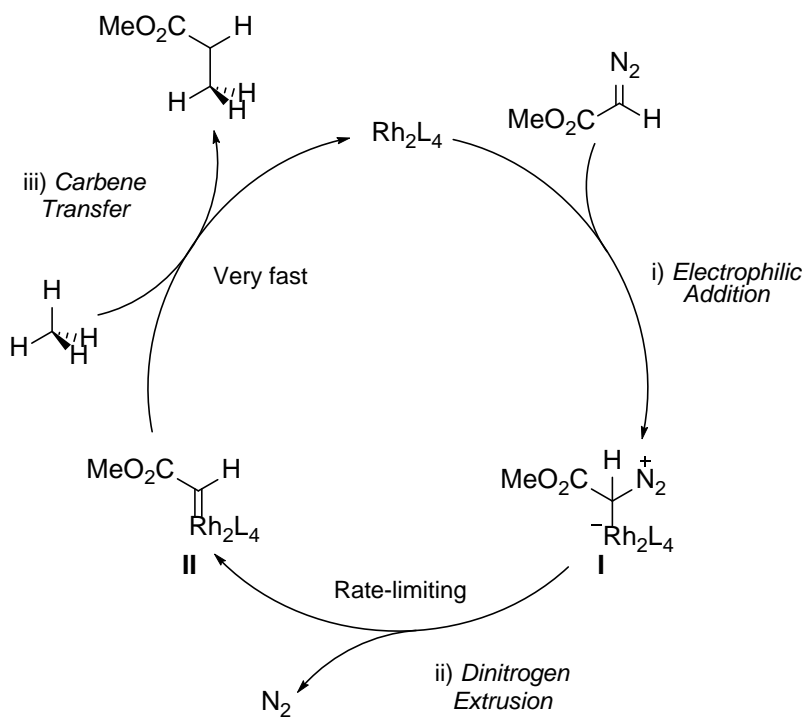


Figure 4. Diazo decomposition and carbene insertion mechanism

Carbene transfer (step iii) is concerted but nonsynchronous as C–H insertion occurs in a single step through a three-centered transition state (TS) with low activation energy (**Figure 6**). Doyle originally proposed¹⁴ that the empty π -orbital on the carbene carbon overlaps with the σ -orbital of the C–H bond. Carbene insertion into a C–H bond occurs with retention of configuration. Doyle’s three-centered concerted TS for the carbene transfer step is generally accepted.

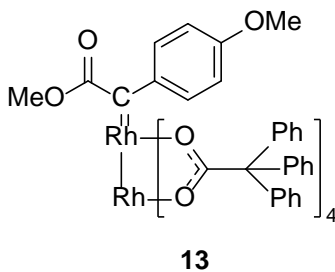


Figure 5. Metastable carbenoid intermediate **13**

A theoretical analysis of the carbene transfer by Nakamura supported Doyle's three-centered TS while further elucidating the mechanistic contribution of the dimetallic core.¹⁶ The Rh^I atom detached from the Rh^{III}-C moiety serves as an 'electron sink', increasing the electrophilicity of the carbene center. After hydride transfer, the Rh^{II}-Rh^{II} bond is regenerated, facilitating cleavage of the Rh^{III}-C bond alongside C-C bond formation (**Figure 7**).

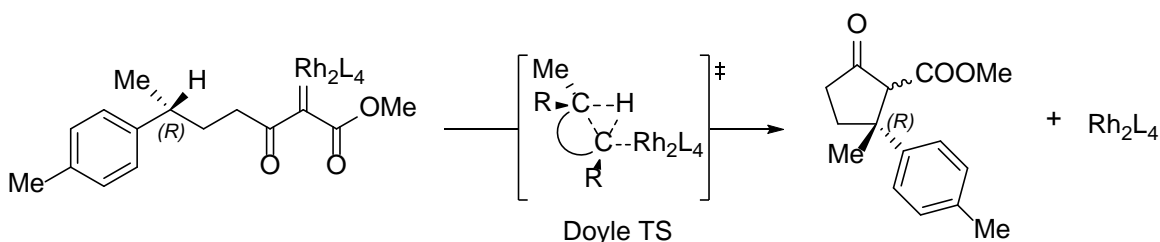


Figure 6. Retention of stereoconfiguration during cyclization¹⁷ and Doyle's three-centered transition state

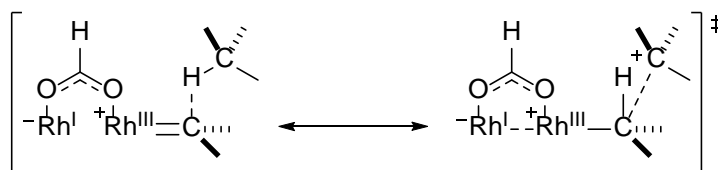


Figure 7. Transition state model of Nakamura's intermediate Rh(II) carbene/alkane complex

1.1.2.2 Donor/Acceptor Diazo Compounds

Diazoalkanes and aryldiazo methanes are impractical carbene precursors for intermolecular C-H insertion reactions due to safety concerns (dangerously explosive) and low regioselectivity.¹⁸ In contrast, α -diazo esters and related compounds (pictured in **Figure 8**) are popular substrates for catalytic C-H insertion reactions due to their relative stability and ease of formation.¹⁹ Diazocarbonyl compounds are resistant to uncatalyzed decomposition over

prolonged storage. For example, the flash point of ethyl diazoacetate is 117 °C²⁰ and is stable toward treatment with glacial acetic acid at room temperature.²¹

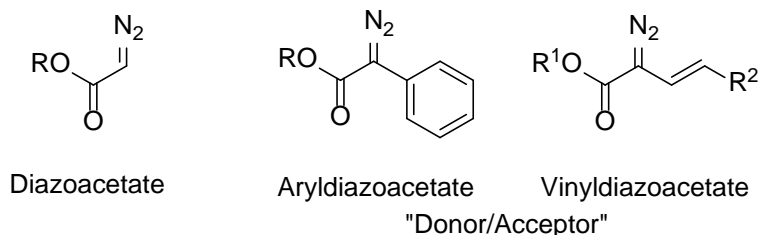


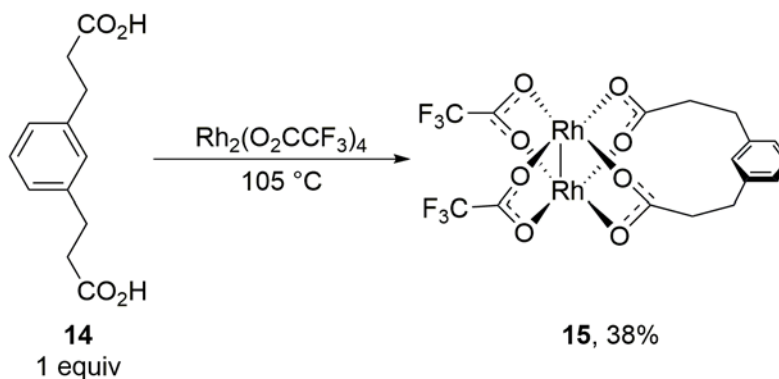
Figure 8. Structures of diazoacetate and two donor/acceptor diazo compounds

Davies investigated the reaction scope toward C–H functionalization with diazo compounds that have two adjacent substituents.²² Diazo compounds with one or two ‘acceptor’ substituents (for example, diazoacetates and diazomalonates) gave high yields only in intramolecular reactions. Selective intermolecular C–H insertion requires attenuated metal carbene reactivity. A ‘donor’ group, typically an aryl or vinyl substituent, stabilizes the electron-deficient metal carbene. Davies’ ‘donor’ nomenclature implies that an aryl substituent stabilizes the carbene through electron donation, but more accurately, the aryl group dissipates positive charge buildup in the C–H insertion TS through resonance delocalization.²³

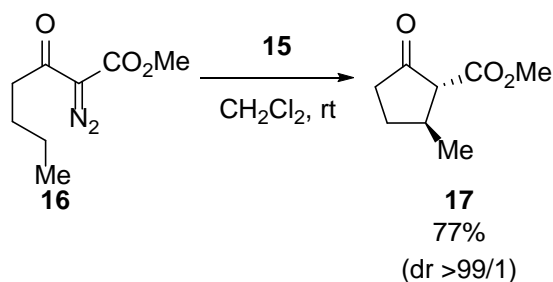
1.1.2.3 Bridged Rh(II) Tetracarboxylate Catalysts

Taber first reported the ligation of two carboxylate groups connected by an organic bridge to a Rh–Rh core with the preparation of monochelated bridged dimer **15** (Scheme 2).²⁴ Benzenedipropanoic acid **14** was added to rhodium(II) trifluoroacetate and the reaction mixture was heated at 105 °C for 5 h to give bridged dimer **15** in 38% yield. When Taber used 2 equiv of diacid **14**, polymeric material was obtained rather than a bis-chelated bridged dimer. Bridged

dimer **15** catalyzed the cyclization of long chain α -diazo β -keto ester **16** to corresponding cyclopentane **17** in 77% yield (**Scheme 3**).

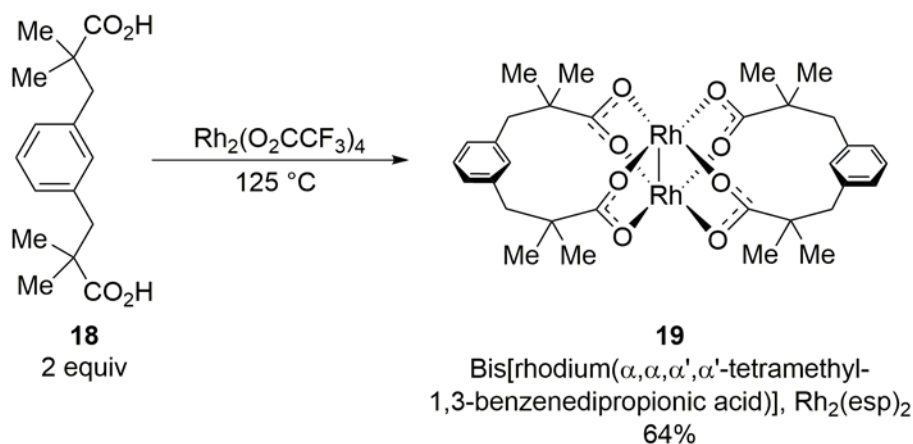


Scheme 2. Preparation of monochelated bridged dimer **15**



Scheme 3. Cyclization of α -diazo β -keto ester **16**

Following earlier work by Bonar-Law,²⁵ Du Bois synthesized tetramethyl diacid **18** where the methyl groups added additional preorganization of the diacids prior to complexation. Tetramethyl benzenedipropionic acid **18** was substituted onto $\text{Rh}_2(\text{O}_2\text{CCF}_3)_4$ to give the fully chelated $\text{Rh}_2(\text{esp})_2$ **22** in 64% yield (**Scheme 4**). Du Bois demonstrated that a $\text{Rh}_2(\text{esp})_2$ **19** catalyzes C–H bond amination.²⁶



Scheme 4. Preparation of $\text{Rh}_2(\text{esp})_2$ **19**

1.1.2.4 Chiral Rh(II) Catalysts with Bridging Ligands

Joining two chiral carboxylate ligands through a linker was first accomplished by Davies to confirm the D_2 -symmetric conformation model of $\text{Rh}_2(S\text{-DOSP})_4$. Second generation proline complexes **20**, **21** and **22** have their aryl-sulfonyl groups conformationally locked in an $\alpha, \beta, \alpha, \beta$ -arrangement (**Figure 9**).²⁷ An advantage of the bridged proline catalysts compared to $\text{Rh}_2(S\text{-DOSP})_4$ is higher observed enantioselectivities in cyclopropanations carried out in polar CH_2Cl_2 versus non-polar hexanes. Vinyl diazoacetate **23** was reacted with styrene and a dirhodium catalyst in either hexanes or CH_2Cl_2 (**Table 1**). When $\text{Rh}_2(S\text{-biTISP})_2$ was the catalyst, the % ee of cyclopropane (S,S)- or (R,R)-**24** equaled or exceeded the % ee observed with $\text{Rh}_2(S\text{-DOSP})_4$ in hexanes (90% / 98% vs 90%).

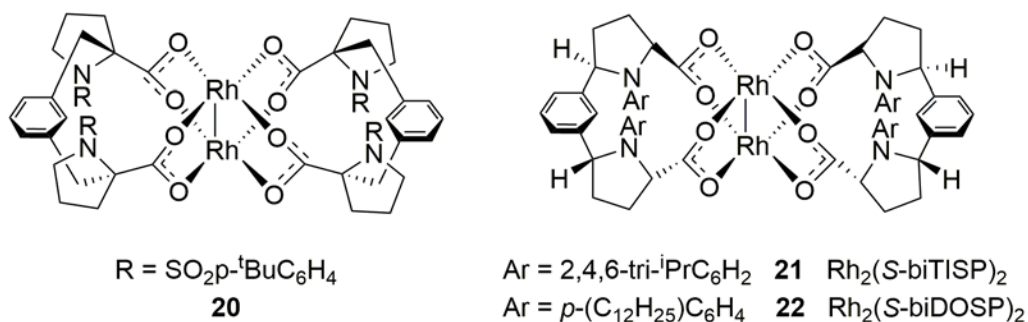
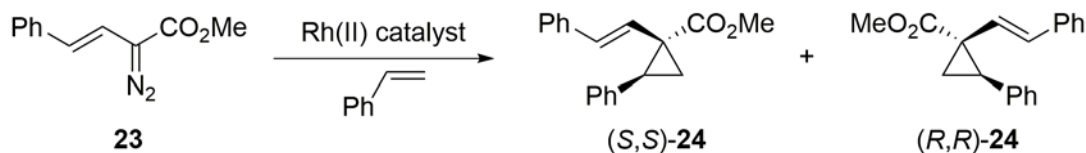


Figure 9. Davies' chiral bridged dirhodium catalysts

Table 1. Solvent effect of rhodium-catalyzed asymmetric cyclopropanation



Solvent	Temperature (°C)	% ee for the formation of 24	
		$\text{Rh}_2(\text{S-biTISP})_2$	$\text{Rh}_2(\text{S-DOSP})_4$
hexanes	25	74 (<i>S,S</i>)	90 (<i>R,R</i>)
CH_2Cl_2	25	90 (<i>S,S</i>)	74 (<i>R,R</i>)
CH_2Cl_2	-50	98 (<i>S,S</i>)	88 (<i>R,R</i>)

1.1.3 Catalytic Carbene Insertion into B–H Bonds

Examples of carbene insertion reactions into B–H bonds are relatively rare when compared to insertion into C–H bonds. B–H insertion reactions have typically required the use of carbene-precursors in large excess (7–40 equiv).²⁸⁻³¹ Prior B–H insertion reactions include reaction of Fischer alkynylcarbene complexes with NaBH_3CN ,²⁸ photo-generated carbethoxycarbene into *o*-carborane B–H bonds,²⁹ samarium carbene insertion into phosphine-borane B–H bonds,³⁰ and dichlorocarbene insertion into phosphine- and amine-boranes (**Figure 10**).³¹

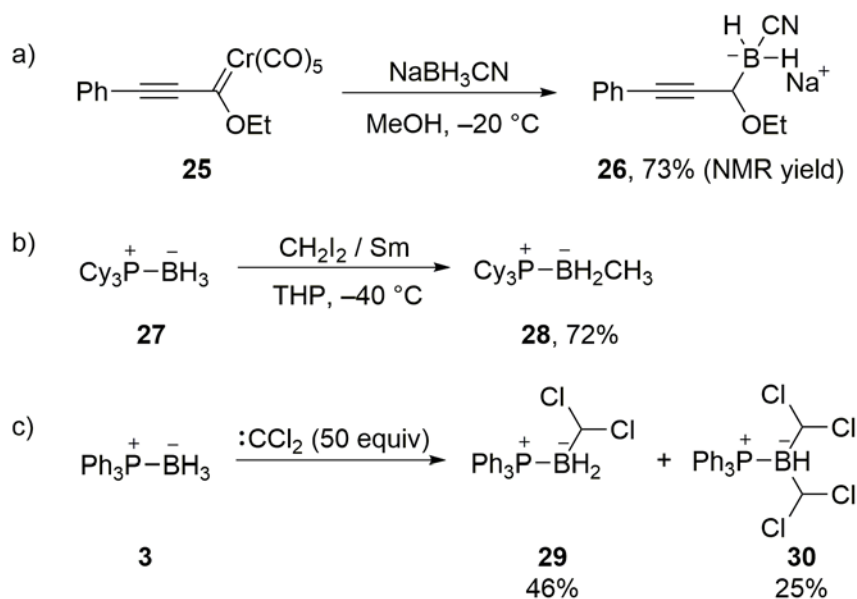
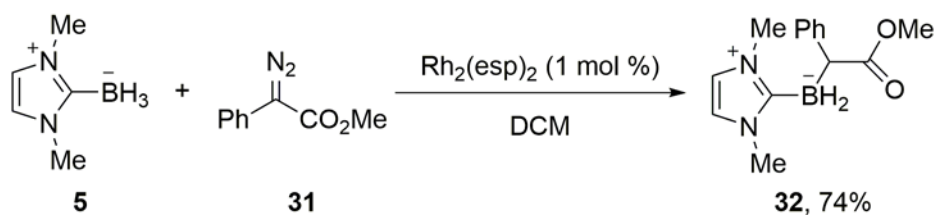


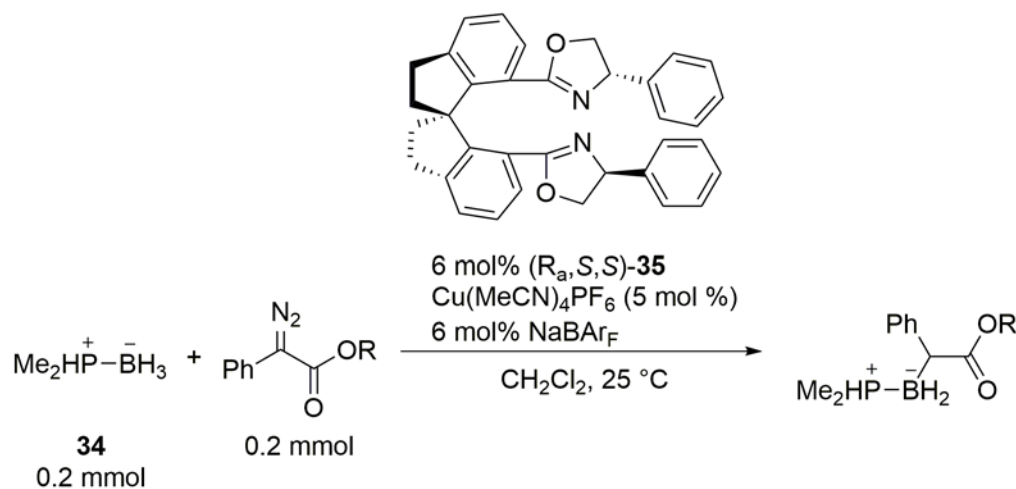
Figure 10. Examples of carbene insertion into B–H bonds, (a) alkynylcarbene insertion, (b) samarium carbene insertion, (c) dichlorocarbene insertion

Recently, Curran and Li reported rhodium(II)-catalyzed carbene insertion into the B–H bonds of NHC-boranes.³²⁻³³ NHC-boranes are among the most nucleophilic neutral hydride donors on Mayr’s nucleophilicity scale³⁴ ($N = 11.88$)³⁵ and are excellent carbenophiles. In a representative example, donor acceptor diazo **31** was added to NHC-borane **5** with $\text{Rh}_2(\text{esp})_2$ to give the insertion product **32** in 74% yield (**Scheme 5**). $\text{Rh}_2(\text{esp})_2$ consistently gave higher yields compared to $\text{Rh}_2(\text{OAc})_4$. This is a reliable procedure for boron-carbon bond formation gives stable α -NHC-boryl carbonyl compounds.

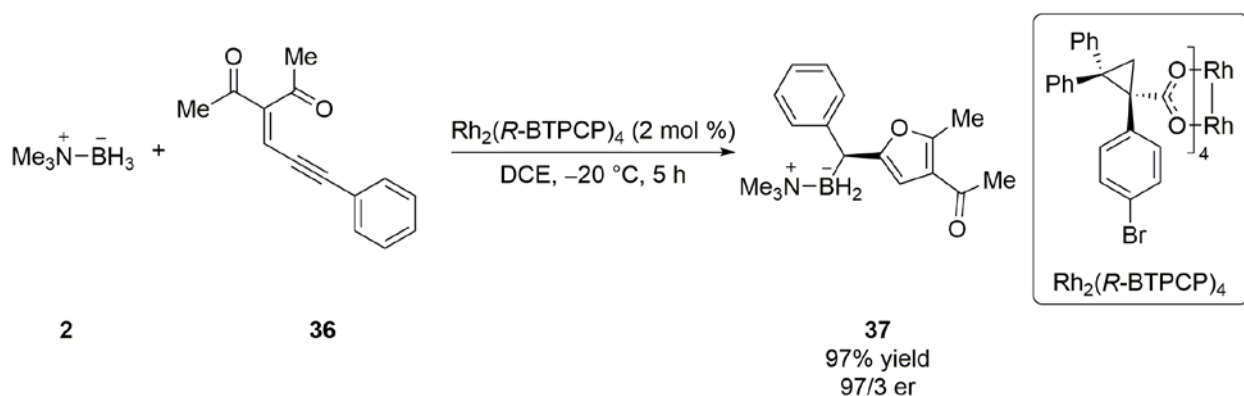


Scheme 5. Rhodium-catalyzed B–H insertion of NHC-borane **5**

Table 2. Enantioselective C–H insertion of dimethylphosphine-borane **34** with Zhou ligand **35**



R	Time (h)	Yield	ee (%)
2,6-Me ₂ C ₆ H ₃	20	86%	88
2,6-Cl ₂ C ₆ H ₃	4	96%	92



Scheme 7. Enantioselective B–H insertion synthesis of boryl furan **37**

The catalyst scope of B–H insertion reactions have been extended to include rhodium(I) salts. Xu and co-workers reported asymmetric rhodium(I)-catalyzed insertions with amine- and NHC-boranes (**Figure 11a**).³⁸ Optimized conditions with methylpyrrolidine-borane **38**, *tert*-butyl

diazophenylacetate **40**, divinylrhodium chloride dimer, and the C_1 -symmetric diene **40** yielded insertion product **41** in 92% yield and >99/1 er. Similar unoptimized conditions with NHC-borane **5** gave modest enantioinduction (80/20 er). The insertion of methyl 2-diazo-2-phenylacetate **31**, catalyzed by a cyclobutadiene rhodium(I) complex, into the B–H bond of triethylamine-borane **42** was demonstrated by Perekalin and co-workers (**Figure 11b**).³⁹

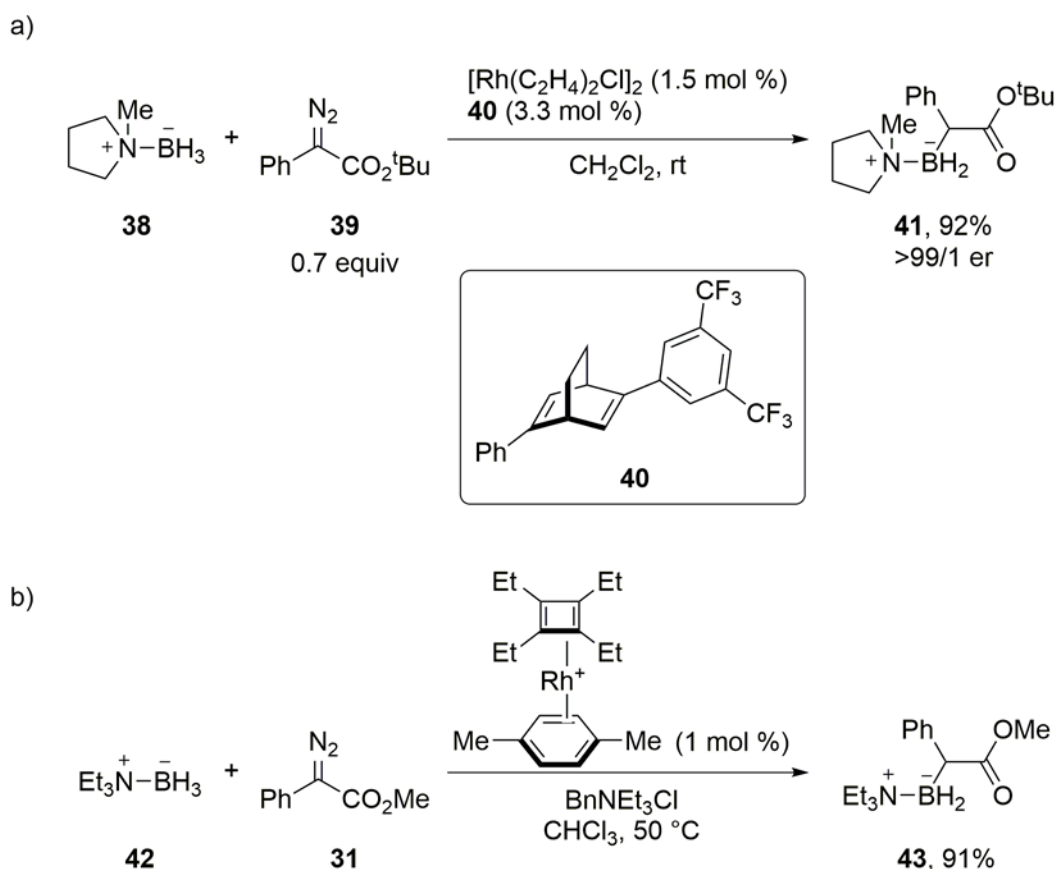
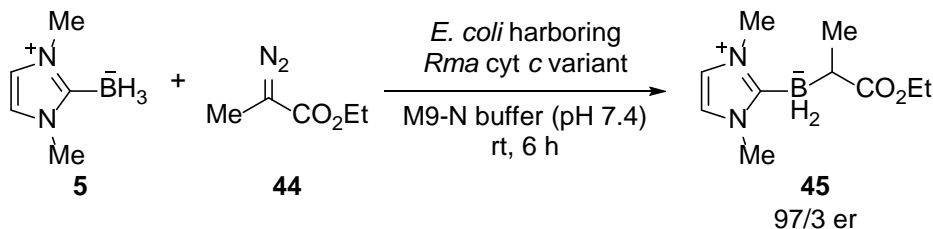


Figure 11. B–H insertion using Rh(I) catalysts

The first B–H insertion reaction of NHC-boranes that produced enantiopure α -NHC-boryl esters was reported by Arnold through the use of an engineered enzyme. Directed evolution of *Rhodothermus marinus* (*Rma* cyt *c*) facilitated carbon–boron bond formation in the

presence of Lewis base borane adducts.⁴⁰ Guided evolution of the bacterial catalyst toward improved enantioinduction allowed access to 16 chiral organoboranes. For example, incubation of NHC-borane **5** and ethyl 2-diazopropanoate **44** with *E. coli* harboring engineered *Rma cyt c* gave boryl ester **45** in excellent enantioselectivity (97:3 er) (**Scheme 8**).



Scheme 8. Enzyme catalyzed enantioselective B–H insertion of NHC-borane **5**

Dr. Li's Rh(II)-catalyzed B–H insertion report contains three unanswered questions: 1) can Rh(II) catalysis conditions be extended to include ligated boranes other than NHC-boranes, 2) can enantioselective B–H insertion be achieved with chiral Rh(II) catalysts, and 3) can the diazo substrate scope be broadened by improving reaction conversion when using 2-alkyl substituted diazo compounds.

The goals addressed in Section 1.2 are: i) to expand the scope of Rh(II)-catalyzed carbene insertion to include ligated boranes beyond NHC-boranes, ii) to develop a relative reactivity profile of ligated boranes in Rh(II)-catalyzed B–H insertion reactions, iii) to apply chiral dirhodium catalysts to enantioselective B–H insertion of NHC-boranes, and iv) to synthesize a chiral variant of Du Bois' Rh₂(esp)₂ benzenedipropionic acid ligand and apply toward B–H insertion reactions and cyclopropanations.

1.2 RESULTS AND DISCUSSION

1.2.1 Rhodium-catalyzed B–H Bond Insertions with Lewis Base Adducts of Borane

The method described in Section 1.1.3 to form carbon-boron bonds through rhodium(II) catalysis was previously applied to reactions between N-heterocyclic carbene boranes and diazocarbonyl compounds.³² We sought to expand the scope of this insertion reaction by exploring other stable donor-acceptor complexes of borane, including amine-, phosphine-, and pyridine-boranes. We also chose tetrabutylammonium borohydride and cyanoborohydride as representative tetravalent, anionic boron reagents, with the cyano group serving as a NHC analog.

1.2.1.1 Synthesis of Stable Lewis Base Complexes of α -Boryl Carbonyl Compounds

Neutral organoboron compounds can exist in either an enol or carbonyl form depending on the nature of the boron functional group. Trivalent boranes usually favor the enol form **46** (**Figure 12**). Tetravalent boron compounds with strongly bound ligands to boron, such as amines,³⁸ phosphines,³⁶ NHCs, and *N*-methyliminodiacetic acid (MIDA),⁴¹ prefer to form as isomeric α -boryl carbonyl compounds **47** rather than enol isomers. The resulting α -boryl aldehydes, ketones and esters ($X = \text{H}, \text{C}, \text{or O}$) are bench-stable compounds, whose stability also translates into reaction tolerance.^{32, 36, 38, 41}

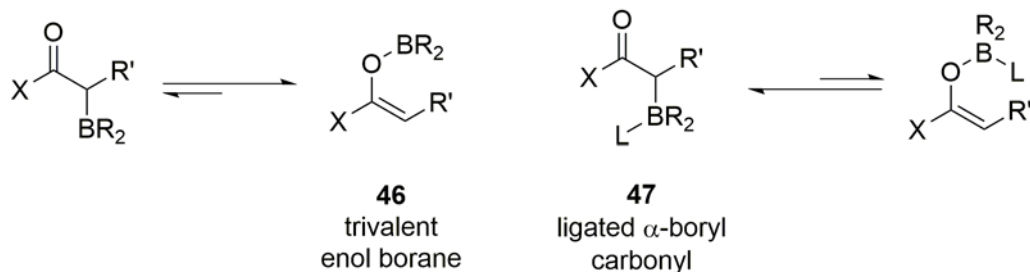


Figure 12. Borane isomer equilibria

Pinacolborane, catecholborane, $\text{BH}_3 \cdot \text{THF}$, and $\text{BH}_3 \cdot \text{SMe}_2$ do not undergo insertion with Fischer-type metal carbenes;³⁶ however, the B–H bond becomes more electron rich upon formation of an amine or phosphine adduct to allow for possible B–H insertion with metal carbenes. We sought to learn whether B–H insertion occurs with a donor/acceptor diazo compound, and if so whether B–H insertion products are stable to isolation by flash chromatography.

Table 3 summarizes the preparation of several ligated borane B–H insertion products. In a typical experiment (Table 4, entry 1, standard conditions), trimethylamine-borane **2** (1 mmol) and $\text{Rh}_2(\text{esp})_2$ (1 mol%) were dissolved in CH_2Cl_2 (0.2 M). Then 1.2 equiv of methyl 2-diazo-2-phenylacetate **31** dissolved in CH_2Cl_2 (0.24 M) was added over 2 h via syringe pump. After addition of the diazo species was complete, the solution color changed from green to orange. Du Bois and coworkers have reported green coloration denotes the presence of the catalytically active $\text{Rh}^{2+}/\text{Rh}^{2+}$ dimer, thus disappearance of green coloration signifies consumption of $(\text{Rh}_2\text{esp}_2)$.⁴²

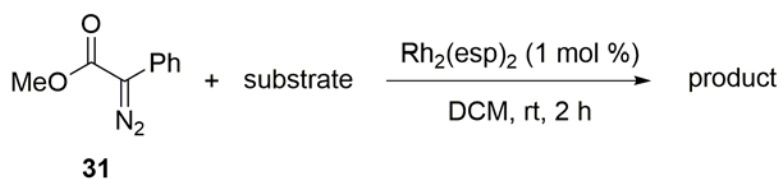
Conversion of starting amine-borane **2** to the desired B–H insertion product **48** was monitored by recording an ^{11}B NMR spectrum of the crude reaction mixture after 2 h. This showed the appearance of a new triplet at -0.9 ppm ($J_{\text{BH}} = 99$ Hz) that we attributed to the B–H

mono-insertion product **48**. The quartet of the starting trimethylamine-borane **2** appeared at -8.3 ppm. Based on integration of the two signals, the ratio of mono-insertion product **48** to unreacted trimethylamine-borane **2** was 70/30.

After evaporation and purification by flash chromatography, α -trimethylamine-boryl ester **48** was isolated in 43% yield as a white solid.⁴³ In addition to the ^{11}B NMR spectrum, the structure of **48** was supported by ^1H and ^{13}C NMR spectra, and mass spectroscopy analysis. Li was not able to observe resonances of carbon bonded to the boron atom (labeled α) in many of the NHC α -boryl carbonyl compounds due to quadrupole broadening.⁴⁴ However, the ^{13}C NMR spectrum of insertion product **48** displayed a broad, weak resonance at 46.5 ppm that we attributed to the α -carbon.

Upon addition of triphenylphosphine-borane **3** to a solution containing Rh_2esp_2 , the solution color changed from green to light orange. When diazo **31** was added, **3** was not consumed and product **33** was not formed. We hypothesized that the presence of free triphenylphosphine in the sample of **3** inactivated the catalyst by complexation. Indeed, a ^{31}P NMR spectrum of the precursor showed triphenylphosphine-borane **3** (20.80 ppm) was contaminated with about 3% free triphenylphosphine (-6.00 ppm).

Table 3. B–H insertion of Lewis base borane adducts

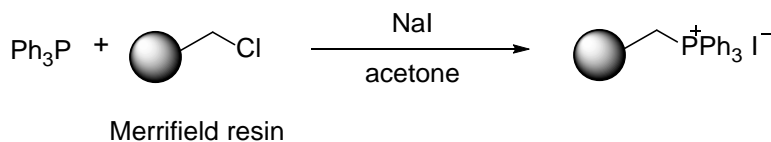


Entry	Substrate	Product	^{11}B NMR ppm (mult).	^{11}B NMR pdt ppm (mult).	Conv. ^a	Yield ^b
1	$\text{Me}_3\text{N}-\text{BH}_3$ 2		−8.3 (q)	−0.9 (t)	70%	43%
2 ^c	$\text{Ph}_3\text{P}-\text{BH}_3$ 3		−38.0 (sex)	−23.1 (br)	70%	50%
3 ^c	$\text{Bu}_3\text{P}-\text{BH}_3$ 49		−41.7 (sex)	−25.8 (br)	86%	30%
4	pyr− BH_3 4		−12.6 (q)	−3.2 (t)	80%	79%
5	$\text{Bu}_4\text{N}\text{BH}_4$ 52		−39.5 (quin)	−22.1 (q)	<15% ^d	N/A ^e
6	$\text{Bu}_4\text{N}\text{BH}_3\text{CN}$ 54		−42.4 (q)	−27.3 (t)	100%	N/A
		55				

^[a] Estimated from ^{11}B NMR spectrum of crude reaction mixture; ^[b] Isolated yield after flash chromatography; ^[c] 4 mol % $\text{Rh}_2(\text{esp})_2$; ^[d] **52** reacted directly with $\text{Rh}_2(\text{esp})_2$, multiple side

products present in crude ^{11}B NMR spectrum; ^[e] Product is a salt and was not isolated after column chromatography.

Our initial approach to circumvent the triphenylphosphine impurity was the Merrifield resin scavenging method. In this method, the resin chloride is converted to iodide, which traps the Ph_3P impurity on the resin by alkylation. The resin-bound phosphonium salt is then filtered and pure starting material is recovered from concentrating the filtrate (**Scheme 9**).⁴⁵ Stirring **3** containing 3% Ph_3P with a slurry of Merrifield resin and sodium iodide in acetone gave pure **3** but in only 10% recovery after filtration. When purified phosphine-borane **3** was reacted with diazo **31** and 1 mol % $\text{Rh}_2(\text{esp})_2$ we observed formation of B–H insertion product **33**. However, the low yield of recovered pure phosphine-borane **3** prompted us to look for a more practical method.



Scheme 9. Triphenylphosphine scavenging with Merrifield resin

We accounted for the impurity by increasing the rhodium(II) catalyst loading to 0.04 equiv, and upon addition of triphenylphosphine-borane **3**, the solution color remained green signifying that the catalyst remained. Reaction between triphenylphosphine-borane **3** (1 mmol) and 1.2 equiv methyl diazo phenylacetate **31** with 4 mol % Rh_2esp_2 (Table 4, entry 2) resulted in 71% conversion to the B–H insertion product **33** (broad singlet at -23.1 ppm) as shown in the ^{11}B NMR spectrum of the crude product. Flash chromatography gave the mono-insertion product **33** in 50% yield as an orange solid. The orange coloration is likely due to a trace amount of

rhodium impurity. A ^{31}P NMR spectrum of **33** showed 93% of target insertion product **33** (13.42 ppm) along with 3.5% triphenylphosphine (-5.40 ppm) and 3.5% triphenylphosphine ylide **56** (29.24 ppm) as impurities. The latter impurity is formed through a modified Staudinger mechanism where triphenylphosphine attacks the terminal diazo nitrogen, resulting in formation of a diazo-ylide. Subsequent loss of dinitrogen leads to the triphenylphosphine ylide **56** (**Figure 13**).

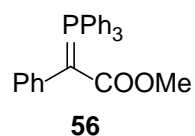


Figure 13. Phosphonium ylide **56**

Next, we reacted commercially available pyridine-borane **4** (6 M solution in THF) with diazo compound **31** under the standard B–H insertion reaction conditions. Unfortunately, formation of B–H mono-insertion product **51** was again not observed in the ^{11}B NMR spectrum of the crude reaction mixture. We again hypothesized that an impurity, this time pyridine, was inactivating the rhodium catalyst.

To obtain a pyridine-borane sample without free ligand, we synthesized pyridine-borane **4** through a Lewis base exchange between pyridine and a borane-tetrahydrofuran complex (1 M in THF). Stirring 0.95 equiv of pyridine with the borane-THF complex at room temperature for 1 h followed by column chromatography gave pyridine-borane **4** as an oil in 64% yield. Subsequent reaction of the homemade pyridine-borane **4** under the standard conditions (**Table 4**, entry 4) resulted in 79% conversion to mono-insertion product **51** (triplet at -3.2 ppm, $J_{\text{BH}} = 101$ Hz), and flash chromatography purification yielded 79% of a colorless oil.

As shown in **Table 3** (Entries 1–5), the α -boryl carbonyl compounds of amine-, phosphine-, and pyridine-boranes reliably exhibit downfield resonances in ^{11}B NMR spectra compared to non-functionalized Lewis base borane precursors. This trend is consistent with Li's data on NHC-boranes and Zhou's copper-catalyzed insertion of amine- and phosphine-boranes.^{32, 36}

The stability of amine-borane insertion product **48** to flash chromatography was examined first by two-dimensional TLC analysis. Moderate streaking of the product spot suggested at least partial instability of insertion product **48** to silica gel. Purification of amine-borane product **48** and phosphine-borane products **33** and **50** by flash chromatography resulted in 20-50% lower isolated yield than expected by ^{11}B NMR spectra conversion estimates (amine: 70% conversion, 43% yield; triphenylphosphine: 70% conversion, 50% yield; tributylphosphine: 86% conversion, 30% yield).

Purification of pyridine-borane insertion product **51** gave a 79% yield (80% conversion). Li reported a 20% reduction between conversion and recovered yield with B–H insertion products of (1,3-dimethyl-1*H*-imidazol-3-ium-2-yl)trihydroborate **5**.³² Quantitative recovery was achieved using bulkier NHC substrates such as dipp-imidazolylidene borane **6**.

Taken together, these results suggest that pyridine-borane α -boryl carbonyl compounds are stable to flash chromatography, whereas analogous amine-, phosphine-, and *N*-alkyl substituted NHC-borane compounds are only partially stable. For these classes of compounds, purification by flash chromatography should be as rapid as possible to minimize product loss. In contrast, once the purified products are isolated, they are quite stable to storage.

Moving beyond neutral donor-acceptor borane complexes, we also sought to apply B–H insertion methodology to borohydrides. Tetrabutylammonium borohydride **52** was initially

chosen for its solubility in CH_2Cl_2 . When B–H insertion reaction of borohydride **52** was attempted under the standard conditions, the solution color changed from green to dark brown prior to addition of diazo compound **31**. Diazo compound **31** was slowly added anyway, but no insertion product **53** was observed by ^{11}B NMR spectra. In a second experiment, diazo compound **33** was premixed with borohydride **52** and $\text{Rh}_2(\text{esp})_2$ was then added to the reaction mixture. Low conversion (<15%) to the borohydride insertion product **53** (–22.4 ppm, $J_{\text{BH}} = 178$, 90 Hz) was observed in the ^{11}B NMR spectrum of the crude reaction mixture. These two experiments suggest that $\text{Rh}_2(\text{esp})_2$ reacts with borohydride faster than with diazo **31**.

We turned to tetrabutylammonium cyanoborohydride **54** as a milder reducing borohydride. On Mayr's nucleophilicity scale, cyanoborohydride has a smaller N value of 11.5 compared to the borohydride N value of 15.0.⁴⁶ The scale is logarithmic so the reactivity difference is large. When **54** was subjected to the standard B–H insertion conditions, we observed 100% conversion to the borohydride insertion product **55** as evidence by a triplet at –27.3 ppm ($J_{\text{BH}} = 94$ Hz) in the ^{11}B NMR. Isolation by flash chromatography was attempted, but the desired cyanoborohydride insertion product was not isolated, presumably because it is a salt. In addition to ^{11}B NMR spectra of the crude product mixture, observance of the typically weak α -carbon signal in the ^{13}C NMR spectrum at 44.7 ppm supported the formation of the insertion product (**Figure 14**).

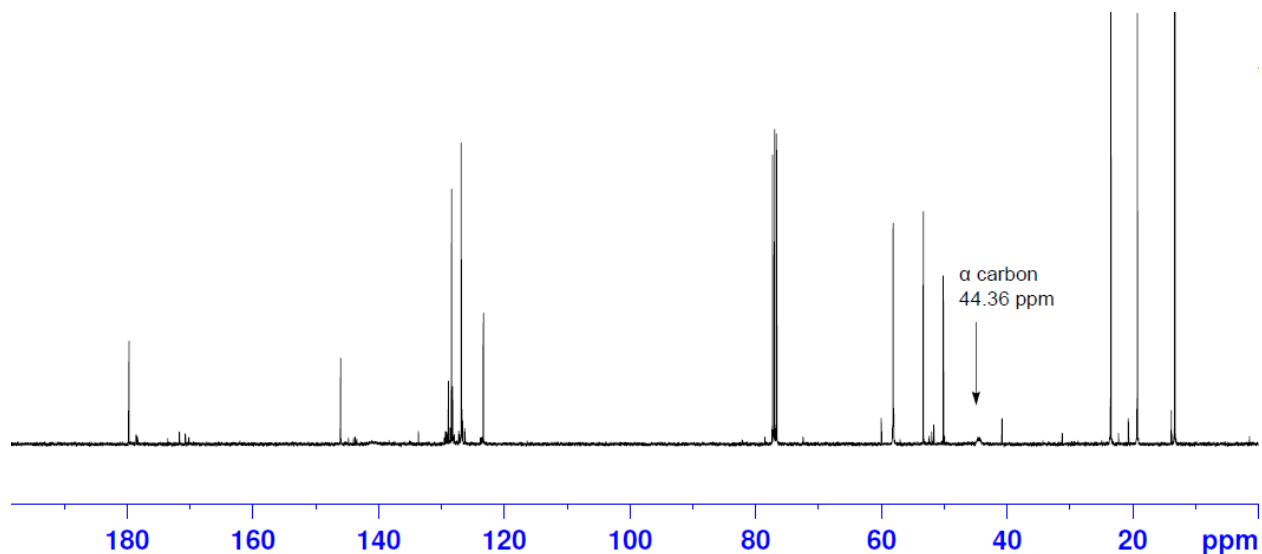


Figure 14. ^{13}C NMR spectra of crude reaction mixture containing cyanoborohydride product **54**

The initial difficulties with B–H insertion reactions of phosphine- and pyridine-boranes suggested that $\text{Rh}_2(\text{esp})_2$ was incompatible with triphenylphosphine and pyridine impurities. To validate this hypothesis, a series of B–H insertion reactions using pyridine-borane as a control were undertaken (**Table 4**). In the control reaction, pyridine-borane **4** (0.2 mmol) and $\text{Rh}_2(\text{esp})_2$ (1 mol %) were dissolved in CH_2Cl_2 (0.5 M). Then 1.8 equiv of methyl phenyl diazo **31** dissolved in CH_2Cl_2 (0.4 M) was added dropwise. Due to the larger amount of diazo **31** used (1.8 rather than 1.2 equiv), the double insertion product **57** (d, -13.9 ppm, $J_{\text{BH}} = 98$ Hz) was observed in the control reaction along with the expected product **51** (**51** / **57** ratio, 74/26) (entry 1). For entries 2–4, the pyridine-borane and $\text{Rh}_2(\text{esp})_2$ reaction mixture was spiked with 0.2 equiv of a Lewis base, then 1.8 equiv of diazo compound **31** was slowly added.

Tetrahydrofuran as an additive decreased conversion of pyridine-borane product **51** from 100% to 93% (entry 2) likely due to competitive C–H insertion of THF.²² Addition of pyridine and triphenylphosphine gave no conversion of **4** (entries 3 and 4). In the latter cases, the reaction solution color transitioned from green, signifying catalytically active Rh(II) species, to pink or

orange, respectively, prior to diazocarbonyl addition. Rhodium(II) dimers have been reported to be solvatochromic upon binding of axial ligands; furthermore, such modified rhodium(II) dimer complexes are not catalytically active.⁴² These results firmly show that pyridine and triphenylphosphine inactivate the catalyst. Further, the simple observation of solution color prior to diazocarbonyl addition indicates whether catalytically active Rh(II) is present (green) or absent (pink or orange) in solution. When ligated boranes are used for B–H insertions, the samples must not contain free ligands as impurities.

Table 4. Lewis base additives in Rh(II) B–H insertion system

Entry	Additive (0.2 Equiv)	Conversion ^a	Ratio 51 / 57
1	None	100%	74/26
2	THF	93%	100/0
3	C ₅ H ₅ N	0%	—
4	Ph ₃ P	0%	—

^[a] Estimated from ¹¹B NMR spectrum of crude reaction mixture.

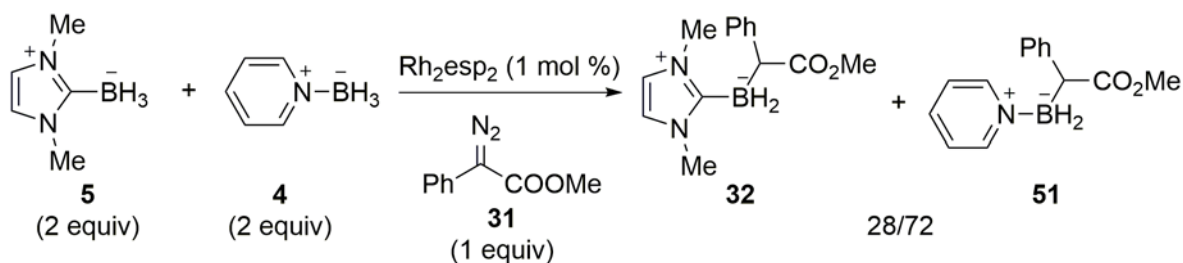
1.2.1.2 Determination of Relative Rates of Ligated Boranes and a Borohydride Salt in Rhodium(II)-Catalyzed Competitive B–H Insertion Experiments

Li's competition experiments with NHC-borane **5** with various carbenophiles established that the B–H bonds in **5** are much more reactive than typical C–H bonds toward electrophilic

rhodium carbenes.³² For example, NHC-borane **5** is approximately 10–12 times more reactive than 1,4-cyclohexadiene (1,4-CHD), and over 100 times more reactive than THF.

Next, we set out to learn the relative reactivity of the NHC-borane B–H bond toward insertion in comparison to other donor-acceptor complexes of borane and borohydrides. Reactions of 0.5 equiv of diazoacetate **31** with equal equiv (1.0) of different ligated boranes and a borohydride were undertaken to produce a relative reactivity profile for boranes toward B–H insertion conditions. The product formation ratios were determined through integration of the ¹¹B NMR signals of the two insertion products.

The initial competitive insertion reaction between NHC-borane **5** and pyridine-borane **4** used Rh₂(esp)₂ and 2-phenyl-diazoacetate **31**. Diazo compound **31** was selected because it was used in Davies and Li's competitive rate experiments and gave high product yields during intermolecular C–H and B–H insertion reactions.^{32, 47} In a typical experiment (**Scheme 10**, standard conditions), NHC-borane **5** (1.00 equiv, 0.37 mmol), pyridine-borane **4** (1.00 equiv, 0.37 mmol) and Rh₂(esp)₂ (1 mol %) were dissolved in CH₂Cl₂ (0.2 M). An ¹¹B NMR spectrum of the crude reaction mixture was taken to determine the accurate starting ratio of the two borane species. Then a solution of diazo compound **31** (0.50 equiv, 0.10 mmol) in CH₂Cl₂ (0.1 M) was added over 15 s by syringe. After addition of the diazo species was complete, the solution color remained light green.



Scheme 10. Competition experiment between NHC-borane **5** and pyridine-borane **4**

Conversions of NHC-borane **5** and pyridine-borane **4** to the B–H insertion products **32** and **51** were determined by recording ^{11}B NMR spectra of the crude reaction mixture immediately after addition of the diazo compound. This showed the appearance of new triplets at -3.4 ppm ($J_{\text{BH}} = 104$ Hz) and -23.7 ppm ($J_{\text{BH}} = 94$ Hz) that belong to B–H mono-insertion products **32** and **51**, respectively. Based on integration of the two signals, a 28 / 72 ratio of **32** / **51** was observed (Table 5, entry 1).

This preliminary experiment suggested that pyridine-borane is approximately two times more reactive ($k_{\text{rel}} = 2.3$) than the NHC-borane towards B–H insertion. We next tried to verify the relative rate by repeating the experiment with increased equivalents of pyridine-borane **4** (entry 2, 5.8 equiv) or NHC-borane **5** (entry 3, 5.0 equiv). Although **4** and **5** were used in small excess, there was not a noticeable decrease in starting material ^{11}B NMR peak integration after the reaction. The relative rates obtained from entries 2 and 3 (2.7 and 2.8) confirm that pyridine-borane is a more reactive substrate in B–H insertion reactions than NHC-boranes.

Moving beyond pyridine-borane, competitive reaction between equimolar amounts of NHC-borane **5** and trimethylamine-borane **2** show that NHC-borane **5** is three times more reactive ($k_{\text{rel}} = 0.33$) than amine-borane **2** (entry 4).

Initial competitive reactions between equimolar amounts of NHC-borane **5** and triphenylphosphine-borane **3** resulted in no formation of phosphine-borane insertion product **33**,

implying that phosphine-boranes are significantly less reactive than NHC-boranes. Competitive reaction of equal equivalents of triphenylphosphine-borane **3** and trimethylamine-borane **2** showed that phosphine-borane is about five times less reactive ($k_{\text{rel}} = 0.19$) than amine-boranes (entry 5). The competitive reaction result between equal equiv of tributylphosphine-borane⁴⁸ **49** with trimethylamine-borane **2** (entry 6) was consistent with phosphine-borane being about five times less reactive than amine-boranes.

Table 5. Competitive B–H insertion experiments

Entry	Unknown (ukn)	Standard (stn)	Equivalents (unk/stn)	Ratio ^a	k_{rel} (unk/stn)
1	pyr–BH ₃ 4	NHC–BH ₃ 5	1.0 / 1.0	72/28	2.3
2	pyr–BH ₃ 4	NHC–BH ₃ 5	5.8 / 1.0	94/6	2.7
3	pyr–BH ₃ 4	NHC–BH ₃ 5	1.0 / 5.0	36/64	2.8
4	Me ₃ N–BH ₃ 2	NHC–BH ₃ 5	1.1 / 1.0	27/73	0.33
5 ^b	Ph ₃ P–BH ₃ 3	Me ₃ N–BH ₃ 2	1.0 / 1.0	16/84	0.19
6 ^b	Bu ₃ P–BH ₃ 49	Me ₃ N–BH ₃ 2	1.0 / 1.0	17/83	0.20
7	Bu ₄ NBH ₃ CN 54	Me ₃ N–BH ₃ 2	1.0 / 1.0	35/65	0.54

^[a] Determined by integration of the ¹¹B NMR spectrum of the reaction mixture; ^[b] 4 mol % Rh₂(esp)₂.

In addition to Lewis base borane adducts, we probed the relative reactivity of cyanoborohydride as well. Reaction between cyanoborohydride **54** and amine-borane **2** produced a relative rate of 0.54; suggesting that cyanoborohydride reactivity is between amine- and phosphine-boranes in B–H insertion reactions (entry 7).

When taken together, a trend of ligated borane reactivity toward B–H insertion can be summarized as shown in the top row of **Table 6**. All k_{rel} values are based on NHC-borane **5**, $k_{\text{rel}} = 1$.

Table 6. Relative rates toward B–H insertion, BDE values, and Mayr N values for various boranes

	pyr–BH ₃	NHC–BH ₃ 5	Me ₃ N–BH ₃	[BH ₃ CN] [–]	R ₃ P–BH ₃
k_{rel}	2.5	1	0.33	0.18	0.06 ^a
BDE (kcal/mol) ⁴⁹	68.8	80.0	102.6	N/A	92.8 ^b
Mayr's Value (N)	10.01 ⁴⁹	11.88 ³⁵	7.97 ⁴⁹	11.52 ⁴⁶	N/A

^[a] Ph₃P–BH₃ and Bu₃P–BH₃; ^[b] Me₃P–BH₃

Also shown in **Table 6** are BDEs and Mayr's nucleophilicity values of the various ligated boranes. A correlation between the relative reactivity trend in B–H insertion and either BDE values⁵⁰ or Mayr's nucleophilicity values is not readily apparent. The high reactivity of pyridine-borane is consistent with its low BDE (68.8 kcal/mol). The trend remains consistent with NHC-borane (80.0 kcal/mol) and trimethylamine-borane (102.6 kcal/mol) decreasing in relative reactivity. However, the BDE of Me₃P–BH₃ (92.8 kcal/mol) is smaller than Me₃N–BH₃ (102.6 kcal/mol) yet the B–H insertion of triphenyl- and tributylphosphine-borane was significantly slower than expected. Likewise, a connection cannot be drawn when comparing our relative reactivity data and Mayr's nucleophilicity scale. NHC-borane **5** is a good hydride donor (11.88) but the similarly nucleophilic cyanoborohydride (11.52) reacts slower under B–H insertion reaction conditions.

When the new scale and Li's³² scale are combined, a general reactivity profile of ligated boranes versus other carbenophiles begins to emerge. The relative reactivity of borane B–H insertion compared with C–H insertion is summarized as shown in **Table 7**.

Table 7. Relative rate of boranes toward B–H insertion

	Pyr- BH ₃	NHC- BH ₃ 5	Me ₃ N- BH ₃	[BH ₃ CN] ⁻	1,4- CHD	R ₃ P- BH ₃	THF
<i>k</i> _{rel}	2.5	1	0.33	0.18	0.08	0.06	0.01

1.2.1.3 Enantioselective NHC B-H Insertions with Donor/Acceptor Rhodium Carbenes

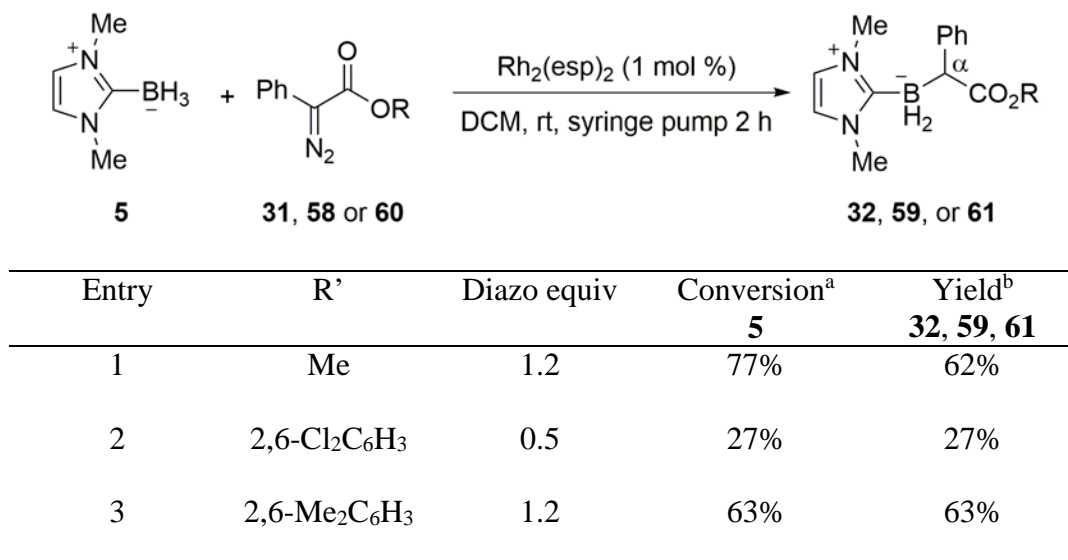
Davies and coworkers have demonstrated that the tetraproline Rh₂(DOSP)₄ exhibits exceptional stereocontrol during intermolecular C–H functionalization when used in conjunction with donor/acceptor stabilized carbenes.⁴⁷ When phenyl diazoesters are used as the donor/acceptor rhodium carbene for NHC-borane B–H insertions, the α -carbon stereocenter of the insertion product (labeled α in **Table 8**), from the donor/acceptor fragment, provides a suitable substrate to probe stereocontrol using various chiral rhodium(II) catalysts.

We first conducted the reaction between NHC-borane **5** and phenyl diazoacetate **31** to determine if insertion product **32** enantiomers can be resolved by chiral HPLC analysis. The racemic standard **32** was synthesized using Li's method for NHC-borane B–H insertion between NHC-borane **5** and 1.2 equiv of diazo compound **31** (**Table 9**, entry 1). After purification by flash chromatography, a 1 mg/1 mL solution of **32** was injected onto an (*S,S*)-Whelk-O1 column with a 30/70 mixture of isopropanol and hexanes as the eluent. UV detection at 231 nm showed the 50/50 ratio of enantiomers.

Two racemic standards with varying diazo ester substitution were also prepared (entries 2 and 3). Reaction of NHC-borane **5** (0.2 mmol) with 2,6-dichlorophenyl diazo **58** (0.5 equiv) gave 27% conversion and recovery of mono-insertion product **58** (t, –23.2 ppm, *J*_{BH} = 96 Hz). Similar conditions between NHC-borane **5** (0.2 mmol) and 2,6-dimethylphenyl diazo **60** (1.2 equiv) resulted in 63% conversion and recovery of mono-insertion product **61** (t, –23.0 ppm, *J*_{BH} = 91

Hz). The 30/70 isopropanol/hexanes HPLC protocol successfully resolved enantiomers of **59** and **61**.

Table 8. Synthesis of racemic standard NHC-borane insertion products



^[a] Estimated from ¹¹B NMR spectrum of crude reaction mixture; ^[b] Isolated yield after flash chromatography.

Next, we studied these reactions catalyzed by chiral rhodium(II) catalysts of three symmetry classes: *D*₂, *C*₂ and *C*₄ (**Figure 15**). Dr. Joseph Fox provided chiral dirhodium catalysts **65** and **66** that are structurally similar to Rh₂(PTTL)₃TPA **63**. We also varied reaction temperature and the diazo ester moiety (**Table 9**).

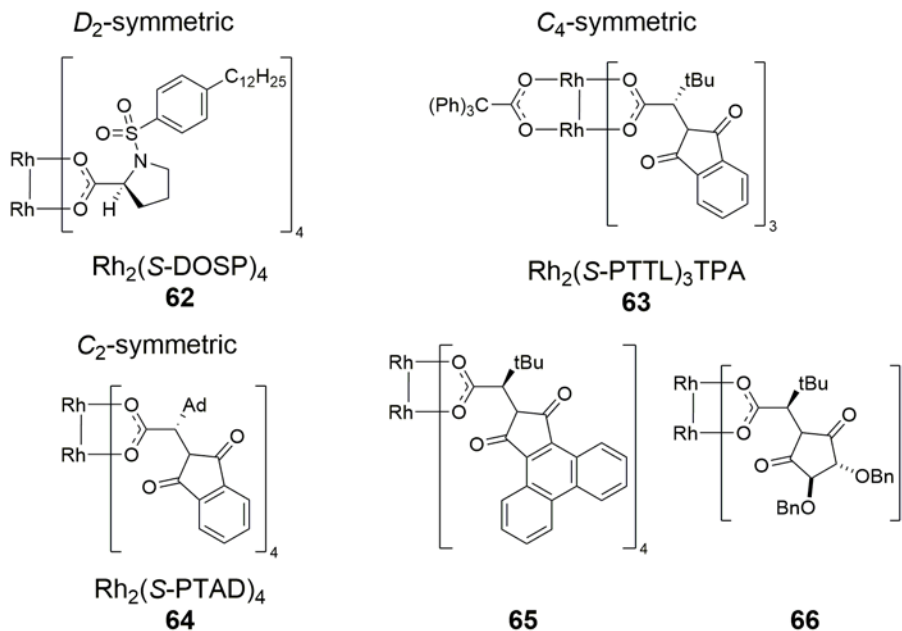
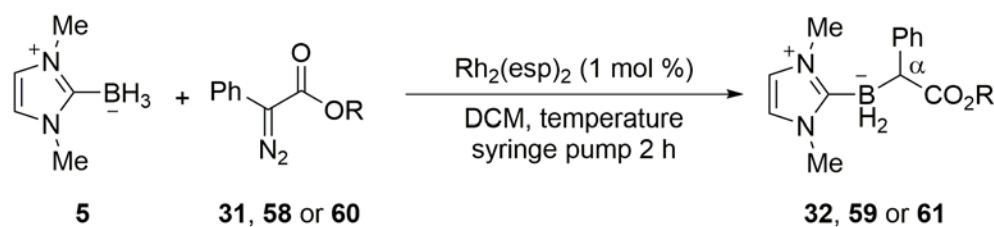


Figure 15. D_2 , C_2 and C_4 symmetric chiral Rh(II) catalysts

Screening NHC-borane **5** B–H insertion with $Rh_2(S-DOSP)_4$ and dichloro diazo compound **58** resulted in a 34/66 er (**Table 9**, entry 1). $Rh_2(PTAD)_4$ and dimethyl diazo **60**, when reacted under reflux conditions, resulted in the highest observed stereinduction during chiral rhodium(II) catalyst screening (70/30 er) (entry 2).

We next turned to Fox's C_4 -symmetric $Rh_2(PTTL)_3TPA$.⁵¹ Due to the low conversions in entries 1–2, dichloromethane was freshly distilled prior to reaction in entries 3–5, resulting in significantly higher observed conversion. The observed enantiomeric ratios with the C_2 -symmetric catalysts remained between 68/32 and 30/70 er.

After screening through three Rh(II) symmetry classes (D_2 , C_2 and C_4), high stereinduction was not apparent for any catalyst. Larger diazo ester moieties also did not dramatically increase enantioselectivity.

Table 9. Chiral rhodium(II) catalyst screening with NHC B–H insertion (α -carbon stereocenter)

Entry	R	Temperature (°C)	Rh(II) catalyst	Diazo equiv	Conversion ^a 5	er ^b
1	2,6-Cl ₂ C ₆ H ₃	20	(<i>S</i> -DOSP) ₄	1.2	33%	34/66
2	2,6-Me ₂ C ₆ H ₃	40	(<i>S</i> -PTAD) ₄	1.2	21%	70/30
3	Me	20	(PTTL) ₃ TPA	3.0	88%	30/70
4	Me	20	65	1.2	51%	68/32
5	Me	20	66	1.2	70%	68/32

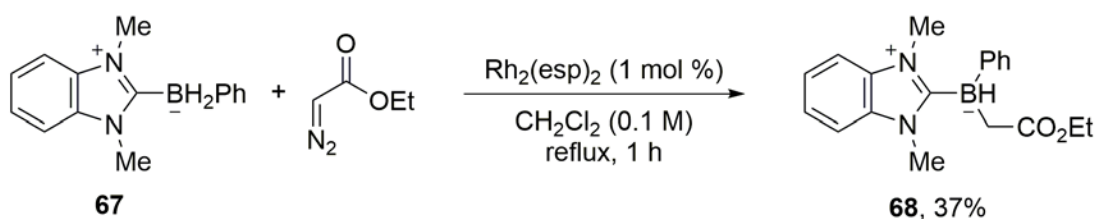
^[a] Estimated from ¹¹B NMR spectrum of crude reaction mixture; ^[b] Ratio of first and second eluting enantiomer.

1.2.1.4 Enantioselective NHC B–H Insertion with Rhodium Carbenes (Boron Stereocenter)

Through back-to-back B–H insertion reactions of two different diazo compounds with benzimidazole NHC-borane **8**, Li isolated a chiral NHC-borane whose only stereocenter is on boron.³² Currently, there is no enantioselective B–H insertion reaction at the boron stereocenter.

We turned to benzimidazole NHC borane **8** because extended conjugation should provide UV active products. Dr Tsuyoshi Taniguchi discovered that NHC-boranes can hydroborate benzyne to give aryl substituted NHC-boranes.⁵² The B–H insertion of ethyl diazoacetate of prochiral aryl NHC-borane **67** affords insertion product **68** with the lone stereocenter at boron.

The racemic standard of benzimidazole aryl borane **68** was synthesized by mixing aryl borane **70** (0.1 mmol) and Rh₂esp₂ (5 mol %) in CH₂Cl₂ (0.03 M). Then 1.2 equiv of ethyl diazoacetate, dissolved in CH₂Cl₂ (0.1 M), was added via syringe pump over 1 h under reflux conditions. An ¹¹B NMR spectrum of the crude reaction mixture showed 46% conversion to benzimidazole aryl **68** (−18.8 ppm, d, J_{BH} = 88 Hz). Purification by flash chromatography gave insertion product **68** as a white solid in 37% yield (**Scheme 11**). During purification, benzimidazole product **68** exhibited strong UV activity on the CombiFlash UV detector at 254 nm. This suggested that benzimidazole **68** was a suitably UV active substrate for HPLC analysis.

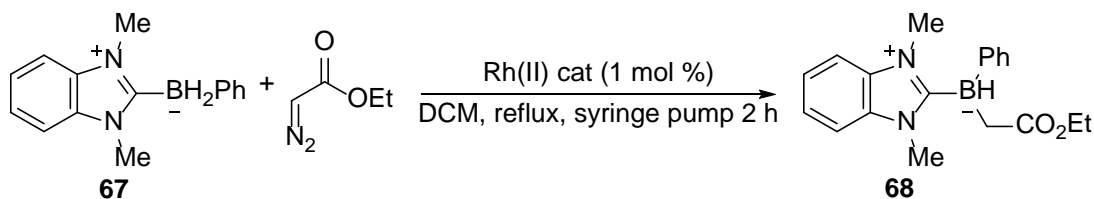


Scheme 11. B–H insertion of benzimidazole aryl borane **67**

Injection of racemic standard **68** onto the (*S,S*)-Whelk-O1 column using 30/70 isopropanol to hexanes, gave two peaks at 12.4 and 15.9 min in a 60/40 ratio. As the isopropanol content of the eluting solvent was increased, the two peaks emerged faster and their ratio approached but did not reach 50/50. At the 85/15 ratio of isopropanol to hexanes, we observed two peaks at 6.3 and 7.2 min in a 53/47 ratio. These unusual results suggest that **68** is somewhat unstable on the Whelk column. The slower eluting enantiomer always under-integrates. Further, as retention time increases, observed under-integration worsens. In practice, we decided that the observed 53/47 ratio was reliable enough for further experiments. We applied a 3% correction to these chromatograms through subtraction from the first eluting enantiomer.

With a method to resolve enantiomers of insertion product **68** in hand, we screened Fox's chiral rhodium(II) catalysts under the standard conditions (**Table 10**). Fox's Rh₂(PTTL)₃TPA produced a racemic mixture of enantiomers (entry 1), while catalyst **65** (entry 2), induced mild enantioselectivity (57/43 er).

Table 10. Chiral rhodium(II) catalyst screening with NHC B–H insertion (boron stereocenter)



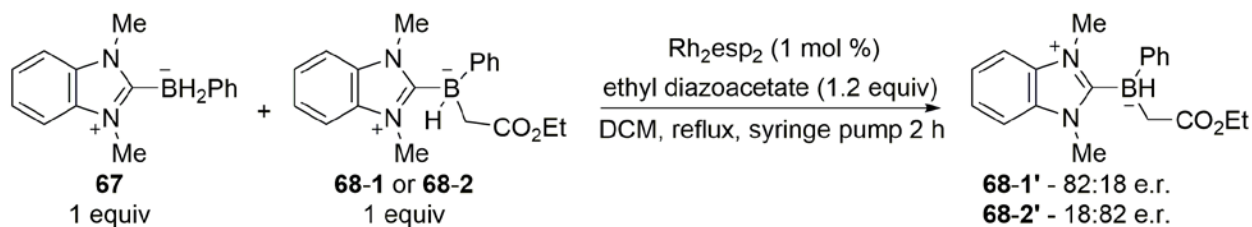
Entry	Rh(II) Catalyst	Diazo equiv	Conversion ^a	
			67	er 68
1	PTTL ₃ (TPA)	1.8	29%	50/50
2	65	1.8	50%	57/43

^[a] Estimated from ¹¹B NMR spectrum of crude reaction mixture.

Because we observed poor stereoinduction at the boron stereocenter, we became concerned that during the B–H insertion mechanism, the stereocenter racemizes during the borenium ion transition state. We hypothesized that if equal amounts of the starting benzimidazole **67** and a resolved enantiomer of insertion product **68** were resubjected to the B–H insertion conditions, the resultant chromatogram would maintain a stereo-enriched ratio of enantiomers if racemization at boron is not occurring. Alternatively, observing a 50/50 mixture of enantiomers would confirm racemization.

The racemate insertion product **68** was preparatively resolved on the chiral column to give both component enantiomers in high enantiopurity. Optical rotations were -156° (first

eluting enantiomer **68-1**) and $+154^\circ$ for **68-2** (both $c = 1$, CHCl_3). The first eluting enantiomer **68-1** (1.00 equiv, 0.02 mmol) was premixed with racemic aryl borane **67** (1.0 equiv), and then reacted with ethyl diazoacetate (1.2 equiv). After isolation the enantioenriched insertion product **68-1'** was injected onto chiral HPLC, resulting in an 82/18 er with the larger component being the previously resolved enantiomer **68-1** (Scheme 13). Repeating the reaction with **68-2'** gave 18/82 er in favor of the other enantiomer. In both experiments, 35% of **68-1'** / **68-2'** was attributed to converted **67** as observed in the ^{11}B NMR spectra. Thus, 17 to 18% of the minor enantiomer was expected in the mixture of **68-1'** / **68-2'** which matched both HPLC chromatograms. This suggests that the boron stereocenter of insertion product **68** does not racemize when subjected to the borenium ion transition state. Thus, the ers in Table 10 reflect poor stereoselectivity.



Scheme 12. Boron stereocenter racemization study with mixed starting material

The enantioselective B–H insertion products of phenyl diazo **31** with NHC-boranes and ethyl diazoacetate with aryl NHC-boranes can be reliably resolved by chiral HPLC analysis. Only moderate stereoselection has been observed with various chiral rhodium catalysts and the Zhou bisoxazoline ligand in the former system. $\text{Rh}_2(\text{S-PTAD})_4$ and $\text{Rh}_2(\text{S-PTTL})_3\text{TPA}$ have resulted in the highest observed stereoselection during chiral rhodium(II) catalyst screening

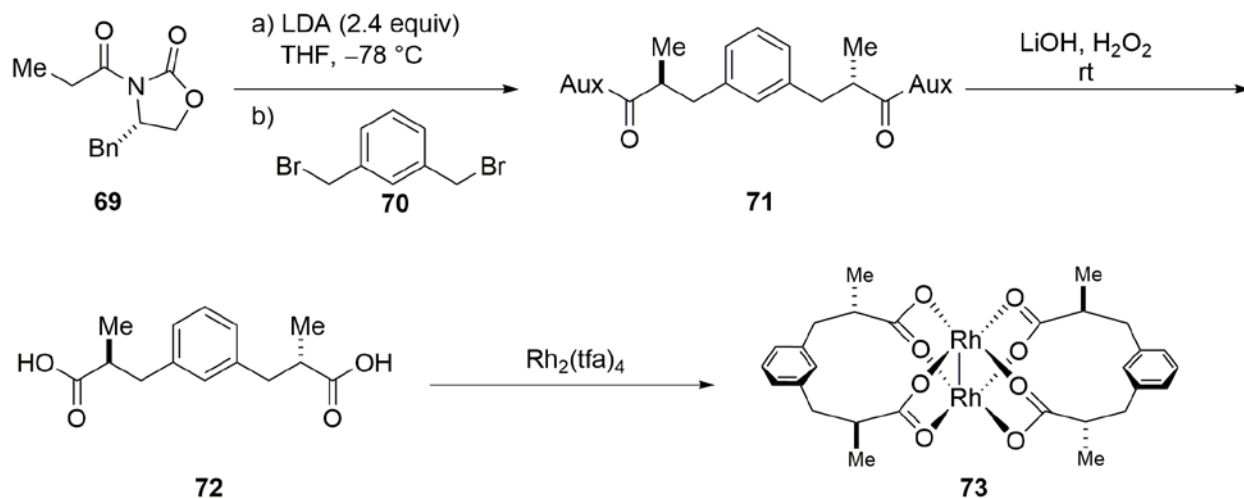
(70/30 and 30/70 er). Little to no stereoinduction has been observed at the NHC boron stereocenter during B–H insertion.

1.2.2 Exploring the Synthesis and Application of a Chiral Rh₂(esp)₂ Analog

Du Bois' Rh₂(esp)₂ is a robust catalyst in facilitating intramolecular²⁶ and intermolecular C–H amination⁴², alongside the synthesis of unprotected aziridines.⁵³ Additionally, Rh₂(esp)₂ typically provides the highest yields within Li's NHC-borane B–H insertion methodology.³² However, there are few examples of chiral Rh(II) catalysts incorporating a bridged dicarboxylate design other than Davies' second-generation prolinates²⁷ and Du Bois' bis-chelated sulfonamide dirhodium catalyst.⁴² We became interested if a chiral variant of Rh₂(esp)₂ could be synthesized and the unique reactive properties of Rh₂(esp)₂ would be retained while also facilitating stereoinduction in various transformations.

1.2.2.1 Synthesis of Methyl and Benzyl Chiral Rh₂(esp)₂ Analogs

We proposed that a proof-of-concept chiral analog of Rh₂(esp)₂ could be obtained through deletion of two methyl groups on the dicarboxylate ligand. Synthesis of the C₂-symmetric dicarboxylic acid **72** could be achieved through double alkylation of 1,3-bis(bromomethyl)benzene **70** with propionyloxazolidinone **69**, followed by hydrolysis.⁵⁴ Subsequent complexation of **72** with Rh₂(tfa)₄ would afford chiral Rh₂(esp)₂ **73** (**Scheme 13**).

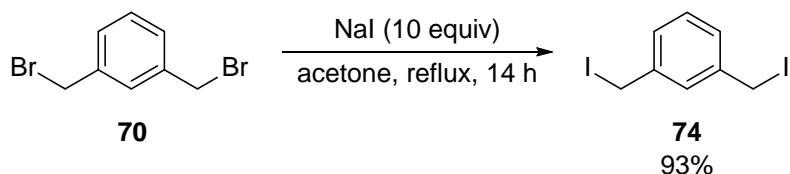


Scheme 13. Proposed synthetic pathway to a chiral Rh₂(esp)₂ analog

Moving forward with the bisbromobenzene double alkylation, reaction progress of the treatment of propionyloxazolidinone **69** (1.00 mmol, 2.2 equiv) with LDA (1.10 mmol, 2.4 equiv) followed by reaction with bis(bromomethyl)benzene **70** (1.0 equiv) was monitored by ¹H NMR spectra of the crude reaction mixture. Only several unidentified side-products were observed. In a second double alkylation experiment, using NaHMDS (1.10 mmol, 2.4 equiv) gave an inseparable mixture of monoalkylated bisbromo benzene and propionyloxazolidinone **69**.

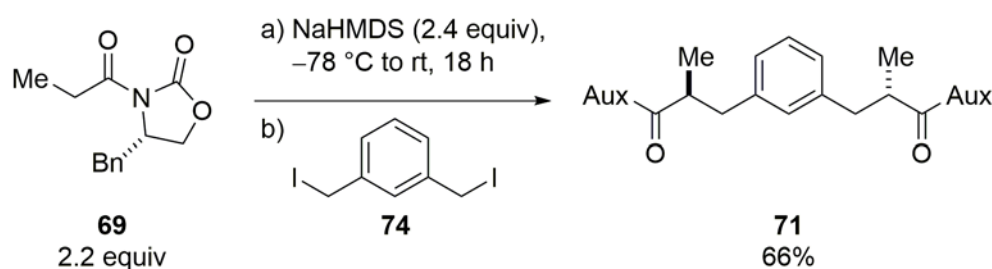
The partial alkylation of bis(bromomethyl)benzene **70** when using NaHMDS prompted us to convert the bromide to an iodide via a Finkelstein reaction (**Scheme 14**).⁵⁵ Bis(bromomethyl)benzene **70** (4.20 mmol, 1.0 equiv) was mixed with sodium iodide (42.0 mmol, 10 equiv) in acetone (0.04 M). The mixture was heated to reflux in absence of light for 14 h. The reaction progress was monitored by a ¹³C NMR spectrum of the crude product mixture. The bromobenzyl carbon resonance (42.0 ppm) disappeared in favor of the iodobenzyl resonance

(4.8 ppm), signifying complete conversion to bis(iodomethyl)benzene **74**. Aqueous workup and evaporation gave bis(iodomethyl)benzene **74** as a light yellow solid in 93% yield.



Scheme 14. Finkelstein reaction of bis(bromoethyl)benzene **70**

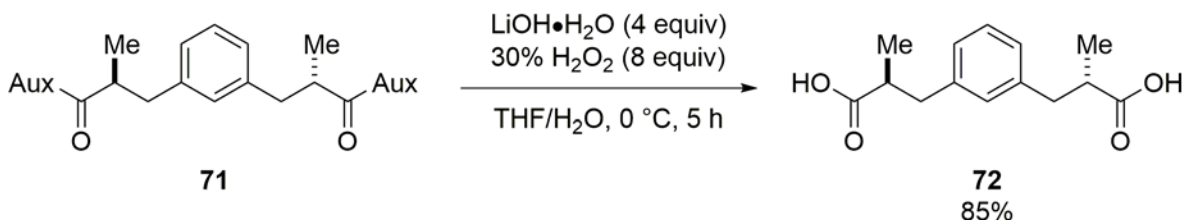
Next, propionyloxazolidinone **72** (7.80 mmol, 2.2 equiv) was deprotonated with NaHMDS (8.51 mmol, 2.4 equiv) (**Scheme 15**). Reaction of the *in situ* enolate with freshly prepared bis(iodomethyl)benzene **74** (3.55 mmol, 1.0 equiv) resulted in observing bis alkylated product **71** in the ¹H NMR spectrum of the crude product mixture. After aqueous workup and flash chromatography purification, we recovered bis alkylated product **71** in 66% yield as a light yellow, foamy solid.



Scheme 15. Double alkylation of bis(iodomethyl)benzene **74**

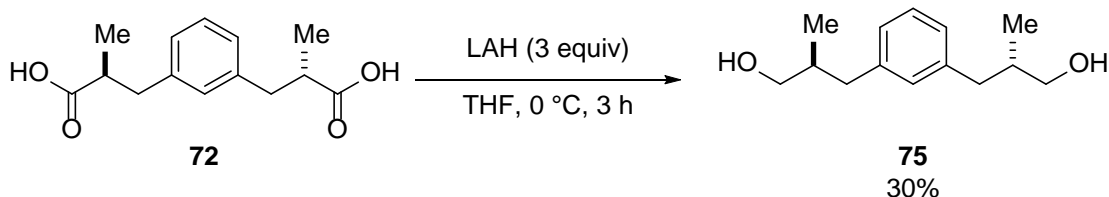
Next, the hydrolysis of bis alkylated benzene **71** (0.17 mmol, 1.0 equiv) proceeded by addition of 30% H₂O₂ (1.34 mmol, 7.8 equiv) and lithium hydroxide monohydrate (0.69 mmol, 4.0 equiv) to a solution of **71** in THF (0.03 M) and stirred at 0 °C for 5 h (**Scheme 16**). The

reaction mixture was acidified with 6 M HCl and after aqueous workup we obtained methyl diacid **72** as a colorless oil in 85% yield.



Scheme 16. Hydrolysis of bis-alkylated benzene **71**

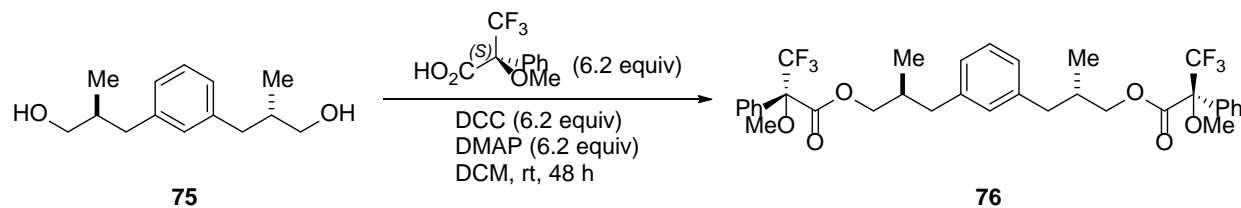
We next used a Mosher acid to determine the enantiopurity of diacid **72**.⁵⁶ Methyl diacid **72** (0.20 mmol, 1.0 equiv) was dissolved in THF (0.13 M) and LAH was added (0.60 mmol, 3.0 equiv) at 0 °C for 3 h (**Scheme 17**). Aqueous workup and flash chromatography purification afforded dialcohol **75** in 30% yield as a colorless oil.



Scheme 17. Reduction of diacid **72** with LAH

Dialcohol **75** (0.06 mmol, 1.0 equiv) was first dissolved in DCM (0.03 M). Then (*S*)-MTPA (0.36 mmol, 6.2 equiv), DCC (0.36 mmol), and DMAP (0.36 mmol, 6.2 equiv) were added sequentially at rt (**Scheme 18**).⁵⁶ After stirring for 45 h, full consumption of dialcohol **75** was confirmed by TLC and ¹H NMR spectra analysis. Following flash chromatography purification, we recovered methyl ester **76** in addition with co-eluted DCC and (*S*)-MTPA. A

single diastereomer (*dr* >98:2) was present in ¹H, ¹³C, and ¹⁹F NMR spectra of the methyl ester **76**, signifying that bis alkylated **71** did not undergo epimerization during hydrolysis.



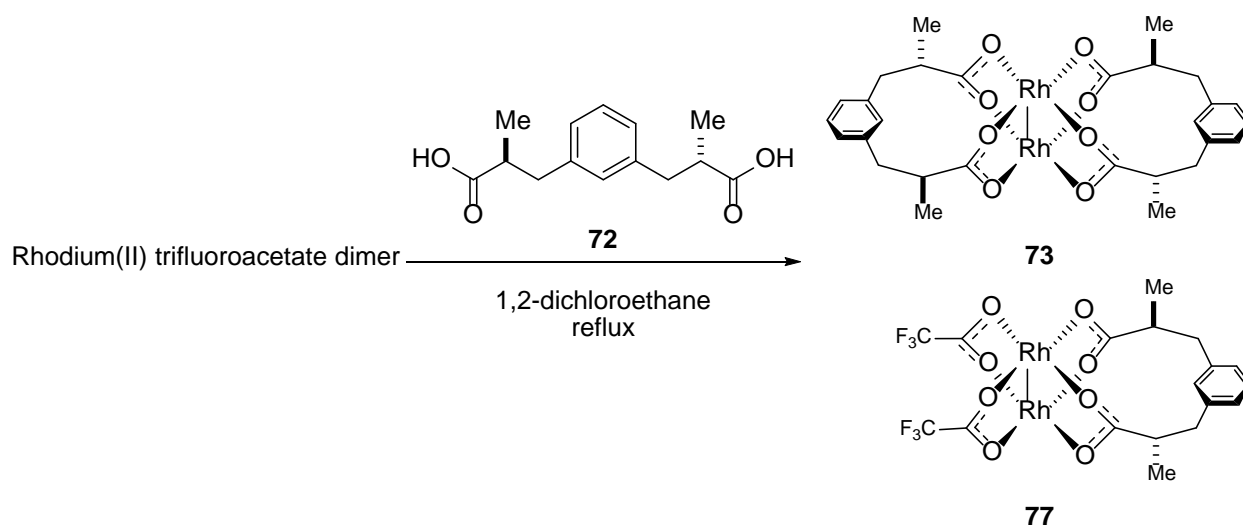
Scheme 18. Mosher's acid esterification of **75**

With the enantiopure methyl diacid **72** ligand in hand, we first attempted complexation of **72** with Rh₂(tfa)₄ through replication of Du Bois' original complexation procedure for Rh₂(esp)₂.²⁶ Rh₂(tfa)₄ (0.07 mmol, 1.0 equiv) was dissolved in 1,2-DCE (0.30 M) and the solution was heated to 125 °C in a pressure tube. Diacid **72** (1 M in 1,2-DCE) was added in 0.2 equiv portions every 20 min. This was continued for the first 1.0 equiv of diacid **72**, and then the reaction was heated at 125 °C for 5 h. The process was repeated for the addition of another 1.0 equiv of diacid **72** (**Table 11**, entry 1).

A significant amount of green precipitate crashed out of solution during the second 5 h heating period. We then filtered off the precipitate and concentrated the remaining crude product mixture. Flash column chromatography of the crude product mixture resulted in the elution of three green bands. The first eluted band was Rh₂(tfa)₄, the second band was monochelated methyl rhodium **77**, and the third band was an uncharacterized oligomeric rhodium species. The monochelated rhodium **77** could be differentiated from the fully chelated rhodium **73** by a strong signal at -76.9 ppm in the ¹⁹F NMR spectrum elucidating the presence of a TFA ligand.

In a second pressure tube experiment, reaction concentration was reduced to 0.07 M and methyl diacid **72** equiv was doubled. Again, a green precipitate crashed out of solution during heating. The three eluted bands from flash column chromatography were characterized in order of elution as monochelated rhodium **77**, the target bischelated methyl rhodium **73** in 10% yield, and an oligomeric rhodium species. The fully complexed bischelated methyl rhodium **73** was characterized by ^1H , ^{13}C and ^{19}F NMR spectra and mass spectroscopy analysis. Unlike monochelated rhodium **77**, there are no signals in the ^{19}F NMR spectrum of bischelated methyl rhodium **73**.

Table 11. Complexation of methyl diacid **72** with $\text{Rh}_2(\text{tfa})_4$



Entry	Concentration (M)	Temperature (°C)	Diacid 72 equiv	Yield ^a (73)	Comment
1	0.30	125	2.0	0%	3 bands (starting material, monochelated 77 , oligomer) + polymer
2	0.07	125	4.0	10%	3 bands (monochelated 77 , 73 , oligomer) + polymer
3	0.02	84	2.0	26%	100% conv (74% 77 , 26% 73)
4	0.02	84	3.0	34%	100% conv (66% 77 , 34% 73)

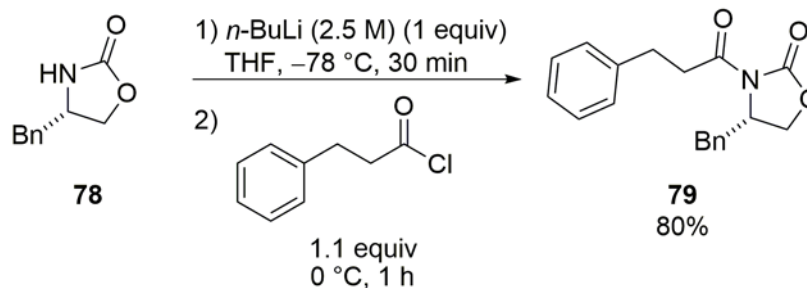
^[a] Isolated yield after flash chromatography.

Transitioning from a pressure tube to a round bottom flask, the reaction concentration was further reduced from 0.07 M to 0.02 M (entry 3). Diacid **72** (2.0 equiv) was added in 0.5 equiv portions in 1 h intervals and the reaction mixture was refluxed at 84 °C for 5 h. Following flash chromatography, a 74/26 ratio of monochelated methyl rhodium **77** and bischelated methyl rhodium **73** was obtained. Treatment of recovered monochelated methyl rhodium **77** (0.03 mmol, 1.0 equiv) with diacid (0.03 mmol, 1.0 equiv) over 12 h at 84 °C gave a 56/44 ratio of mono to bischelated product. The combined yield over the two experiments was 59%. Repeating the conditions of entry 3 with 3.0 equiv of diacid **72** gave a 66/34 ratio of mono to bischelated product (entry 4).

Taber reported that *m*-benzenedipropionic acid **14** only gave monochelated product **15** upon complexation with Rh₂(tfa)₄.²⁴ Du Bois reasoned that Rh₂(esp)₂'s geminal methyl groups provided needed conformational rigidity for diacid preorganization prior to complexation.²⁶ The ability for a singly methylated diacid to fully complex with Rh₂(tfa)₄ was not known. Ultimately, we obtained a 59% yield of bischelated methyl rhodium **73** using 3.0 equiv of diacid **72**, which is comparable to Du Bois' 64% yield using 2.0 equiv of diacid in his Rh₂(esp)₂ synthesis. In general, the complexation of methyl diacid **72** with Rh₂(tfa)₄ requires low concentration to avoid formation of polymeric by-products. The highest yielding pathway that also conserves both synthetically useful chiral diacid **72** and monochelated rhodium **77** is to treat Rh₂(tfa)₄ with 2.0 equiv of diacid, and then resubject recovered monochelated rhodium **77** with 1.0 equiv of diacid.

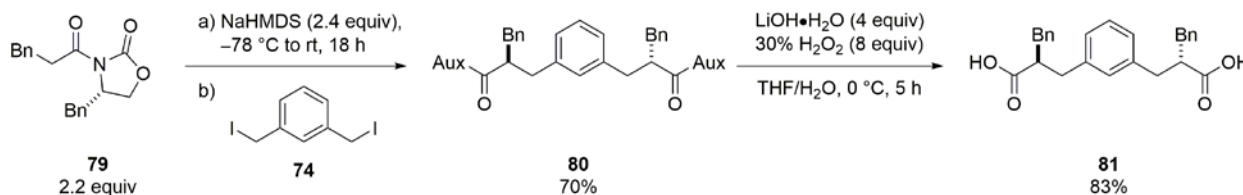
With a viable synthetic route to a chiral analog of Rh₂(esp)₂ accessible, we increased the steric bulk of the chiral ligand through substituting methyl with a benzyl group. The necessary hydrocinnamoyloxazolidinone **78** chiral auxiliary was synthesized through deprotonation of (*S*)-

benzyl oxazolidinone **78** (1.00 mmol, 1.0 equiv) with *n*-BuLi (1.00 mmol, 1.0 equiv) at $-78\text{ }^{\circ}\text{C}$ followed by treatment with hydrocinnamoyl chloride (1.10 mmol, 1.1 equiv) at $0\text{ }^{\circ}\text{C}$ (**Scheme 19**). Flash chromatography purification gave hydrocinnamoyloxazolidinone **79** in 80% yield as a white solid.



Scheme 19. Synthesis of hydrocinnamoyloxazolidinone **79**

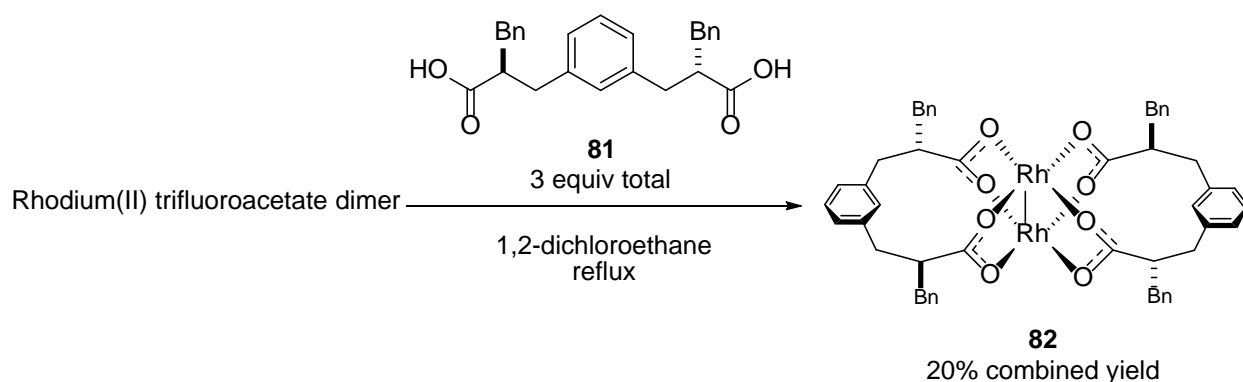
Reaction of hydrocinnamoyloxazolidinone **79** (8.70 mmol) under the chiral diacid standard conditions gave bis alkylated benzene **80** in 70% yield and benzyl diacid **81** in 83% yield (**Scheme 20**).



Scheme 20. Synthesis of chiral benzyl diacid **81**

Replicating the high yielding, two-reaction method that gave bis-chelated rhodium **73**, we reacted Rh₂(tfa)₄ (0.29 mmol, 1.0 equiv) with benzyl diacid **81** (0.58 mmol, 2.0 equiv) in a round bottom flask for 18 h under reflux (**Scheme 21**). After flash column chromatography, we

obtained 87% monochelated and 13% bischelated benzyl rhodium **82**. Subjecting the monochelated benzyl rhodium dimer (0.29 mmol, 1.0 equiv) to the same conditions with 1.0 equiv of diacid **81**, resulted in reappearance of the insoluble polymeric species. A 93/7 mixture of mono to bischelated benzyl rhodium **82** was recovered after flash column chromatography. The combined yield between the two reactions was 20%, a decrease from 59% of the methyl diacid **72** complexation.



Scheme 21. Complexation of benzyl diacid **81** with $\text{Rh}_2(\text{tfa})_2$

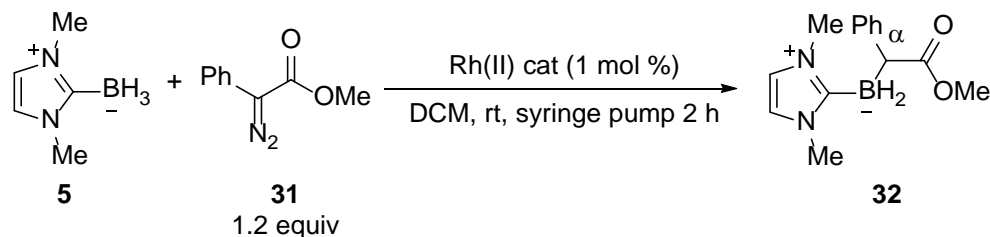
1.2.2.2 Application of Methyl and Benzyl Chiral $\text{Rh}_2(\text{esp})_2$ Analogs

Preliminary organic transformations that we have explored with chiral $\text{Rh}_2(\text{esp})_2$ analogs include B–H insertion of a NHC-borane and a styrene cyclopropanation.

First, we applied chiral methyl dirhodium **73** to our NHC-borane B–H insertion system in Section 1.2.1.3. Reaction between NHC-borane **5** and phenyl diazo **31** resulted in 9% conversion to insertion product **32** and 69/31 er (**Table 12**, entry 1). Chiral benzyl dirhodium **82** gave a mildly higher yield of 19% but er decreased to 63/37 (entry 2). Li had observed that the reactivity of $\text{Rh}_2(\text{DOSP})_4$ and $\text{Rh}_2(\text{PTAD})_4$ decreased dramatically in contrast to $\text{Rh}_2(\text{esp})_2$ when solvent was not freshly distilled. Presumably the chiral Rh(II) catalysts are not stable to oxygen

dissolved in solvent. Unfortunately, based on product conversions our chiral Rh₂(esp)₂ analogs do not retain the same stability of achiral Rh₂(esp)₂.

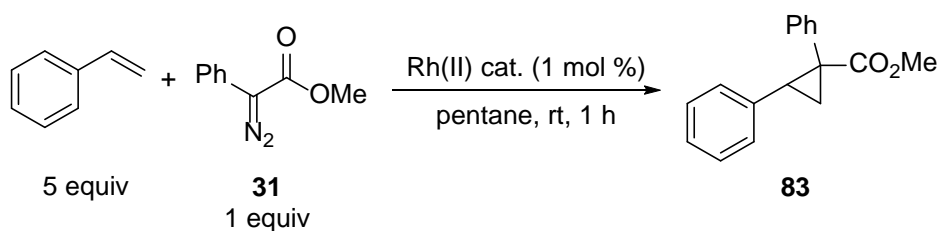
Table 12. Enantioselective NHC B–H insertion (α -carbon stereocenter)



Entry	Catalyst	Conversion ^a	er
		5	32
1	73	9%	69/31
2	82	19%	63/37

^[a] Estimated from ¹¹B NMR spectrum of crude reaction mixture.

We next screened the cyclopropanation of styrene. In the control reaction, styrene (1.00 mmol, 5.0 equiv) and Rh₂(DOSP)₄ (1 mol%) was dissolved in pentane (0.5 M). Then diazo **31** was added over 1 h by syringe pump. Flash chromatography yielded 60% **83** as a white solid in 93/7 er (**Table 13**, entry 1).⁵⁷ Chiral methyl dirhodium **73** (entry 2) gave 45% **83** in 59/41 er, while chiral benzyl dirhodium **82** (entry 3) resulted in increased yield (51%) and er (73/27).

Table 13. Enantioselective styrene cyclopropanation

Entry	Catalyst	Yield ^a	er
1	(<i>S</i> -DOSP) ₄	60%	93/7
2	73	45%	59/41
3	82	51%	73/27

^[a] Isolated yield by flash chromatography.

1.3 CONCLUSIONS

Li's dirhodium catalyzed intermolecular B–H insertion methodology was expanded beyond NHC-boranes to amine-, phosphine-, pyridine-boranes and a cyanoborohydride salt. The boryl adducts are stable in regards to purification by flash chromatography and long term storage. A reactivity profile of ligated borane adducts toward B–H insertion reaction conditions was developed. All of the substrates are either comparable to or more reactive than 1,4-cyclohexadiene. The range of reactivity between the most reactive pyridine-borane and the least reactive phosphine-borane is a factor of approximately 40.

Continued efforts to solve the enantioselective B–H insertion of NHC-boranes, at either a carbon or boron stereocenter, have yielded low to moderate enantiomeric ratios. Various chiral dirhodium catalysts have resulted in only mild stereinduction.

Chiral $\text{Rh}_2(\text{esp})_2$ analogs have been successfully isolated and characterized, although additional project goals may include i) obtain an X-ray crystal structure to elucidate the symmetry class of this group of catalysts, and ii) find a signature enantioselective reaction and continue optimizing the catalyst alkyl substituents.

2.0 RADICAL AND THERMAL REACTIONS OF N-HETEROCYCLIC CARBENE BORANES WITH ELECTROPHILIC DIAZO COMPOUNDS

2.1 INTRODUCTION

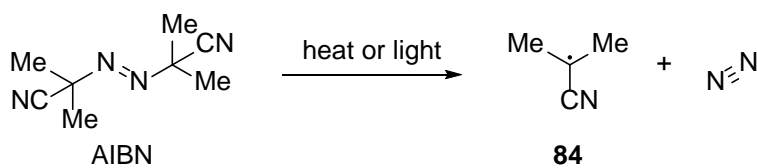
2.1.1 Radical Initiators

The homolytic cleavage of a covalent bond often initiates a radical chain reaction. The conditions required to achieve homolysis can be harsh. Accordingly, compounds that can be used to initiate radical chain processes under mild conditions are valued in modern radical synthesis. Radical initiators are compounds that are susceptible to homolytic cleavage at lower temperatures. Radical initiators contain relatively weak covalent bonds that are usually cleaved through thermolysis or photolysis.⁵⁸ Common radical initiators include azo compounds, organic peroxides, and hyponitrites.

2.1.1.1 Azo initiators

Azo compounds are a class of radical initiator consisting of R–N=N–R functional groups. The R–N bond (usually a C–N bond) can be cleaved with either heat or light as an initiation step. Two of the most commonly used azo initiators are 2,2'-azobis(2-methylpropionitrile) (AIBN) and 2,2'-azobis(2,4-dimethylvaleronitrile) (V-65).⁵⁹ The temperature of the reaction can have a dramatic effect on which azo initiator should be used in a particular reaction. For example, AIBN

has a half-life of 10 h in toluene at 65 °C, whereas V-65 has a half-life of 10 h in toluene at 51 °C. Thermolysis or photolysis of AIBN causes homolysis of the C–N bonds to generate two 2-cyanoprop-2-yl radicals **84** and dinitrogen (**Scheme 22**).⁶⁰ Typically, 40% of the newly formed cyanopropyl radicals **84** recombine before escaping the surrounding solvent cage while the remaining 60% escape for initiation.⁵⁸



Scheme 22. Radical fragmentation of AIBN

2.1.2 Radical chemistry of NHC-boranes

Boranes (BR₃) react with oxygen, nitrogen, sulfur, and halogen radicals (X•) to expel carbon radicals (C•).⁶¹ Triethylboron and related boranes are common initiators and reagents in synthetic radical chemistry.⁶² In contrast, homolytic substitution reactions with ligated boranes instead generate boron-centered radicals. The relatively weak NHC-borane B–H bond can be cleaved to give an NHC-boryl radical (NHC–BH₂•).⁶³ Evidence for NHC–BH₂• formation has been obtained from observation of NHC-boryl radicals by EPR spectroscopy⁶⁴ and by UV-visible spectroscopy during laser flash photolysis (LFP).⁶⁵

Since the discovery of NHC-boryl radicals in 2008, their synthetic application has included addition to xanthates⁶⁶ and electron-poor alkenes,⁶⁷ bromine and iodine abstraction from alkyl⁶⁸ and aryl halides,⁸ and reaction with disulfides to yield boryl sulfide and boryl

thioamide products.⁶⁹ Recently, Kawamoto and Curran observed that NHC boryl radicals can abstract cyano groups from dinitriles to give NHC-boryl cyanides.⁷⁰

2.1.3 Radical chemistry of diazo compounds

The synthetic utility of diazo compounds is broad, including common reaction classes such as carbenoid heteroatom insertions and 1,3-dipolar cycloadditions.⁷¹ However, radical reactions of diazo compounds have received less attention in comparison. There are a few examples of triorganotin radical addition to diazo compounds to afford carbon-centered radicals after dinitrogen extrusion. Kim investigated the use of α -diazocarbonyl compounds as radical precursors.⁷² Reaction of diazomalonate **85** with Bu_3SnH and AIBN in refluxing benzene- d_6 initially generates diazo tin radical intermediate **86** or **87** (Figure 16). Subsequent loss of dinitrogen gives tin malonate radical **88**, and Kim isolated reduced tin malonate **89**. Soon after, Karady and coworkers demonstrated that benzophenone radicals, derived from the corresponding diazonium salts, undergo rapid 1,5-hydrogen transfer to give an equilibrium of three aryl radical intermediates.⁷³ Subsequent Pschorr cyclization affords several fluorenone isomer products.

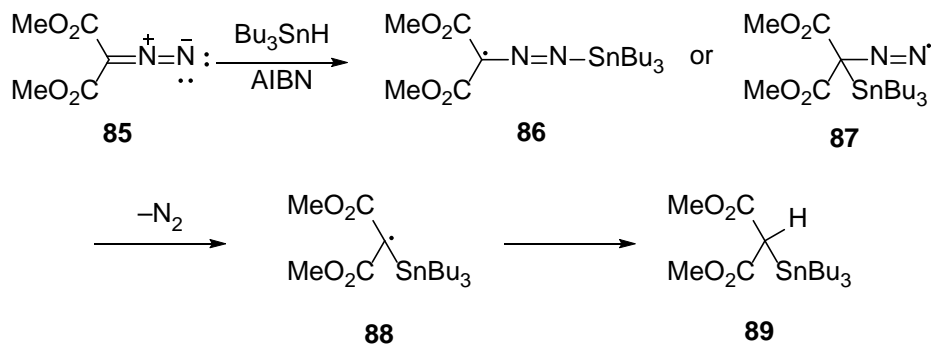


Figure 16. Tributyltin hydride radical addition to diazomalonate **85**

Given that NHC-boranes and diazo compounds are both subject to radical reactions, we hypothesized that when an NHC-borane is reacted under conditions of radical generation with a diazo compound, an α -NHC-boryl insertion product would be formed upon boryl radical addition to a diazo compound and subsequent dinitrogen extrusion.

2.2 RESULTS AND DISCUSSION

2.2.1 Reaction of NHC-boranes and Diazo Compounds with Radical Initiators

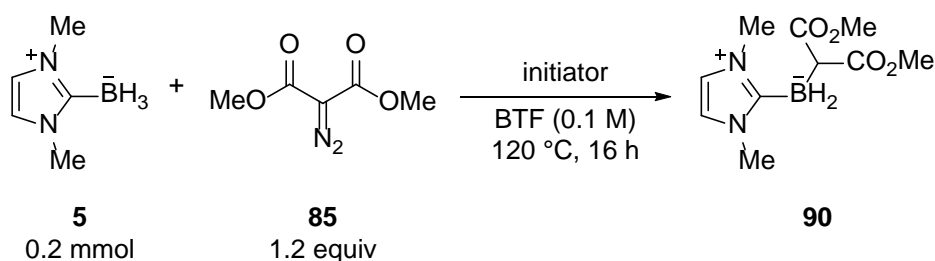
The initial aim was to study the reaction between NHC-boranes and diazo compounds with radical initiators. We chose dimethyl diazomalonate **85** as the diazo substrate because it undergoes radical chemistry when reacted with azo-bis-isobutyronitrile (AIBN) and tributyltin hydride.⁷² **Table 14** summarizes the results of reaction between 1,3-dimethylimidazol-2-ylidene borane **5** and diazo malonate **85** with di-*tert*-butyl peroxide (DTBP) and AIBN radical initiators.

In an initial control experiment (entry 1), a mixture of diazomalonate **85** and NHC-borane **5** in benzotrifluoride (C₆H₅CF₃, abbreviated BTF) was heated to 120 °C. The ¹¹B NMR spectrum of the crude reaction mixture showed 19% conversion of the starting material. A trace amount (5%) of product with the same shift as B–H insertion compound **90** (–25.4 ppm) was formed.

In a standard reaction (entry 2), 0.2 mmol NHC-borane **5**, 1.2 equiv diazomalonate **85**, and 20 mol % DTBP was loaded into a pressure tube with 2 mL BTF. The reaction mixture was then heated to 120 °C. Over 16 h, the reaction mixture turned a yellow-orange color. The ¹¹B NMR spectrum of the crude reaction mixture showed 39% conversion of NHC-borane **5**. We observed a small triplet (2%) in the ¹¹B NMR region where expected B–H insertion product **90**

appears (−25.4 ppm). Additional resonances were observed at −19.1 ppm (15%), −13.3 ppm (4%) and 18.0 ppm (18%). The 18.0 ppm resonance can be attributed to boric acid-like decomposition products. Increasing the DTBP loading to 100 mol % (entry 3) resulted in higher conversion (84%) but also a larger amount of decomposition products.

Table 14. Radical initiator screening



Entry	Initiator	Conversion ^a	Product 90 ^a	Other ¹¹ B NMR resonances (NMR Yield) ^a
1	None	19%	5%	−13.4 (5%), 18.0 (9%)
2	DTBP (20 mol %)	39%	2%	−19.1 (15%), −13.3 (4%), 18.0 (18%)
3	DTBP (100 mol %)	84%	0%	−23.7 (3%), −19.1 (12%), −13.3 (5%), 18.0 (64%)
4	AIBN (20 mol %)	14%	0%	−17.6 (14%)
5	AIBN (100 mol %)	85% ^b	0%	−19.0 (15%), −17.7 (60%), 18.0 (10%)

^[a] Estimated from ¹¹B NMR spectrum of crude reaction mixture; ^[b] 22% isolated yield of NHC-boryl hydrazone **91**.

When 20% AIBN was used in place of DTBP (entry 4), we observed formation of a broad resonance at −17.6 ppm. After increasing AIBN loading to a stoichiometric amount (entry 5), the resonance was resolved as a pair of triplets with major boron-containing components at −17.7 (60%) and −19.0 ppm (15%). Following flash chromatography purification of the reaction

mixture, we concentrated a polar fraction at 100% EtOAc. The isolated yellow solid (22% yield, mp 113–116 °C) exhibited a broad triplet at –17.9 ppm in the ^{11}B NMR spectrum (CDCl_3). The product exhibited a methyl proton resonance (1.71 ppm) and cyano carbon resonance (118.8 ppm) in the ^1H and ^{13}C NMR spectra, showing that it possessed a 2-cyanoprop-2-yl group. It also exhibited the vinyl NHC-borane resonances and two methyl esters. This suggests that the structure is **91**. In addition, the product was identified as *N*-boryl-*N*-2-(2-cyanopropyl) hydrazone **91** based on HRMS data.

Crystals of the compound were grown from a dichloromethane/pentane solution, and the X-ray structure was solved by Dr. Steve Geib. As shown in **Figure 17**, both the 2-cyanopropyl group and the NHC-boryl group are bonded to the same nitrogen atom of the hydrazone **91**.

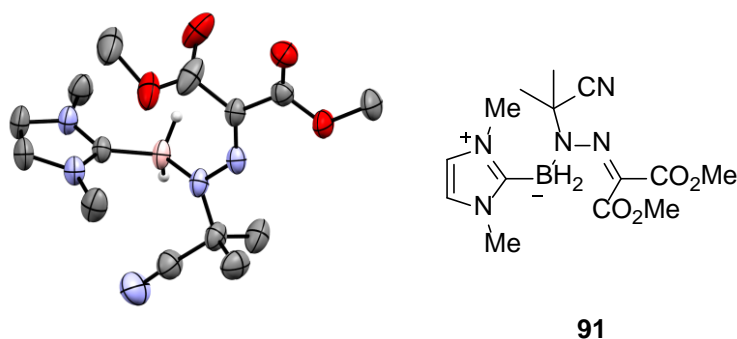
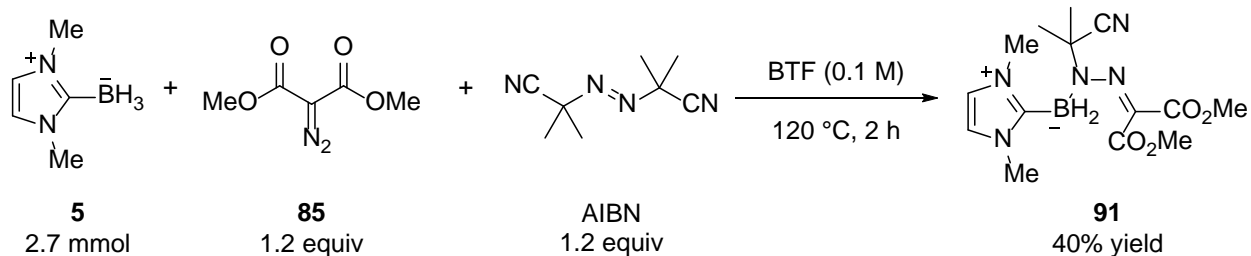


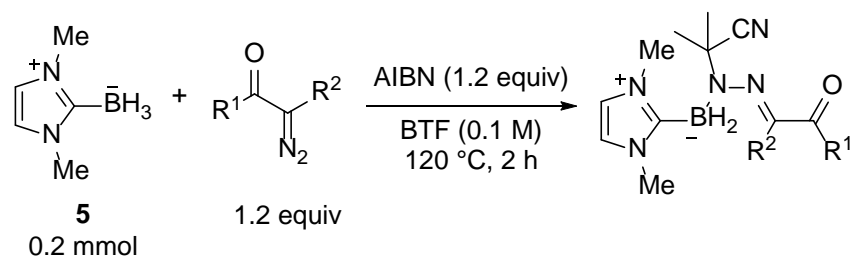
Figure 17. X-ray structure of NHC-boryl hydrazone **91**

We next increased the amounts of AIBN and NHC-borane **5** in an effort to improve the isolated yield of NHC-hydrazone **91**. A BTF solution of 1 equiv of NHC-borane **5**, 1.2 equiv of diazomalonate **85**, and 1.2 equiv of AIBN was heated in a pressure tube at 120 °C for 2 h (**Scheme 23**). About 95% of NHC-borane **5** was consumed, and NHC-boryl hydrazone **91** was isolated as a yellow solid in 40% yield by standard flash chromatography (100% EtOAc).⁷⁴



Scheme 23. Preparative scale synthesis of NHC-boryl hydrazone **91**

We briefly surveyed this reaction with four other diazo compounds, and the results are summarized in **Table 15**. Reaction of NHC-borane **5** and AIBN (1.2 equiv) with ethyl diazoacetate (entry 1) provided the corresponding NHC-boryl hydrazone in 7% yield as a yellow solid after isolation by flash chromatography. In separate reactions with ethyl diazo ketone, phenyl diazoacetate **31**, and benzyl diazoacetate (entries 2–4), we observed moderate formation (40–60%) of presumed NHC-boryl hydrazone products (peaks at –17 ppm region in ^{11}B NMR spectrum), but the target hydrazone products were not isolated after flash chromatography purification.

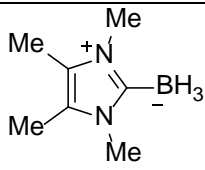
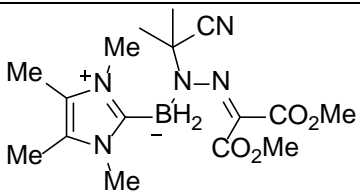
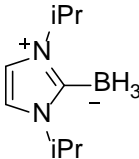
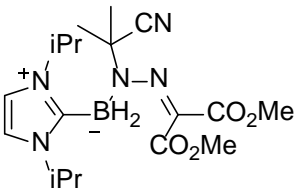
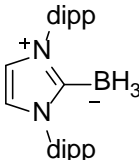
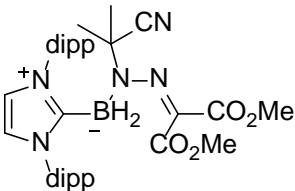
Table 15. Screening substituted diazo compounds

Entry	R ¹	R ²	NMR yield ^a	Isolated Yield
1	H	OEt	20%	7%
2	H	Et	43%	0%
3	Ph	OMe	66%	0%
4	Bn	OMe	43%	0%

^[a] Estimated from ¹¹B NMR spectrum of crude reaction mixture.

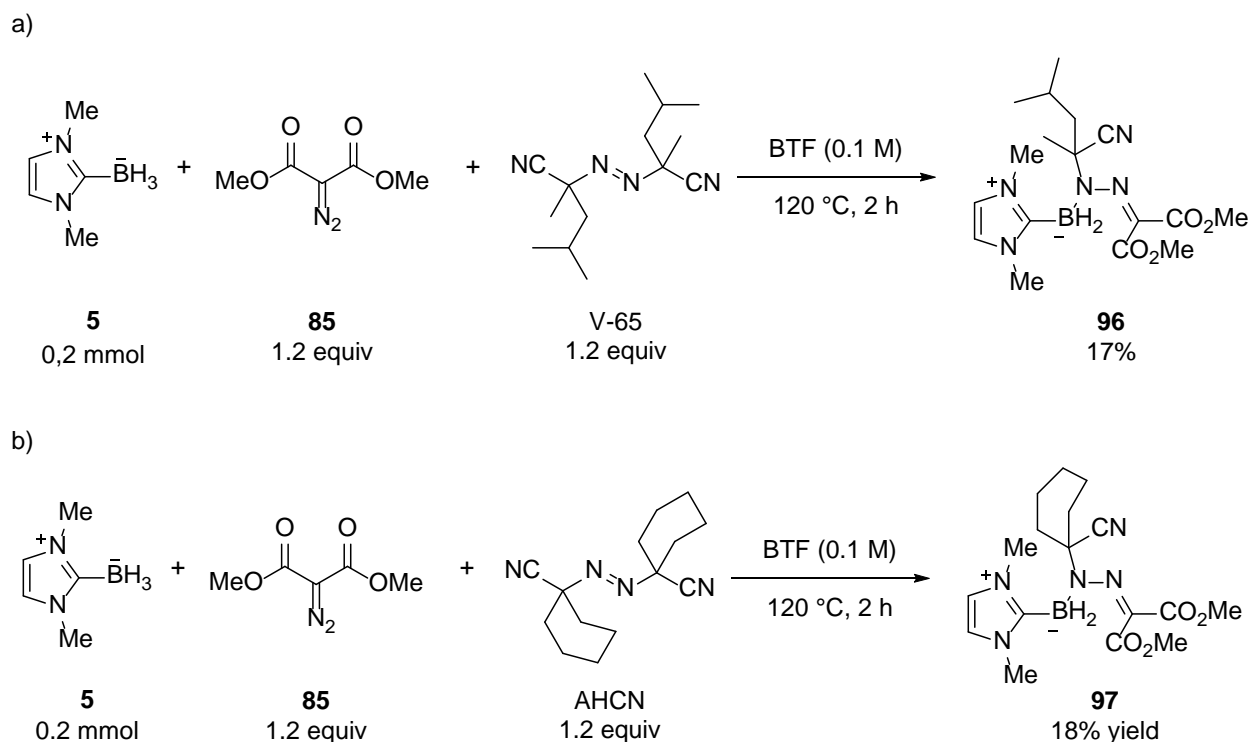
Next, we screened three different NHC-boranes. **Table 16** summarizes the results. Reactions of diazomalonate **85** and AIBN with 1,2,4,5-tetramethylimidazol-2-ylidene borane **92** and 1,3-diisopropylimidazol-2-ylidene borane **7** provided the corresponding NHC-boryl hydrazones **93** (33%) and **94** (43%) after isolation by flash chromatography (entries 1 and 2). Both products were stable yellow solids. When hindered dipp-NHC-borane **6** was used (entry 3), low conversion was observed and target hydrazone **95** was not isolated after flash chromatography.

Table 16. Screening differentially substituted NHC-boranes

Entry	NHC-borane	NMR Yield ^a	Isolated Yield
1	 <p>92</p>	92%	 <p>93</p>
2	 <p>7</p>	78%	 <p>94</p>
3	 <p>6</p>	11%	 <p>95</p>
			0%

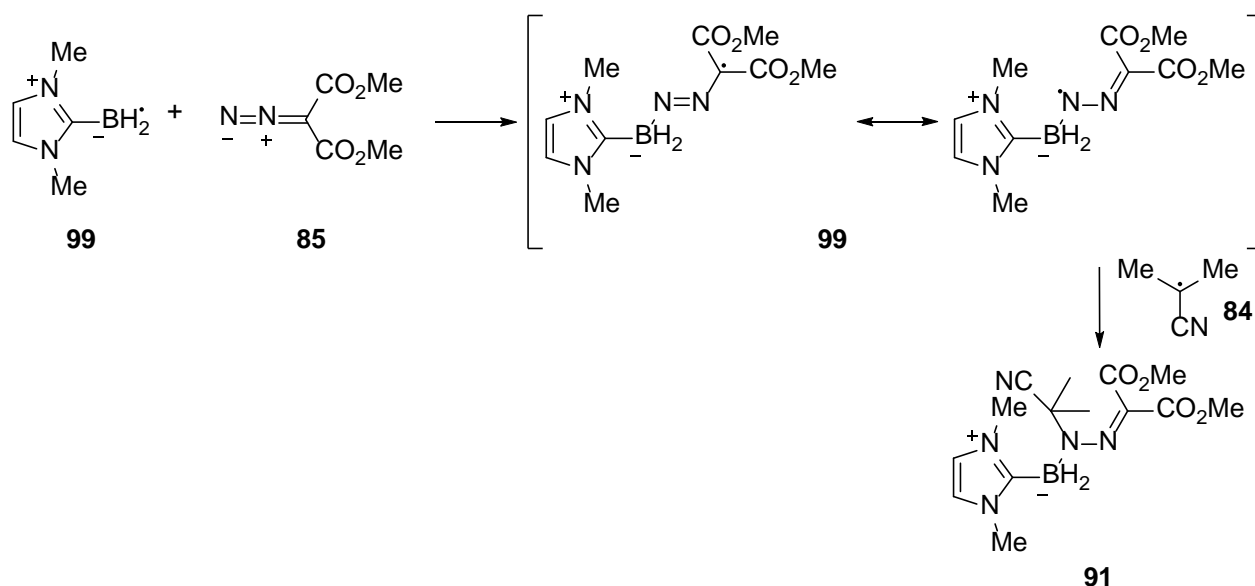
^[a] Estimated from ¹¹B NMR spectrum of crude reaction mixture.

Finally, we tested two other thermally labile azo initiators, 2,2'-azobis[2,4-dimethylvaleronitrile] (V-65) and 1,1'-azobis(cyclohexanecarbonitrile) (ACHN). Reactions of **85** and 1,3-dimethylimidazol-2-ylidene borane **5** with V-65 (**Scheme 24a**) and AHCN (**Scheme 24b**) produced the yellow hydrazones **96** (17%) and **97** (18%) after flash chromatography.



Scheme 24. Synthesis of azo initiator NHC-boryl hydrazone analogs

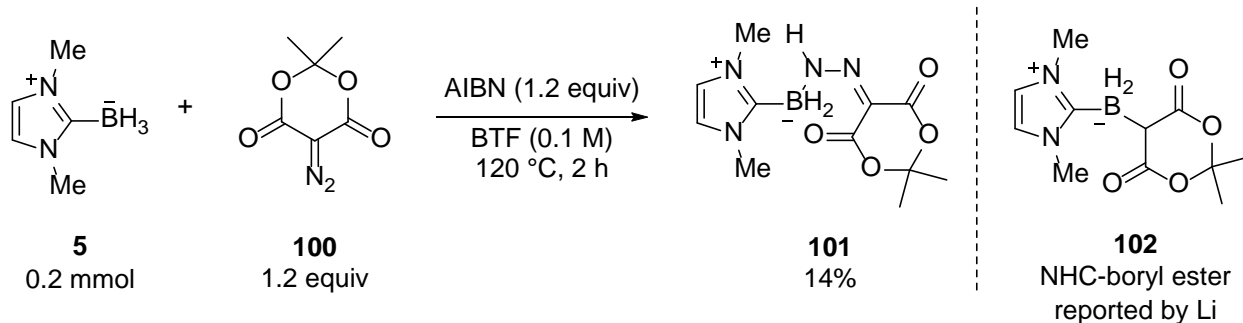
The moderate isolated yields of the NHC-boryl hydrazone compounds (17–43%) support the notion that these products are formed in nonchain radical reactions from radical recombinations. The NHC-boryl radical (NHC–BH₂• **98**) is presumably formed by reaction of a 2-propanenitrile radical with the starting borane. Then **98** adds to the diazomalonate **85** to boryl hydrazone radical intermediate **99** (**Scheme 25**). Finally, termination with 2-propanenitrile radical **84** produces NHC-boryl hydrazone **91**. Some radical reactions of diazo compounds occur on the carbon atom (which typically leads to loss of N₂), but these new reactions evidently occur on the terminal nitrogen atom. In short, we hypothesized that boryl radicals would add to the carbon atom of diazomalonate, but instead, they added to the nitrogen atom.



Scheme 25. Proposed mechanism for the formation of NHC-boryl hydrazone **91**

2.2.2 Synthesis of an NHC-boryl Hydrazone via 1,1-Hydroboration

Diester 5-diazo-2,2-dimethyl-1,3-dioxane-4,6-dione **100** is a cyclic analog of diazo malonate **85**. The reaction conditions established in **Scheme 23** were repeated by heating of NHC-borane **5**, AIBN, and diazo dione **100** in BTF. The ^{11}B NMR spectrum of the crude reaction mixture showed the complete consumption of NHC-borane **5** and appearance of a boron–nitrogen resonance at -19.3 ppm. However, the polar product **101** isolated after flash column chromatography (100% EtOAc in 14% yield) incorporated the diazo dione and the NHC-borane, but had no 2-cyanopropyl group (**Scheme 26**).



Scheme 26. Reaction of NHC-borane **5** with diazo dione **100** (AIBN present)

The structure of **101** was evident from the similarities of its spectra to the spectra of the previous *N*-boryl hydrazone adduct **91**. For example, **101** exhibited a triplet at -18.7 ppm in its ^{11}B NMR spectrum, which is very close to the resonance of **91**. A broad singlet at -12.42 ppm in the ^1H NMR spectrum of **101** was attributed to an N–H proton. We also considered that the product could be structure **102**, a compound previously reported by Li.³² However, compound **101** has a plane of symmetry perpendicular to that of **102**, and the observed simplification in both ^1H and ^{13}C NMR spectra (the geminal methyl groups are equivalent) is consistent with **101**, not **102**. The HRMS confirmed that dinitrogen was not eliminated in **101**, which is a direct adduct of **5** and **100**. Like **91**, *N*-boryl hydrazone **101** is a stable yellow solid. Crystals were grown from dichloromethane/pentane, mp 193 – 195 °C, and the X-ray structure shown in **Figure 18** confirmed the structure assignment.

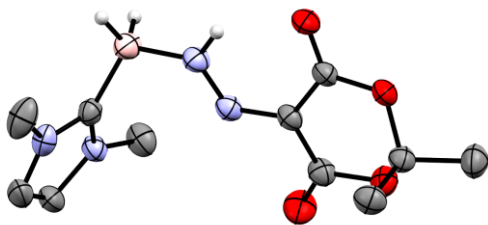
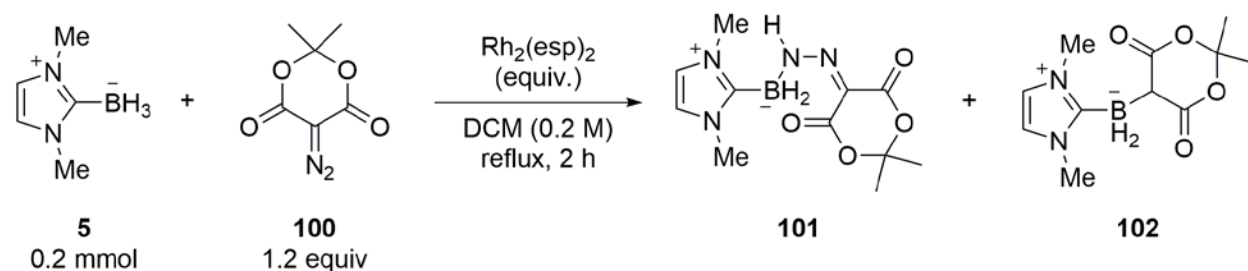


Figure 18. Structure of NHC-boryl hydrazone **101**

Product **101** has the same spectra as those reported for the Rh-catalyzed insertion product **102** by Dr. Xiben Li (**Scheme 26**, right).³² These results mean the assigned structure of **102** reported in 2013 as the product of the Rh-catalyzed reaction of **5** and **100** is incorrect.

To verify this, we conducted three reactions of **5** and **100**, with $\text{Rh}_2(\text{esp})_2$ (**Table 17**). The first reaction mimicked Li's conditions. The diazo dione **100** was added via syringe pump into a refluxing solution of NHC-borane **5** and 1% $\text{Rh}_2(\text{esp})_2$ in DCM (entry 1). After 4 h, ^{11}B NMR analysis showed clean formation of **101**, with no evidence of **102**. Next, we changed the reaction vessel from a round-bottom flask to a pressure tube. NHC-borane **5**, dione diazo **100**, and 1% $\text{Rh}_2(\text{esp})_2$ were mixed in DCM and the mixture was heated at 60 °C for 2 h (entry 2). The ^{11}B NMR spectrum of the crude reaction mixture exhibited two peaks: the boryl hydrazone product (41%) and a new triplet at -24.0 ppm (56%). This chemical shift is consistent with Li's other α -NHC boryl ester products, so the new product is probably **102**. Finally, we repeated the pressure tube experiment with increased $\text{Rh}_2(\text{esp})_2$ loading (5 mol %). After 2 h, all starting NHC-borane **5** was consumed and the α -NHC B-C adduct **102** was the only product (entry 3). Unfortunately, the NHC boryl dione ester product was not isolated by column chromatography purification. These results show that the thermal 1,1-hydroboration of **5** and **100** can supersede the Rh-catalyzed insertion reaction under reaction conditions with low catalyst loadings.

Table 17. Formation of NHC B–N and B–C adducts with dione diazo **100**

Entry	$\text{Rh}_2(\text{esp})_2$ (Equivalents)	Method	NMR yield 101 ^a	NMR yield 102 ^a
1	0.01	Syringe pump	100%	0%
2	0.01	Pressure tube	41%	59%
3	0.05	Pressure tube	0%	100%

^[a] Estimated from ¹¹B NMR spectrum of crude reaction mixture.

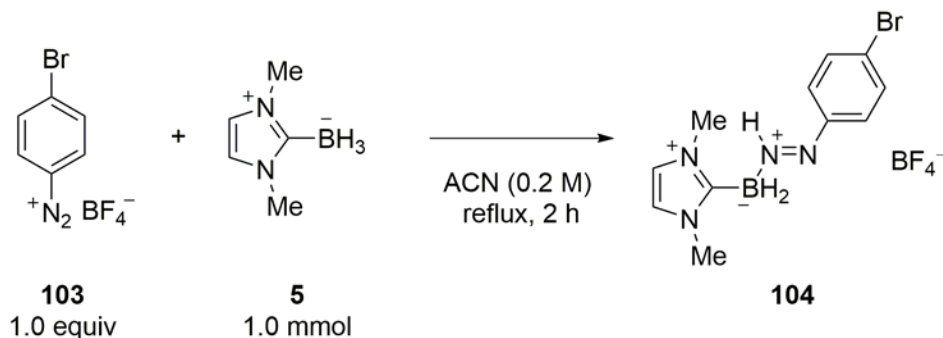
With the new spectra and information, we then checked the data for the 14 structures of the Rh-catalyzed B–H insertion products in the original 2013 report.³² However, only the structure in the reaction of 5-diazo-2,2-dimethyl-1,3-dioxane-4,6-dione **100** is incorrect as indicated by its ¹¹B NMR resonance (–18.7 ppm). All the other products are correctly assigned as α -NHC-boryl esters, with ¹¹B NMR shifts at approximately –25 ppm, resulting from B–H insertion reactions of diazocarbonyl compounds.

A control reaction in BTF without the AIBN initiator provided boryl hydrazone **101** in 18% yield; a mild improvement compared to the 14% yield from the original reaction with AIBN (**Scheme 27**). Furthermore, heating **5** and **100** (1.2 equiv) in CH_2Cl_2 for 20 h afforded target boryl hydrazone **101** in much improved yield (61%). This result is consistent with the NHC boryl hydrazone **101** yield originally reported by Li.

2.2.3 Thermal Reaction of an NHC-borane with a Diazonium Salt

Finally, we speculated that more electrophilic diazo compounds could also lead to 1,1-hydroboration products. If 1,1-hydroboration occurs between NHC-borane **5** and a diazonium salt, then the product will be a NHC boryl diazene salt ($[\text{NHC-BH}_2\text{NH}=\text{NAr}]^+$).⁷⁶

Slow addition of 4-bromobenzenediazonium tetrafluoroborate **103** in acetonitrile to a refluxing solution of NHC-borane **5** in acetonitrile (**Scheme 28**) gave a crude product that showed three substantial resonances in the ^{11}B NMR spectrum. There is a sharp peak at -0.48 ppm from BF_4^- , a quartet at 0.42 ppm from 1,3-dimethylimidazol-2-ylidene trifluoroborane (NHC- BF_3), and a very broad peak between -18.0 and -22.0 ppm. We anticipated that the third signal corresponded to the proposed boryl diazene product **104**.



Scheme 28. Pathway to proposed NHC boryl diazene **104**

Purification of the crude reaction mixture by flash chromatography with 100% EtOAc yielded a light yellow oil. The residue exhibited two resonances in the ^{11}B NMR spectrum: a sharp BF_4^- singlet at -1.31 ppm and a broad very broad peak at -20.0 ppm (**Figure 20**). The NHC- BF_3 impurity was removed by column chromatography purification. The BF_4^- peak integrated 2:1 with the B-N peak, hinting that the isolated residue was a dicationic salt.

Furthermore, two broad singlets at 5.55 ppm (1H) and 6.58 ppm (2H) in the ^1H NMR spectrum (**Figure 21**) disappeared upon addition of D_2O to the NMR sample. We attributed these two resonances to exchangeable protons on the diazene nitrogen atoms. Finally, the residue exhibited satisfactory HRMS data (m/z [M^+] calculated for $\text{C}_{11}\text{H}_{17}\text{N}_4\text{BBr}$ 295.0724, found 295.0718).

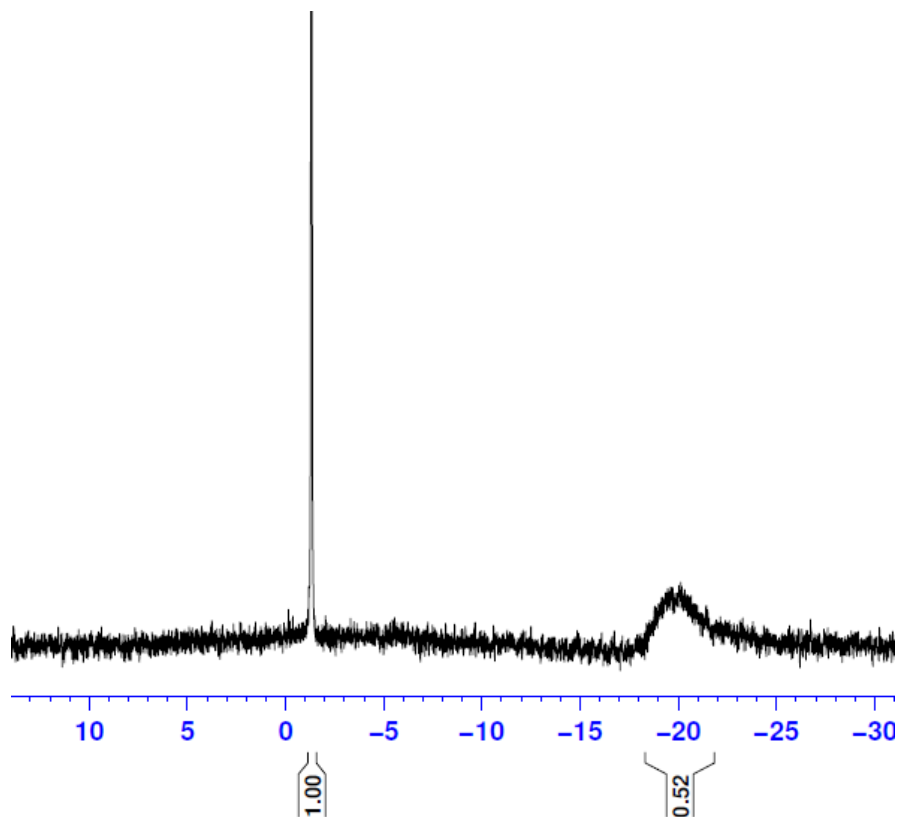


Figure 20. ^{11}B NMR spectra of isolated boryl salt intermediate

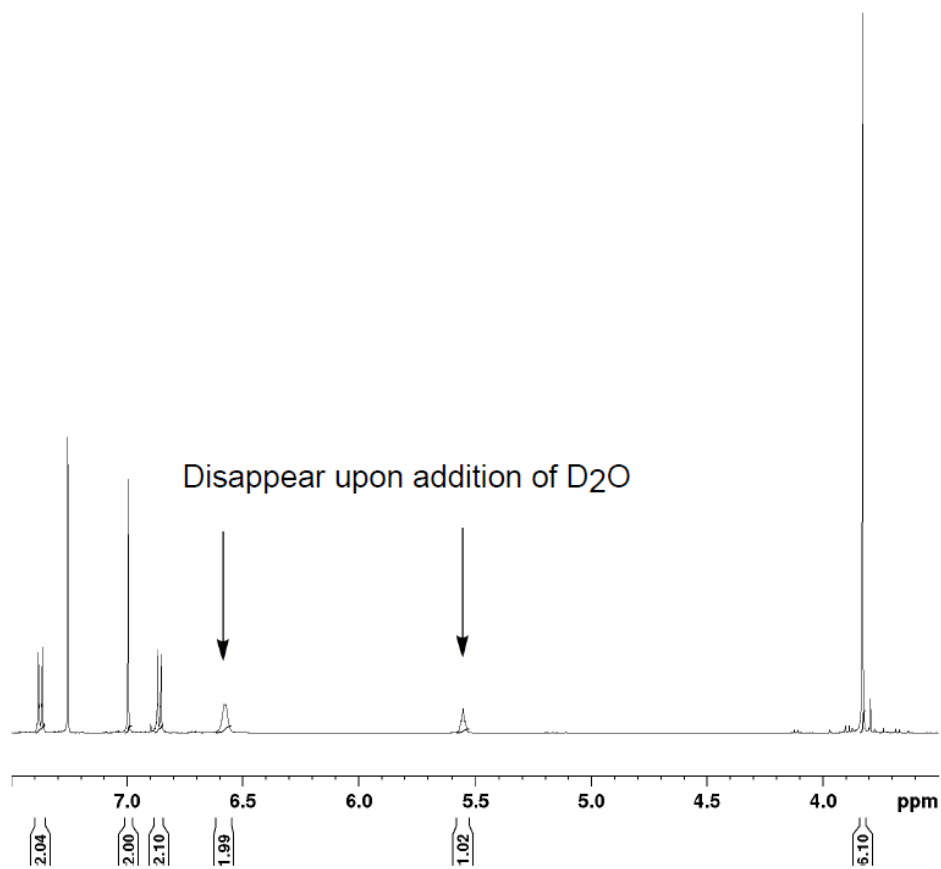


Figure 21. ¹H NMR spectrum of isolated boryl salt intermediate

Based on this spectroscopic data, we propose that the structure of the isolated dicationic salt to be either NHC diazaborirane **105** or NHC boryl hydrazine **106** (**Figure 22**).

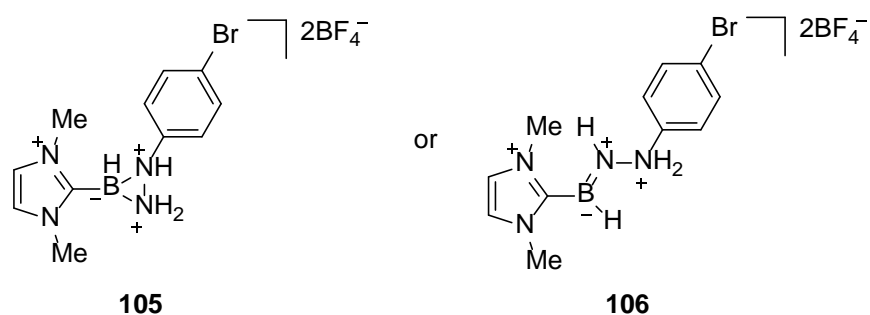
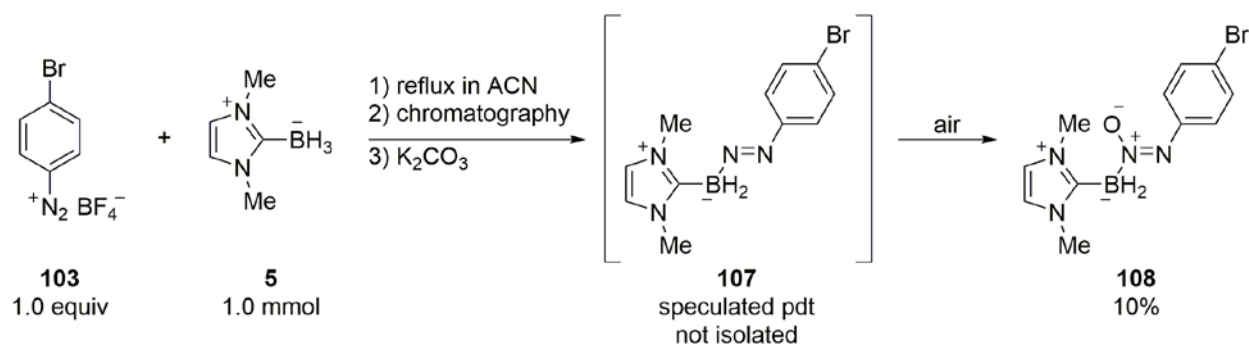


Figure 22. Proposed structures of dicationic boryl salt intermediate

To access target boryl diazene product **104** from the salt intermediate, we proposed that addition of a base would deprotonate the nitrogen atoms of either **105** or **106**. Treatment of the NHC-boryl salt intermediate in CH_2Cl_2 with aqueous K_2CO_3 resulted in the solution immediately turning a dark maroon color. A triplet at -12.0 ppm ($J = 95$ Hz) was now present the crude ^{11}B NMR spectrum (**Scheme 29**). The combined organic layers were dried over Na_2SO_4 and concentrated to give a purple solid in 10% yield (mp $67\text{--}70$ °C). This was identified by its spectra as the diazene *N*-oxide **108**. The added oxygen atom of the *N*-oxide was evident from HRMS. Presumably **108** arises from air oxidation of NHC-boryl diazene **107**.



Scheme 29. Synthesis of NHC boryl diazene oxide **108**

Crystals of **108** were grown from THF/pentane, and the structure was confirmed by X-ray crystallography, as shown in **Figure 23**. Compound **108** is the first example of an NHC-borane bonded to an azoxy group.

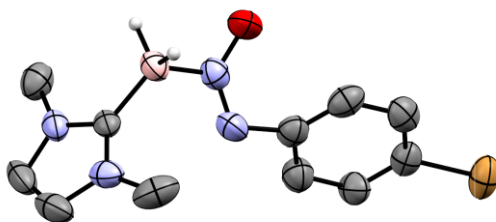


Figure 23. X-ray structure of NHC boryl diazene oxide **108**

2.3 CONCLUSIONS

In summary, thermal reactions of NHC-boranes with several diazo compounds and one diazonium salt have been studied. We originally hypothesized that NHC-boryl radicals would add to the carbon atom of diazo compounds to afford α -NHC-boryl esters after dinitrogen extrusion. Chain reactions between NHC-boranes and diazo compounds are not initiated by azo initiators such as AIBN. Instead, *N*-(cyanoalkyl)-*N*-borylhydrazones are formed, probably from nonchain radical reactions. Contrary to our hypothesis, NHC-boryl radicals add to the terminal nitrogen atom of diazo compounds. This type of reaction does not occur with diazo 2,2-dimethyl-1,3-dioxane-4,6-dione. Instead, this reacts directly with the NHC-borane (no azo initiator needed) to give an *N*-boryl hydrazone product arising formally from 1,1-hydroboration. A similar thermal reaction of an NHC-borane with a diazonium salt gave an intermediate that upon neutralization underwent air oxidation to provide an NHC-boryl azoxy compound.

The structures of three key compounds (one of each structural type) have been confirmed by X-ray crystallography. The new classes of products join a small list of stable NHC-boryl compounds with boron–nitrogen bonds, including several boryl azides and triazoles,⁷⁷ and a boryl isonitrile and nitro.⁷⁸

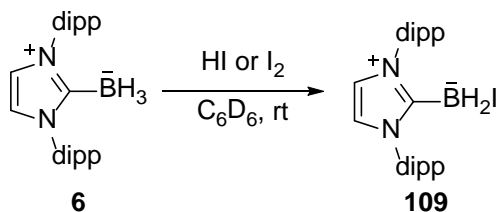
3.0 BORENIUM ION EQUIVALENT CATALYZED B–H INSERTION REACTIONS OF N-HETEROCYCLIC CARBENE BORANES

3.1 INTRODUCTION

3.1.1 Borenum ion chemistry of NHC-boranes

The activation of amine- and phosphine-boranes generates a borenum ion (LB-BH_2^+) or a borenum ion equivalent.⁷⁹ These equivalents include charged complexes of borenum ions with solvent or another Lewis base, or neutral, covalent LB–borane complexes with a good leaving group ($\text{LB-BH}_2\text{X}$ where X is the leaving group). Borenum ions and borenum ion equivalents are reactive in hydroboration.⁸⁰

Like amine- and phosphine-boranes, NHC-boranes react with strong acids and various electrophiles to give electrophilic substitution products (**Scheme 30**).⁷⁷ For example, the reaction of dipp-NHC-borane **6** and 1 equiv of HI or 0.5 equiv of I_2 gave the mono-substituted product dipp-NHC– BH_2I **109**.



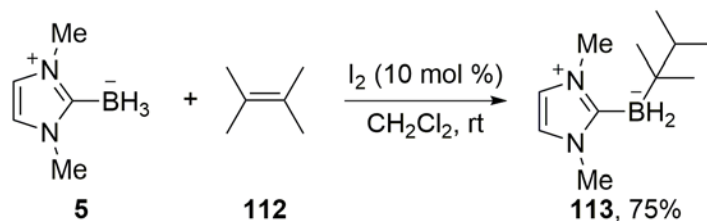
Scheme 30. Electrophilic halogenation of NHC-borane **6**

Although boron bears a formal negative charge in NHC-boranes, nucleophilic substitutions on a boron atom with a good leaving group can be achieved. For example, substitution of electrophilic NHC-boryl iodide **109** with sodium azide or cyanide provided boryl azide **110** or boryl cyanide **111** (**Scheme 31**).⁷⁷



Scheme 31. Nucleophilic substitutions of NHC-boryl iodide **109** with NaN₃ or NaCN

Pan and Curran demonstrated that NHC-boranes activated with 10 mol % diiodine can hydroborate alkenes.⁸¹ For example, reaction of NHC-borane **5** with 10% I₂ followed by addition of 2,3-dimethyl-2-butene **112** gave the hexyl NHC-borane **113** in 75% yield (**Scheme 32**).



Scheme 32. Hydroboration of 2,3-dimethyl-2-butene by NHC-borane **5**

3.2 RESULTS AND DISCUSSION

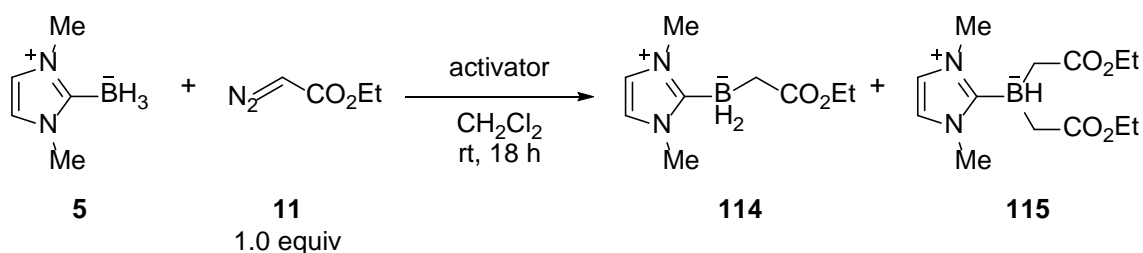
Diazoesters can function as nucleophiles on carbon in the absence of metal catalysts.⁸²⁻⁸³ For example, ethyl diazoacetate is a weak neutral nucleophile with an *N* value of 4.91 on the Mayr scale.⁸⁴ Unlike uncatalyzed ligated tetravalent boranes, trivalent boranes typically react with diazoesters by addition and 1,2-shift.⁸⁵ However, electrophilic borenium ions or their functional equivalents sometimes mimic the reactivity of trivalent boranes. Thus, we hypothesized that boryl electrophile catalysts would be alkylated by diazoesters and would thereby provide a pathway to B–H bond insertion reaction between diazo compounds and ligated boranes.

3.2.1 Optimization of B–H Insertion Reaction Conditions with Excess Diazo Component

The beginning purpose of this study was to test the mutual reactivity between ethyl diazoacetate and a NHC-boryl electrophile. Dr. Takuji Kawamoto and Mr. Sean Gardner first observed that reaction of 1,3-dimethylimidazol-2-ylidene borane **5** with ethyl diazoacetate **11**, upon addition of a substoichiometric amount of electrophiles or strong acids, gave NHC-boryl ester **114**. The results of the preliminary screening reactions by Kawamoto and Gardner are summarized in **Table 18**. The first activators screened were triflic acid (TfOH) and triflimide (Tf₂NH) (entries 1

and 2). Moderate conversions (38–47%) of NHC-borane **5** to the target B–H insertion product **114** were observed in the ^{11}B NMR spectra. A small amount of double adduct **115** was present in both cases. When the activator was switched to diiodine (entry 3), NHC-boryl ester **114** was isolated in 58% yield after flash column chromatography. A weaker acid, camphor sulfonic acid (10-CSA), did not produce the target product.

Table 18. Initial discovery of B–H reaction with NHC-boranes and activators



Entry	5 (mmol)	Activator	Concentration	Conversion ^a	114 / 115
1	0.3	TfOH (10 mol %)	0.7 M	47%	94/6
2	0.3	Tf ₂ NH (10 mol %)	0.6 M	38%	92/8
3	1.0	I ₂ (10 mol %)	1.0 M	58% ^b	– ^c
4	1.0	10-CSA (1.0 equiv)	0.2 M	0%	None

^[a] Estimated from ^{11}B NMR spectrum of crude reaction mixture; ^[b] Isolated yield after flash chromatography; ^[c] ^{11}B NMR spectrum of crude reaction mixture was not obtained.

Based on the preliminary results in **Table 18**, we sought to further develop reaction conditions with electrophilic activators to afford α -NHC-boryl esters in good yields. The donor-acceptor diazo compound **31** and 10 mol % I₂ activator were applied in the first reaction. At 0.1 M concentration (**Table 19**, entry 1), the reaction proceeded slowly, requiring 18 h to reach 50% conversion of the starting NHC-borane. A tenfold increase in concentration (entry 2) resulted in

complete conversion after 1 h. The less sterically bulky diazo compound **11** was then used to screen the activators as to determine the ratio between single and double insertion products.

Next, we screened four other activators: bromine, triflic acid, triflimide, and camphor sulfonic acid (entries 4–7). Twenty mol % loading of activator was used for each experiment. The bromine-catalyzed reaction proceeded to 95% consumption of NHC-borane with a 98/2 ratio of single and double adducts in the ^{11}B NMR spectrum after 1 h (entry 4). After an additional 17 h, the starting material was consumed and the double adduct increased moderately to 25%. NHC-borane was completely consumed after 1 h with triflic acid activation (entry 5). The ratio of single and double adduct changed slightly from 90/10 to 86/14 after 18 h. Triflimide catalysis gave a similar result to triflic acid with complete conversion after 1 h, and a minimal change in double adduct formation after 18 h (93/7 to 91/9) (entry 6). No target product was observed after 18 h when the weak acid, camphor sulfonic acid, was used as the activator (entry 7). The control reaction with activator absent (Entry 8) also resulted in no conversion to the insertion product.

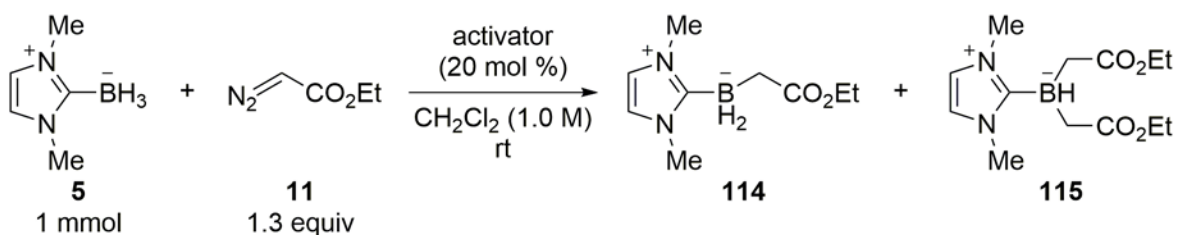
To reduce conversion to the double insertion product, the amount of **11** was reduced to 1.2 equiv and the reaction was stopped after 1 h (entry 9). The observed product ratio of 82/18 favored the single adduct compared to similar conditions with 1.3 equiv **11** (63/37). On a larger scale reaction of NHC-borane (10 mmol), a reduced loading of I_2 (3 mol %) was screened (entry 10). After 1 h, gas evolution ceased and only 7% conversion of NHC-borane was observed by ^{11}B NMR analysis.

When the reaction with diiodine as activator proceeded over 18 h (entry 3), the ratio of single and double adducts in the ^{11}B NMR spectrum changed from 63/37 to 36/64. A ratio of 36/64 is not theoretically possible given 1.3 equiv of diazo **11** used in the reaction. Therefore, the single adduct **114** is likely unstable when exposed to the diiodine activated reaction condition

over an extended time period. Limiting the reaction time to 1 h prevents degradation of the desired mono insertion product **114**.

In summary, the optimized reaction conditions to form a mono NHC-boryl ester product are shown in Entry 9: 1.2 diazo equivalents, 10 mol % I₂, CH₂Cl₂ (1.0 M), 1 h, rt.

Table 19. Reaction conditions screening with diazo compound in excess

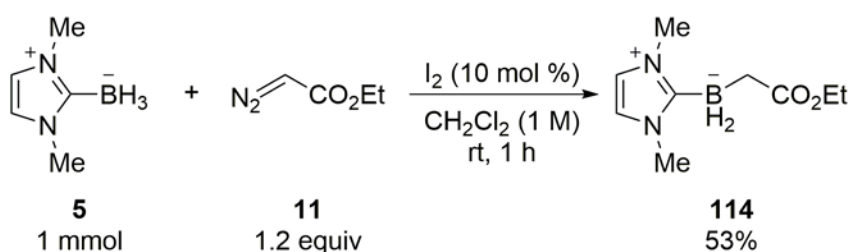


Entry	Activator	Conversion after 1 h (114 / 115)	Conversion after 18 h (114 / 115)
1 ^a	I ₂ (10 mol %)	8% (100/0)	50% (100/0)
2 ^b	I ₂ (10 mol %)	>99% (100/0)	–
3	I ₂ (10 mol %)	>99% (63/37)	>99% (36/64)
4	Br ₂	95% (98/2)	>99% (75/25)
5	TfOH	>99% (90/10)	>99% (86/14)
6	Tf ₂ NH	>99% (93/7)	>99% (91/9)
7	10-CSA	0%	0%
8	None	0%	0%
9 ^c	I ₂ (10 mol %)	>99% (82/18)	–
10 ^d	I ₂ (3 mol %)	7% (100/0)	–

^[a] 0.1 M, 1.2 equiv diazo **31**; ^[b] 1.2 equiv diazo **31**; ^[c] 1.2 equiv diazo **11**; ^[d] 10 mmol NHC-borane **5**.

3.2.2 Preparative B–H Insertion Reactions of NHC-boranes with Ethyl Diazoacetate

The next goal was to study the scope of this reaction with other NHC-boranes. For preparative scale reactions, we selected iodine as the activator because it reacts quickly and quantitatively with NHC-boranes to make NHC-boryl iodides. Iodine is easier to handle than bromine and triflic acid, and does not require manipulation under inert atmosphere compared to triflimide. In a standard reaction, NHC-borane **5** (1 mmol) was dissolved in dichloromethane (1 mL), and then diiodine (10 mol %) was added. The iodine color dissipated quickly accompanied by bubbling due to the formation of hydrogen gas. After 5 min, the neat diazo compound **11** (1.2 equiv) was added. Vigorous bubbling ensued, this time due to formation of nitrogen gas. After 1 h, an ^{11}B NMR spectrum of the reaction mixture showed that starting NHC-borane **5** was absent. Present were monoinsertion product **114** (t, -28.2 ppm) and the corresponding double insertion product NHC-BH(CH₂CO₂Et)₂ (d, -20.3 ppm) in a ratio of about 80/20. Solvent evaporation and flash chromatography of the residue provided stable α -boryl ester **114** in 53% yield.⁸⁶



Scheme 33. Preparation of α -NHC boryl ester **114**

Table 20 summarizes preparative reactions of **11** with other NHC-boranes under the conditions described in **Scheme 33**. The stable α -boryl ester products were isolated by concentration and direct flash chromatography. Reaction of 1,3-diisopropyl-imidazol-2-ylidene

borane **7** provided **116** in 57% yield (entry 1). Differentially substituted imidazolium boranes **117** (*N*-Me, *N*-iPr) and **119** (*N*-Me, *N*-Bu) provided products **118** and **120** in 50% and 58% yield, respectively (entries 2 and 3). 1,3,4,5-Tetramethylimidazol-2-ylidene borane **92** gave α -boryl ester **121** in 37% yield (entry 4), while the corresponding benzimidazole analog **8** gave **122** in 63% yield (entry 5). In contrast to these successes, the reactions with *N*-Me, *N*-Bn substituted NHC-borane **123** and the hindered 1,3-*bis*-(2,6-diisopropylphenyl)imidazole-2-ylidene borane **6** did not give the corresponding insertion products (entries 6 and 7). Similarly, Dr. Xiangcheng Pan reported that diiodine catalyzed hydroboration of alkenes did not occur when using dipp-NHC borane **6**.⁸¹ In both cases, the steric environment around the boryl iodide is likely too hindered for the incoming nucleophile to access.

Most of the products in **Table 20** are new compounds, though benzimidazole NHC-boryl ester **122** has been made by the rhodium-catalyzed reaction in about the same isolated yield.³² In the diiodine-catalyzed reactions, the formation of both the boryl iodide and the boryl ester can be conveniently followed by ¹¹B NMR spectroscopy, if desired. Spectra of most reaction mixtures showed that small amounts (roughly 10%) of double insertion products were formed. These are rather polar and were not isolated. The exception was entry 4, the reaction of tetramethylimidazol-2-ylidene borane **92**. In this case, the ratio of monoinsertion product **121** to the corresponding double insertion product was 66/34 according to the ¹¹B NMR spectrum of the crude product. Thus, the lower yield in entry 4 is due at least in part to over-reaction of the product **121**.

Table 20. Isolated yields in preparative reaction of NHC-boranes with ethyl diazoacetate

Entry	NHC-borane ^a	R ¹	R ²	Product	Yield
1	7	iPr	iPr	116	57%
2	117	Me	iPr	118	50%
3	119	Me	Bu	120	58%
4	123	Me	Bn	124	0%
5	6	dipp	dipp	125	0%
6					37%
7					63%

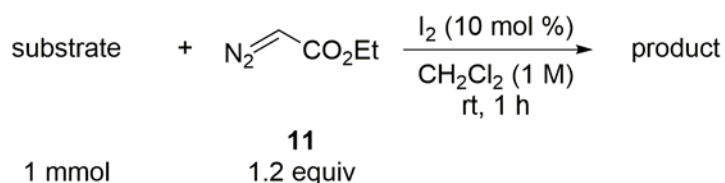
^[a] Conditions: 1 mmol of NHC-borane, 10 % I₂, 1.2 equiv of **11**, 1 mL dichloromethane, 1 h at rt.

3.2.3 Diiodine-Catalyzed B–H Insertion Screening with other Ligated Boranes

Next, we briefly surveyed other kinds of stable ligated boranes with ethyl diazoacetate **11** under the standard conditions, summarized in **Table 21**. Reactions with trimethylamine borane (Me₃N–BH₃ **2**) and triphenylphosphine borane (Ph₃P–BH₃ **3**) gave small amounts of boryl iodide

intermediates but no target insertion products as assessed by ^{11}B NMR spectroscopy. The reaction with pyridine-borane (pyr-BH₃ **4**) gave some product with the same ^{11}B NMR chemical shift as insertion product **128** (t, -5.7 ppm) but the conversion was low (<40%) and there was also a significant unidentified peak in the spectrum ($\delta = 2.2$ ppm). At least under these conditions then, NHC-boranes are a superior class for the B-H insertion reaction.

Table 21. Diiodine-catalyzed B-H insertion of ligated boranes



Entry	Substrate	Product	δ , ^{11}B NMR	Conversion
1	Me ₃ N-BH ₃ 2	Me ₃ N ⁺ -B ⁻ (H) ₂ -CH ₂ -CO ₂ Et 126	–	0%
2	Ph ₃ P-BH ₃ 3	Ph ₃ P ⁺ -B ⁻ (H) ₂ -CH ₂ -CO ₂ Et 127	–	0%
3	pyr-BH ₃ 4	pyr ⁺ -B ⁻ (H) ₂ -CH ₂ -CO ₂ Et 128	t, (-5.7 ppm)	<40%

3.2.4 Preparative Reactions of 1,3-Dimethylimidazol-2-ylidene Borane with Substituted Diazoacetates

Many boron analogs of amino acids exist, but typically the boron functionality replaces the carboxy carbon of the amino acid.⁸⁷⁻⁸⁸ Diazo compounds that gave B-H insertion products with

2-alkyl substituents gave low yields in Li's rhodium-catalyzed reactions. The diazo esters chosen for this scope study feature natural or common unnatural amino acid side chains.

The diazo compounds were prepared by literature methods. 2-diazopropanoates with methyl (**44**) and benzyl (**129**) esters were obtained by treatment of 2-methylacetoacetate precursors with 4-acetamidobenzenesulfonyl azide (*p*-ABSA) in a Regitz diazo transfer reaction.⁸⁹ Similarly, treatment of ethyl 2-isopropylacetoacetate with *p*-ABSA afforded methyl 2-diazo-3-methylbutanoate **131**. The remaining diazo compounds, other than **31** and **85**, were prepared by diazotization of the corresponding α -amino acid ester with isopentyl nitrite.⁹⁰

Table 22 summarizes the results of a survey of reaction of various diazoesters with readily available NHC-borane **5**. The standard conditions were used (1 mmol NHC-borane **5**, 10% I₂, 1.2 equiv of diazo ester, 1 mL of dichloromethane, 1 h of rt) unless otherwise noted. Yields are reported after concentration and flash chromatography.

Reactions of **5** with 2-diazopropanoates with methyl (**44**) and benzyl (**129**) esters provided the corresponding NHC-boryl alanine esters **45** and **130** in 68% and 43% yields (entries 1 and 2). Reaction with methyl 2-diazo-3-methylbutanoate **131** gave the boryl valine analog **132** in only 20% yield (entry 3). However, reactions of diazoesters **133** and **135** with phenylalanine and methionine side chains gave **134** and **136** in 71% and 52% yields (entries 4 and 5). The reaction with **134** was slow and was allowed to progress for 18 h before purification.

The diazoesters with natural tyrosine and tryptophan side chains did not provide insertion products in reactions with **5** (entries 6 and 8). However, the corresponding methylated analogs **139** and **143** provided protected tyrosine and tryptophan NHC-boryl esters **140** and **144** in 58% and 46% yields (entries 7 and 9).

Table 22. Isolated yields in preparative reactions of NHC-borane **5** with substituted diazoacetates

Entry ^a	NHC-borane	R ¹	R ²	Product	Yield
1	44	Me	Et	45	68%
2	129	Me	Bn	130	43%
3	131	iPr	Et	132	20% ^b
4	133	Bn	Me	134	71%
5	135	CH ₂ CH ₂ SMe	Me	136	52% ^c
6	137	CH ₂ C ₆ H ₄ OH	Me	138	0%
7	139	CH ₂ C ₆ H ₄ OMe	Me	140	58%
8	141	CH ₂ -tryptophan	Me	142	0%
9	143	CH ₂ -NMe-tryptophan	Me	144	46%
10	31	Ph	Me	32	64%
11	60	Ph	2,6-Me ₂ C ₆ H ₃	61	54%
12	58	Ph	2,6-Cl ₂ C ₆ H ₃	59	26% ^d
13	85	CO ₂ Me	Me	90	0%
14					0%
15					0%

^[a] Conditions: 1 mmol of NHC-borane **5**, 10 % I₂, 1.2 equiv of diazo, 1 mL of dichloromethane, 1 h at rt; ^[b] 25% conversion of **5**; ^[c] 18 h reaction time; ^[d] 61% conversion of **5**.

Next, 2-phenyl-diazoacetates with methyl (**31**), 2,6-dimethylphenyl (**60**) and 2,6-dichlorophenyl (**58**) esters provided the corresponding NHC-boryl phenylglycines **32**, **61**, and **59** in 64%, 54%, and 26% yields, respectively (entries 10, 11, and 12).

Finally, dimethyl diazo malonate **85** did not yield target boryl ester product **90** (entry 13). Diethyl diazomalonate has an *N* value of -0.35 on the Mayr scale and, therefore, is less nucleophilic than the other tested diazo substrates. We also screened dimethyl 2-diazosuccinate **145** and dimethyl 2-diazopentanedioate **147** (aspartic and glutamic acid precursor analogs), but the desired products were also not obtained (entries 14 and 15).

The progress of these reactions was followed by ^{11}B NMR spectroscopy as usual, and in many cases the conversion of **5** was high (90–100%). Exceptions were the lower yielding reactions in entries 3 and 10. These were not plagued by side-product formation. Instead, they seemed to stop with substantial amounts of NHC-borane **5** remaining (75% and 39%, respectively).

3.2.5 Optimization of B–H Insertion Reaction Condition with Excess Borane Component

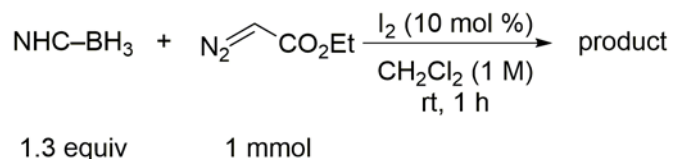
To further reduce formation of the double insertion product, we screened several reactions with NHC-borane in excess (**Table 23**). Boron–hydrogen insertion reactions with *N*-methyl substituted NHC-boranes give a higher ratio of double insertion side product compared to NHC-boranes with bulky *N*-substituents. When 1.3 equiv of diMe-NHC borane **5** or benzimidazole-NHC borane **8** were reacted with 1 mmol ethyl diazoacetate (Entries 1 and 4), formation of the desired mono-insertion product was heavily favored (99/1 and 98/2 single to double adduct). Furthermore, the isolated yield of the mono-adduct was higher compared to the insertion reaction with excess diazo compound (75% and 78% versus 53% and 65%).

The double insertion product does not appear when the hindered diIPr-NHC borane **7** or -*N*-Bu NHC borane **119** are reacted with excess diazo compound. When either NHC borane is reacted in excess (Entries 2 and 3), no double adduct is formed and the isolated yield is within \pm

6% of the standard conditions result (63% and 55% versus 57% and 58%). Similar results are obtained when the bulkier diazo methionine **135** and phenyl diazoacetate **31** are reacted with diMe-NHC borane **5** in excess (entries 5 and 6). Again, double adduct formation was not observed, and there was no improvement in isolated yield of the target product (49% and 61% versus 52% and 64%).

In summary, if a combination of NHC borane and diazo compound results in significant formation of undesired double insertion product, the NHC borane component should be used in excess to increase the isolated yield of the single insertion product.

Table 23. Reaction conditions screening with NHC-borane in excess



Entry	NHC-borane	Product	Conversion (1 h)	Single /Double	Yield	Yield (std conditions)
1	5	114	84%	99/1	75%	53% ^a
2	7	116	90%	100/0	63%	57% ^b
3	119	120	96%	98/2	55%	58% ^c
4	8	122	88%	100/0	78%	65% ^d
5 ^e	5	136	70% ^f	100/0	49%	52% ^g
6 ^h	5	32	75%	100/0	61%	64% ⁱ

^[a] Scheme 31; ^[b] Table 20, entry 1; ^[c] Table 20, entry 3; ^[d] Table 20, entry ; ^[e] Diazo **135**; ^[f] 18 h;

^[g] Table 22, entry 5; ^[h] Diazo **31**; ^[i] Table 22, entry 10.

3.2.6 Structure and Stability of α -NHC-Boryl Esters

Unlike the crystalline NHC-borane starting materials, many α -NHC-boryl esters in **Table 20** and **22** are clear, free-flowing liquids. Exceptions included benzimidazole derivative **122**, tryptophan analog **144**, and the two aryl esters **59** and **61** with the phenylglycine motif. These four products are white solids. Crystals of the tryptophan analog **144** were grown by vapor phase diffusion from dichloromethane/pentane. The X-ray crystal structure was solved by Dr. Steve Geib, and the resulting ORTEP diagram is shown in **Figure 24**.

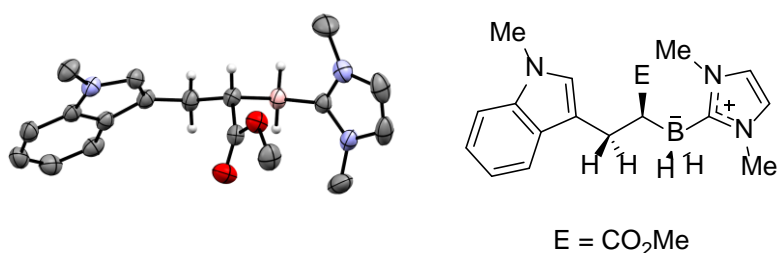


Figure 24. X-ray structure of NHC-boryl ester **144**

This is the first crystal structure of an NHC-boryl ester, and it confirms the assignment of constitution that was made by NMR methods (specifically, the compounds are α -NHC-boryl esters, not isomeric enol boranes). The molecule adopts an extended conformation from the tryptophan ring on the left through to the NHC-ring on the right. This leaves the bond from the chain to the ester (CH–CO₂Me) as gauche to both the CH₂–tryptophan bond on one side and the BH₂–NHC bond on the other side.

The chiral α -boryl esters in **Table 22** are racemates. To learn if the individual enantiomers resist racemization, the two enantiomers of 2,6-dichlorophenyl ester **59** were resolved by chiral HPLC ((*S,S*)-Whelk-O column, hexane/*i*PrOH = 70:30, first enantiomer t_R =

12.04 min, second enantiomer $t_R = 15.45$ min). The enantioenriched samples were stable and did not racemize for several years at rt.

3.2.7 Mechanistic Experiments

Figure 25 shows a plausible mechanism for this reaction that is based on analogies between borane (BH_3) and NHC-borenium ions (NHC-BH_2^+), both of which are reactive Lewis acids. It is unlikely that free borenium ions are involved in this reaction, but NHC-boranes bearing excellent leaving groups ($\text{NHC-BH}_2\text{X}$) exhibit borenium-like reactivity.

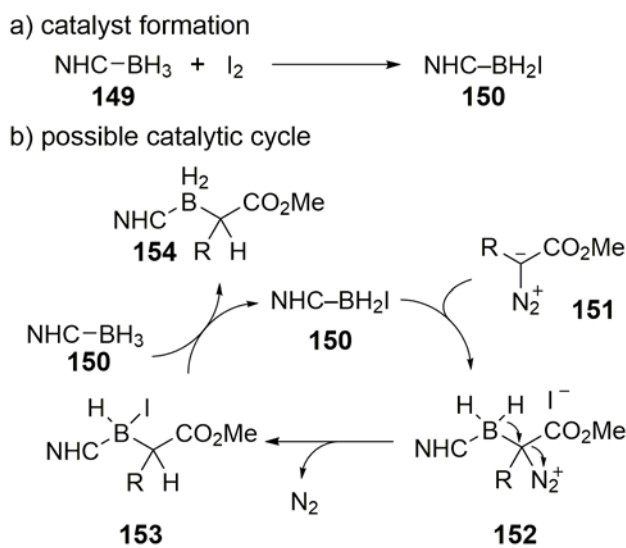
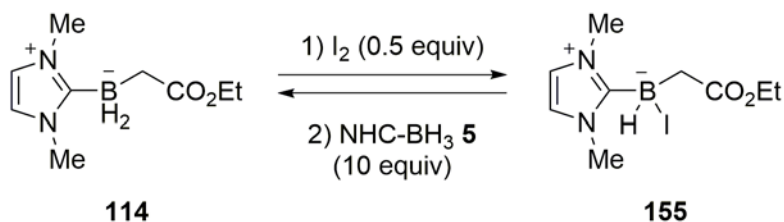


Figure 25. Proposed catalytic cycle

The rapid formation of boryl iodide catalyst **150** by reaction of NHC-BH_3 **149** with diiodine was verified by ^{11}B NMR spectroscopy. Subsequent C-borylation of diazoester **151** provides α -NHC-boryl diazonium iodide **152** that then undergoes 1,2-hydride shift with loss of dinitrogen. Collapse of the iodide upon the forming borenium ion generates boryl iodide **153**.

The observed product **154** arises from hydride/iodide exchange between starting NHC–BH₃ **149** and **153** with regeneration of the catalyst **150**. The hydride/iodide exchange reaction has precedent in 1,2-hydroboration reactions of NHC-boranes, which are also catalyzed by NHC-boryl iodides and related molecules.⁹¹

The second hydride transfer step was probed by generation of an iodide like **154** by treatment of boryl ester **114** with 0.5 equiv of iodine (**Scheme 34**). The ¹¹B NMR spectrum showed formation of boryl iodide **155** as a doublet at –21.0 ppm (**Figure 26**, top). Next, the catalytic conditions were mimicked by addition of excess NHC–BH₃ **5** (10 equiv). The complete conversion of **155** back to boryl ester **114** (t, –28.0 ppm) after 1 h as observed in the ¹¹B NMR spectrum (**Figure 26**, bottom) confirmed that the hydride transfer step was viable.



Scheme 34. Experimental confirmation of turnover step

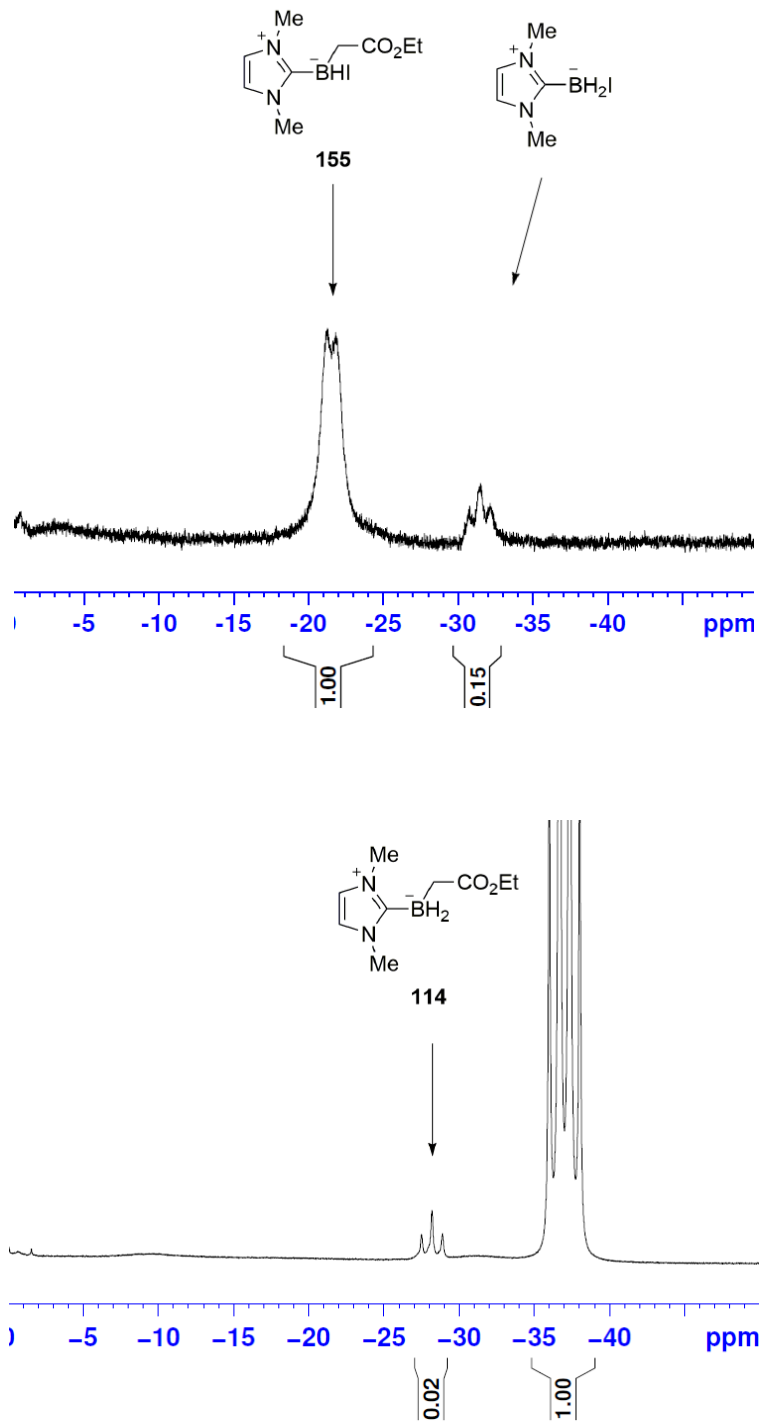


Figure 26. (Top) ^{11}B NMR spectrum NHC-boryl iodide **155**; (Bottom) Regeneration of NHC-boryl ester **114**.

3.3 CONCLUSIONS

In summary, we have discovered that formal B–H insertion reactions of NHC-boranes with diazoesters are facilitated by substoichiometric amounts of diiodine and other activators. The diiodine is a precatalyst that reacts rapidly with the NHC-borane to produce an NHC-boryl iodide catalyst. In this new transformation, the NHC-BH₂I catalyst acts as an electrophile with the diazoester attacking as a nucleophile. Carbon–boron bond formation leads, then followed by hydride transfer by an NHC-borane molecule. The ability of NHC-boranes to donate hydride to borenium ion equivalent species is critical to the regeneration of the boryl iodide catalyst.

Overall, the borenium ion catalyzed B–H insertion reaction resembles Li's previous Rh(II)-catalyzed transformation in both starting substrates and end products. However, the mechanisms of these two reactions are, generally, opposites of each other. In the Rh-catalyzed reactions, the key catalytic species (a rhodium carbene) comes from the diazo ester and reacts directly with the NHC-borane. In the leading step, the NHC-borane donates a hydride to the electrophilic rhodium carbene. Subsequent C–B bond formation gives the requisite boryl ester product.

These different mechanisms are reflected in the diverging scope of compatible diazo compounds. The two reactions give comparable yields with unsubstituted and α -aryl-substituted diazoacetates. In contrast, the previous Rh-catalysis method looks superior for electron-poor diazoesters (diazomalonates give high yields) while the boryl iodide catalysis method looks superior for 2-alkyl-substituted diazoacetates. Building on this feature, we have produced a number of α -NHC-boryl esters with amino acid side chains in the α -position. This paves the way for study of such molecules as analogs of amino acids where the unusual, electron-donating NHC-boryl group replaces the usual, electron-withdrawing amino group.

While NHC-boranes do not react like trivalent boranes, such borane-like reactivity can be expressed with a borenium ion equivalent catalyst. In turn, reactions of borenium ions loosely resemble those of trivalent boranes. The chemistry of tetravalent NHC-boranes could continue to broaden if additional reactions utilizing trivalent boranes are applied to activated NHC-boranes.

In conclusion, the boryl iodide catalysis method is the only reported methodology that is compatible with 2-alkyl substituted diazoesters, in contrast to Li's Rh(II) catalyzed method and the other carbene B–H insertion methods mentioned in Section 1.1.3. However, the boryl iodide method is not compatible with ligated boranes other than NHC-boranes. The Rh(II) carbene method is applicable to non-NHC ligated boranes, *N*-aryl substituted NHC-boranes, and electrophilic diazo compounds.^{32, 43} Another current limitation of the boryl iodide method is that the reaction produces only racemic products. Enantiopure boryl carbonyl products have been synthesized using Cu(I) salts (phosphine-boranes),³⁶ Rh(I) salts (pyrrolidine-boranes),³⁸ and a cytochrome c enzyme (NHC-boranes).⁴⁰ The door is open to explore an asymmetric boryl iodide catalysis method by introduction of a chiral element to the NHC-borane starting substrate.

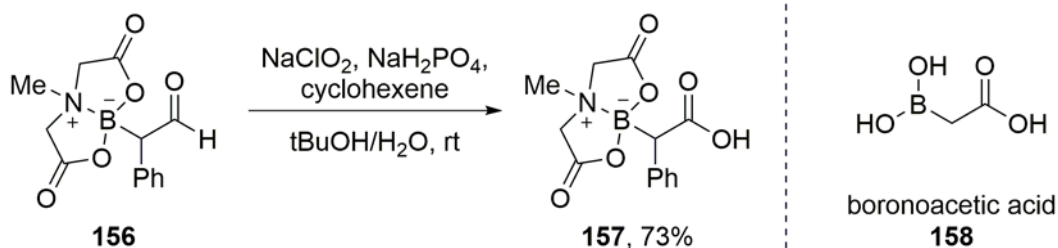
4.0 SYNTHESIS AND CHARACTERIZATION OF LIGATED BORYL ACETIC ACIDS

ACIDS

4.1 INTRODUCTION

4.1.1 α -Boryl Carboxylic Acids

Few examples of α -boryl carboxylic acids exist. Recently, Yudin and co-workers have described the synthesis of α -MIDA-boryl carboxylic acids.⁴¹ Yudin's α -MIDA-boryl aldehyde **156** is oxidized with sodium chlorite to give MIDA-boryl carboxylic acid **157** in 73% yield (Scheme 35, left).⁹² Yudin then treated boryl acid **157** with diphenylphosphoryl azide to give the boryl isocyanate by which additional boryl functional groups can be accessed.⁹³ MIDA-boryl carboxylic acid **157** is formally a derivative of unknown compound boronoacetic acid **158** (Scheme 35, right).



Scheme 35. Yudin's synthesis of α -MIDA-boryl acid **157**

Two acetic acid derivatives with carborane substituents are known. Zakharkin and Petrovskii reported the preparation α -carborane acid acid **159** and diacid **160** (Figure 27).⁹⁴⁻⁹⁵ Acid dissociation constants for either the MIDA-boryl acids or carborane acetic acids are not known.

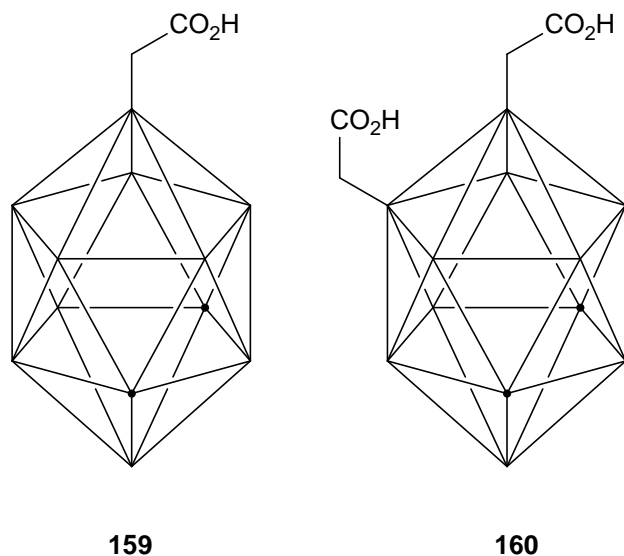


Figure 27. α -Boryl acetic acids with carborane substituents (CH vertex indicated by black dot)

Similar to boronoacetic acid **158**, there are no examples of the reduced analog boroacetic acid **161** (Figure 28), likely because of the mutual reactivity of boranes and acids. Boroacetic acid is formally a Lewis acid/base complexes of a borane and a carboxylic acid. Further, there are no known ligated α -boryl acid derivatives of borane. It is not clear that its ligated derivatives will be stable because ligated boranes and carboxylic acids are subject to acid/base reactions to form dihydrogen.^{2, 6}

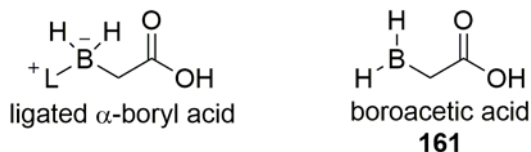


Figure 28. Unknown compound boroacetic acid and its ligated derivative

Our goal for this study is to determine if ligated α -boryl esters can be hydrolyzed under basic conditions, and if the formed boryl acetic acid products are stable to isolation and storage. Stable ligated α -boryl acids will then be further characterized by X-ray crystallography and acidity constant (pK_a) measurements.

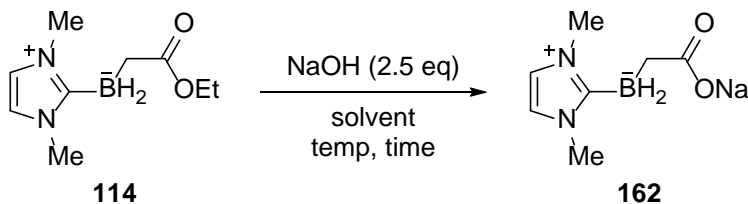
4.2 RESULTS AND DISCUSSION

4.2.1 Hydrolysis of Ligated α -Boryl Esters

The hydrolysis study began with readily available α -ligated boryl esters that were prepared from both the rhodium(II) and borenium ion methods.^{43, 86} NHC-boryl ester **114** (0.15 mmol) with 2.5 equiv NaOH in acetonitrile was heated at 70 °C in a sealed, 20 dram vial. Reaction progress was followed by ^{11}B NMR spectroscopy (**Table 24**, entry 1). Over 18 h, a new peak gradually appeared 1 ppm downfield from the boryl ester triplet at -27 ppm. To verify that this new signal was the desired carboxylate intermediate, the hydrolysis experiment was repeated in $MeOH-d_4$ at 55 °C to monitor reaction progress by 1H NMR analysis (entry 2). The appearance of a triplet at 0.99 ppm in the 1H NMR spectrum after 18 h was consistent with the formation of ethanol. The corresponding triplet signal of the ester starting material also disappeared. The completion of the

hydrolysis was confirmed by a clean triplet at -26 ppm in the ^{11}B NMR spectrum. A larger scale reaction with 1.6 mmol NHC-boryl ester **114** required 3 d for complete consumption of the starting material (entry 3).

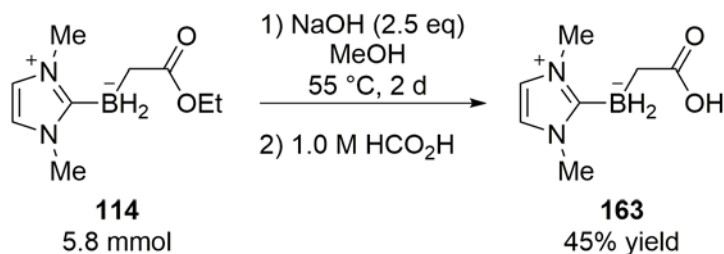
Table 24. Hydrolysis of NHC-boryl ester **114**



Entry	NHC-boryl ester (mmol)	Solvent	Temperature (°C)	Time	Conversion
1	0.15	CH ₃ CN	70	18 h	incomplete
2	0.15	MeOH- <i>d</i> ₄	55	18 h	100% ^a
3	1.6	MeOH- <i>d</i> ₄	55	3 d	100% ^a

^[a] Monitored by formation of ethanol in ^1H NMR spectrum of crude reaction mixture.

To isolate the NHC-boryl acetic acid, we first formed the NHC-boryl carboxylate by heating 5.8 mmol NHC-boryl ester **114** with 2.5 equiv NaOH for 2 d (**Scheme 36**). Because NHC-boranes undergo acid/base reactions when treated with strong acids, we initially chose a weak acid (formic) as the proton source during workup. After 2 d, the mixture was cooled, excess 1.0 M formic acid was added, and the resulting acidic aqueous phase was extracted with CH₂Cl₂. Drying and concentrating of the CH₂Cl₂ layer gave good quality α -NHC-boryl acid **163** in 45% yield as a stable white solid, melting point 137–140 °C.⁹⁶



Scheme 36. Synthesis of NHC-boryl acetic acid **163**

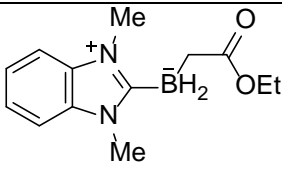
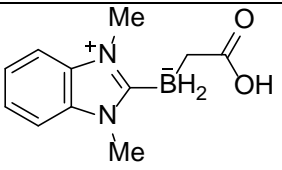
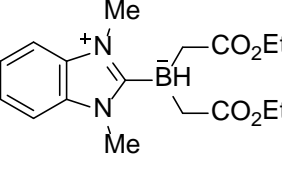
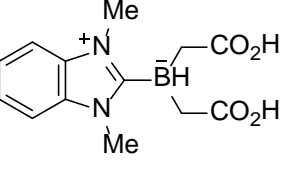
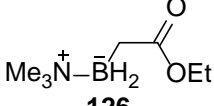
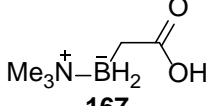
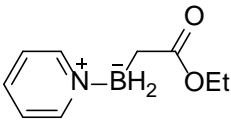
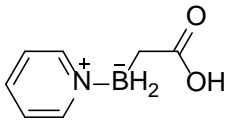
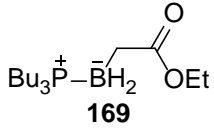
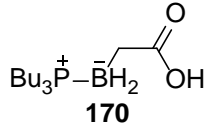
Table 25 summarizes structures, hydrolysis times, and isolated yields of five other ligated α -boryl acids. Benzimidazole-NHC-boryl ester **122** hydrolysis required 2 days for complete consumption of the starting material as determined by ^{11}B NMR analysis (entry 1). Formic acid workup gave benzimidazole-NHC-boryl acid **164** in 78% yield as a white solid, melting point 175–177 $^\circ\text{C}$. Benzimidazole-NHC-boryl diester **165** in $\text{MeOH-}d_4$ was heated at 55 $^\circ\text{C}$ with 5.0 equiv NaOH for 3 days (entry 2). The NHC-boryl diester doublet in the ^{11}B NMR spectrum broadened rather than exhibiting a discernable shift to carboxylate intermediates. Reaction progress was monitored by ^1H NMR spectroscopy. Upon addition of the formic acid solution during workup, a white precipitate formed instantaneously. The solid was filtered and dried under reduced pressure. NMR analysis confirmed that the solid was the target benzimidazole-NHC-boryl diacid **166**. Diacid **166** was isolated in 45% yield as a white solid, melting point 202–203 $^\circ\text{C}$.

Next, we screened three ligated boryl esters: trimethylamine-borane, pyridine-borane, and tributylphosphine-borane B–H insertion adducts. The starting boryl ester products were prepared by $\text{Rh}_2(\text{esp})_2$ catalyzed B–H insertion with ethyl diazoacetate. First, the hydrolysis of trimethylamine-boryl ester **126** was complete after heating 2.5 equiv NaOH at 55 $^\circ\text{C}$ for 1 day (entry 3). Subsequent acid workup afforded trimethylamine-boryl acid **167** in 24% yield as a white solid, mp 113–115 $^\circ\text{C}$. Unlike the relatively clean ^{11}B NMR spectra of the NHC-borane

ester hydrolyses, a significant impurity (~25%) was present at 2.5 ppm in the amine-boryl ester ^{11}B NMR spectrum. Pyridine-boryl ester **128** decomposed when heated at 55 °C with 2.5 equiv NaOH, probably because pyridine-borane adducts are prone to decomplexation at elevated temperature. The hydrolysis was repeated at rt and proceeded smoothly over 4 days (entry 4). Pyridine-boryl acid **168** was isolated in 54% yield (mp 76–78 °C) after acid workup. Hydrolysis of tributylphosphine-boryl ester **169** proceeded slowly over 2 weeks at rt (entry 5). Unfortunately, the desired boryl acid **170** was not isolated after acid workup. Reaction progress of the three ligated boryl esters was monitored by ^1H NMR of the crude reaction mixtures because the ^{11}B NMR signals were too broad to determine formation of the carboxylate intermediate.

The isolated yields are likely a reflection of partitioning of the small, polar acids into the aqueous phase during extractions. Trimethylamine-boryl acid **167** is the smallest and most water soluble of the boryl acids, and **167** was isolated in the lowest yield. Benzimidazole boryl acid **164** is less water soluble and was isolated in higher yield (78%) than imidazole boryl acid **163** (45%). The α -boryl acids in **Table 25** are stable to strong base and mild acid, and they are stable to prolonged storage either in the solid state or in solution. They are not amenable to standard silica gel chromatography because they are highly polar ($R_f \approx 0$ in 100% EtOAc).

Table 25. Synthesis of ligated boryl acetic acids

Entry	Boryl Ester	Boryl Acid	Time	Temperature (°C)	Yield
1	 <p>122</p>	 <p>164</p>	2 d	55	78%
2 ^a	 <p>165</p>	 <p>166</p>	3 d	55	45%
3	 <p>126</p>	 <p>167</p>	1 d	55	24%
4	 <p>128</p>	 <p>168</p>	4 d	rt	54%
5	 <p>169</p>	 <p>170</p>	2 weeks	rt	0%

4.2.2 X-ray Structures of Ligated α -Boryl Acetic Acids

The X-ray crystal structures of all five ligated α -boryl acetic acids were solved by Dr. Steve Geib. Figures **29**, **30**, **31** and **32** show ORTEP representations of the imidazole-boryl acid **163**, benzimidazole-boryl acid **164**, trimethylamine-boryl acid **167**, and pyridine-boryl acid **168**.

Despite the unusually low acidity of these acids (see Section 4.2.3.), they all form hydrogen-bond complexes in the solid state. Imidazole-boryl acid **163** is a typical eight-membered ring dimer of two acids face-to-face as shown in **Figure 29**. The $\text{BH}_2\text{-CH}_2$ bond is *gauche* in both molecules. The benzimidazole-boryl acid **164** dimer has a $\text{BH}_2\text{-CH}_2$ bond *anti* in one molecule and *gauche* in the other (**Figure 30**). Trimethylamine-boryl acid **167** dimer has both $\text{BH}_2\text{-CH}_2$ bonds adopt an *anti* conformation (**Figure 31**), while the pyridine-boryl acid **168** dimer $\text{BH}_2\text{-CH}_2$ bonds adopt a *gauche* conformation (**Figure 32**).

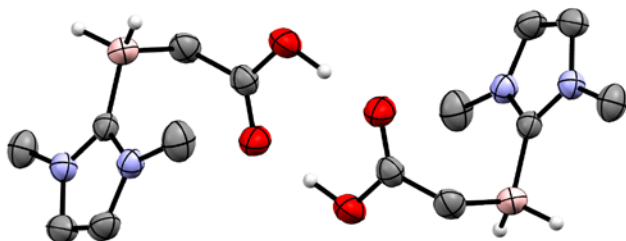


Figure 29. X-ray structure of imidazole-boryl acid **163** dimer

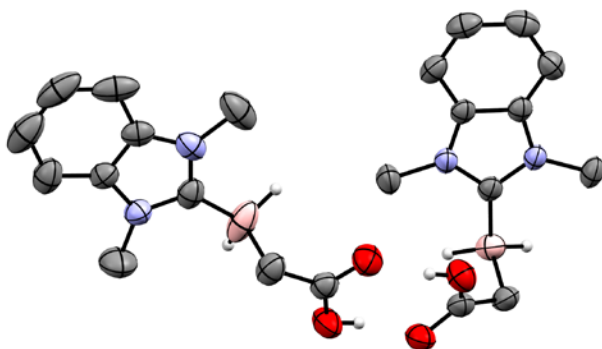


Figure 30. X-ray structure of benzimidazole-boryl acid **164** dimer

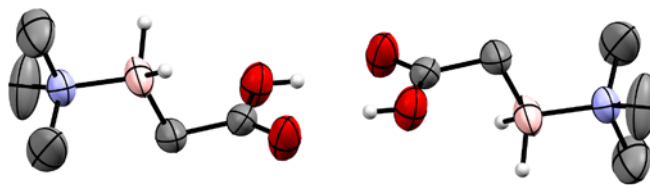


Figure 31. X-ray structure of trimethylamine-boryl acid **167** dimer

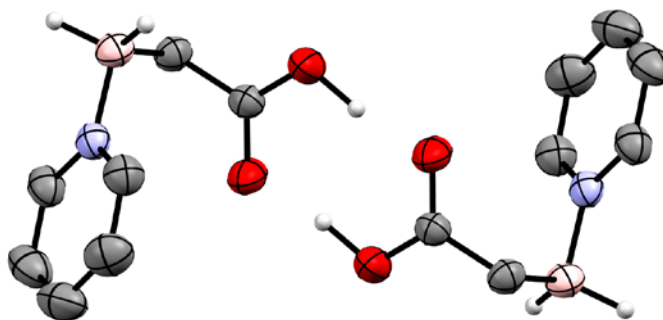


Figure 32. X-ray structure of pyridine-boryl acid **170** dimer

For the diacid **166**, the two acids form hydrogen bonds to two different molecules in the crystal. This organization then allows the benzimidazole NHC rings to exhibit a π stacking-like arrangement. A small segment of the resulting ladder-like structure is shown in **Figure 33**. In this structure, all the BH-CH₂ bonds are *anti*.

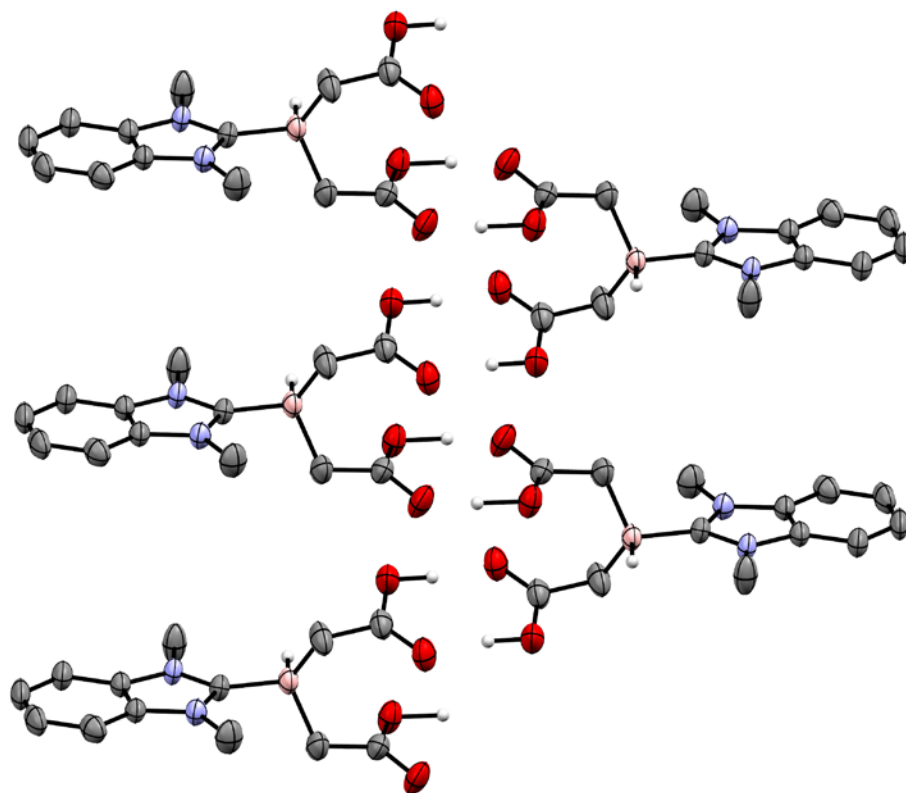


Figure 33. Hydrogen bonding network of benzimidazole-boryl diacids

4.2.3 Acidity Constant Measurements

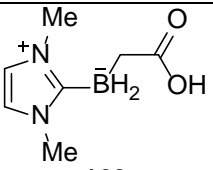
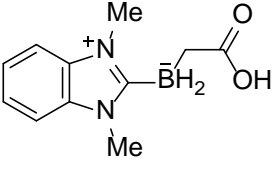
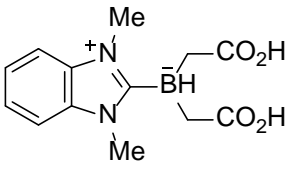
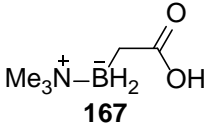
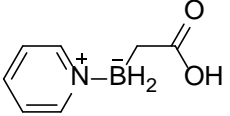
Acidity constant (pK_a) values for the isolated ligated α -boryl acetic acids were measured by Dr. Stephen Weber and Mr. Anthony Horner from fitting an equilibrium model to potentiometric titration data. In a representative titration experiment of imidazole-boryl acid **163**, a syringe pump delivered titrant, 72.5 mM NaOH, to the analyte solution. The titrant was standardized using a potassium hydrogen phthalate solution and contained 100 mM NaCl to minimize change in ionic activity coefficient. The pH was acquired every three seconds by computer. Data of NHC-boryl acid **163** was fit between 20 and 80% of the equivalence point.⁹⁷

The pK_a values of the ligated boryl acetic acids are shown in **Table 26**. Imidazole- and benzimidazole-boryl acids **163** and **164** have pK_a values of 6.88 ± 0.01 and 6.70 ± 0.02 (entries 1 and 2). Trimethylamine- and pyridine-boryl acids **167** and **168** are slightly more acidic, with pK_a values of 6.42 ± 0.00 and 6.41 ± 0.01 , respectively (entries 4 and 5). Benzimidazole-boryl diacid **166** has two pK_a values (entry 3). Diacid **166** was poorly soluble, but the single deprotonated form was more soluble. The value of the second, more robustly fit, pK_a was measured at 7.68 ± 0.02 . The best estimate from comparisons to various pentanedioic acids for the first pK_a is 6.5.

Few monosubstituted acetic acids, summarized in **Figure 34**,⁹⁸ are less acidic than acetic acid itself (pK_a 4.76). Typically, alkyl-substituted acetic acids are modestly less acidic than unsubstituted acetic acid. For example, butanoic acid has a pK_a of 4.82. The trimethylsilyl functional group is one of the strongest electron-donating substituents ($\sigma_{para} = -0.17$). Yet, trimethylsilyl acetic acid has a pK_a of only 5.22.⁹⁹ Compared to the ligated boryl acids in **Table 26**, the illustrated monosubstituted acetic acids are 50–100 times more acidic.

Select di- and trisubstituted acetic acids are markedly less acidic than monosubstituted variants. In comparison to alkyl-substituted butanoic acid, disubstituted cyclohexane carboxylic acid has a pK_a of 4.90 while trisubstituted pivalic acid (2,2-dimethylpropanoic acid) has a pK_a of 5.01. Certain bicyclic carboxylic acids have acidity constants that are nearly the same as the measured values in **Table 26**. For example, bicyclo[2.2.2]octane-1-carboxylic acid has a pK_a of 6.75.

Table 26. Acidity constant measurements of ligated boryl acetic acids

Entry	α -Boryl Acetic Acid	$pK_a \pm \text{SEM}$
1	 163	6.88 ± 0.01
2	 164	6.70 ± 0.02
3	 166	6.5^a and 7.68 ± 0.02
4	 167	6.42 ± 0.00
5	 168	6.41 ± 0.01

^[a] Estimated value.

Diacid **166** can be viewed as pentanedioic acid (glutaric acid) with the third carbon atom substituted by a boron atom and a benzimidazole substituent. In contrast to either **166** pK_a value, pentanedioic acid exhibits low pK_a values of 4.34 and 5.42. The only second pK_a values approaching 7.68 are exhibited by pentanedioic acids with 3,3-disubstitution. Accordingly, 3,3-

dipropylpentanedioic acid has a high second pK_a of 7.31, yet its first pK_a is consistent with most acetic acid derivatives (3.69). The two long-chain alkyl substituents forces the pentanedioic carboxylate anions to be in close proximity. The resulting anion repulsion (*syn*-pentane effect) elevates the second pK_a . Since diacid **166** does not have such proximity constraints, the high pK_a values are likely due to the electron-donating ability of the benzimidazole-borane substituent. In summary, ligated α -boryl acetic acids are among the least acidic carboxylic acids known.

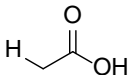
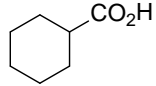
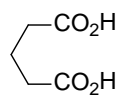
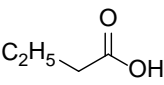
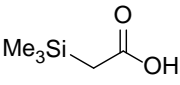

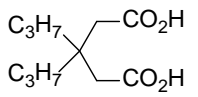
acetic acid and mono-substituted derivatives		di- and trisubstituted acetic acids		diacids	
	p <i>K</i> _a		p <i>K</i> _a		p <i>K</i> _a
acetic acid		cyclohexane- carboxylic acid		pentanedioic acid	
	4.76	$(\text{CH}_3)_3\text{CCO}_2\text{H}$	4.90	4.34 and 5.42	
butanoic acid		pivalic acid		3.69 and 7.31	
	5.22		6.75		
2-TMS-acetic acid		bicyclo[2.2.2]octane- 1-carboxylic acid		3,3-dipropylpentane- dioic acid	

Figure 34. Acidity constant measurements of comparable acids

Ligated boryl acids have pK_a values equivalent to imidazolium (pK_a , 7.05) and 4-nitrophenol (pK_a , 7.14), a stabilized phenol. These compounds are approximately 100 times less acidic than pyridinium (pK_a , 5.14). Therefore, ligated boryl carboxylate salts are strong bases relative to most known carboxylates.

4.2.4 NHC-borane Hammett Values Derived from ^{13}C NMR Chemical Shift Correlation

We next quantified the electron donating ability of L-BH_2 substituents by deriving electrophilic substituent constants (σ_{p}^+)¹⁰⁰ from ^{13}C NMR chemical shift correlation. Electrophilic substituent constant σ_{p}^+ values were originally derived by Brown from the solvolysis of *para*-substituted (2-chloropropan-2-yl)benzene derivatives. A σ_{p}^+ value quantifies how a substituent stabilizes a positive charge via resonance. Electron donating groups have increasingly negative σ_{p}^+ values. Similar to other σ_{para} values, substituents that can participate via resonance have larger absolute σ_{p}^+ values. Extensive correlations of ^{13}C chemical shifts in monosubstituted benzenes with Hammett σ constants were first reported by Spiesscke and Schneider.¹⁰¹ By using the regression line for the $\Delta\delta(\text{C}_{\text{p}})$ correlation, σ_{p}^+ values were calculated for various substituents on benzene. Data for monosubstituted benzenes in acetone solution are summarized in **Figure 35**.¹⁰²

$$\Delta\delta(\text{C}_{\text{p}}) = 9.809\sigma_{\text{p}}^+ - 0.814$$

$n = 14$
 n is number of substituted benzene derivatives tested

$$r = 0.992$$

Figure 35. Correlation of $\delta(\text{C}_{\text{p}})$ of monosubstituted benzenes with σ_{p}^+

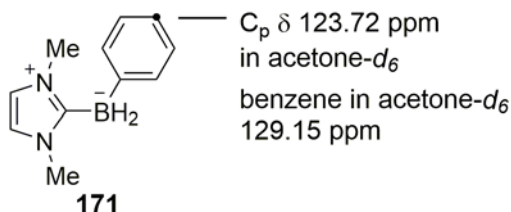


Figure 36. Hammett correlation equation applied to NHC-boryl arene **171**

The ^{13}C NMR chemical shift of a ligated boryl arene para carbon (**Figure 36**) provides a σ_{p}^+ value for a ligated boryl substituent when equation 1 is applied. Ligated boryl arenes were prepared by Dr. Tsuyoshi Taniguchi, Dr. Swapnil Nerkar, and Mr. Daniel Bolt. The chemical shifts of the para phenyl carbon in relation to other aromatic carbons must first be confirmed by HSQC NMR analysis. In a representative example, HSQC analysis of imidazole-BH₂Ph **171** in acetone-*d*₆ confirmed that the most upfield signal (123.72 ppm) in the aromatic region (excluding the imidazole carbon) was the para carbon resonance. A σ_{p}^+ value of -0.47 was calculated for imidazole-BH₂ substituent (**Table 27**, entry 3). The para carbon resonances of the other compounds were assigned by additional experiments conducted by Dr. Taniguchi. **Table 27** summarizes the calculated σ_{p}^+ values for 11 ligated borane substituents. Also shown in **Table 27** are Tolman electronic parameter (TEP) values for NHC ligands. TEP values are a measurement of the electron donating or withdrawing ability of a ligand.¹⁰³ A smaller TEP value corresponds to a more electron donating ligand.

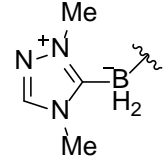
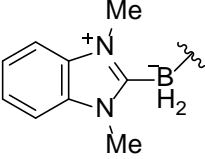
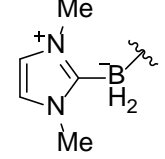
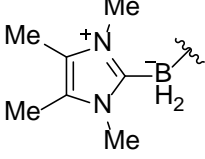
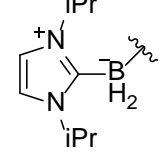
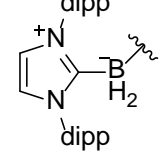
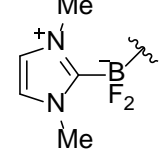
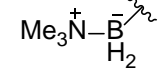
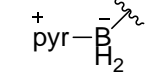
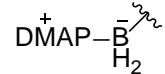
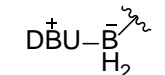
Benzimidazole-BH₂ has a slightly less negative Hammett value (entry 2) than imidazole-BH₂ which is reflected by benzimidazole-boryl acid **164** being more acidic than imidazole-boryl acid **163**. Triazole-borane is the least electron donating of the NHC-BH₂ substituents (entry 1). Tetramethyl-NHC-borane and diisopropyl-NHC-borane are more electron donating than imidazole-BH₂ (entries 4 and 5), and the *N*-aryl dipp-NHC-BH₂ substituent is the most electron donating group of the NHC ligands (entry 6).

Substituting NHC-BH₂ boron-hydrogen atoms with fluorine dramatically reduces the electron donating ability of the substituent (entry 7). Trimethylamine-borane and pyridine-borane substituents have less negative sigma values than the NHC analogs (entries 8 and 9). These Hammett values are consistent with the lower $\text{p}K_{\text{a}}$ values measured for amine-boryl acid **167** and

pyridine-boryl acid **168**. DMAP-borane has a more negative Hammett value than pyridine-borane because of the addition of an electron donating dimethylamino group (entry 10). Finally, the DBU-borane substituent is as strongly electron donating as the NHC-borane substituents (entry 11).

The calculated sigma values correlate nicely with Tolman electronic parameter (TEP) data of NHC ligands.¹⁰⁴ In general for entries 1–6, a larger TEP value (more electron donating) corresponds to a more negative sigma value. The range of NHC-BH₂ sigma values (–0.50 to –0.40) lies below the sigma values for methyl (–0.31) and phenyl (–0.18) substituents, but is less negative than methoxy (–0.78) and amine (–1.3) functional groups. This data suggests that NHC-BH₂ substituents are among the strongest inductive electron donating groups. Only groups that can participate in resonance have more negative σ_p^+ values.

Table 27. Electrophilic Hammett constants for ligated borane substituents

Entry	Substituent, L	NHC TEP (cm ⁻¹) ¹⁰⁴	¹³ C _{para} δ (ppm)	σ _p ⁺
1		2060.0	124.23	-0.42
2		2057.0	124.04	-0.44
3		2054.1	123.72	-0.47
4		2051.7	123.61	-0.48
5		2051.5	123.67	-0.48
6		2050.5	123.33	-0.51
7		N/A	126.92	-0.14
8		N/A	126.16	-0.22
9		N/A	125.40	-0.30
10		N/A	124.69	-0.37
11		N/A	123.93	-0.45

4.3 CONCLUSIONS

In summary, we have described the synthesis, structure, and acidity constants of the first ligated derivatives of the simple but unknown compound boroacetic acid. α -Boryl acetic acids with *N*-heterocyclic carbene, amine, and pyridine ligands are all stable solids that do not self-destruct by acid/base reactions, because they are exceptionally weak acids. Indeed, a series of pK_a measurements show that they are among the weakest of all known carboxylic acids. In turn, this means that their conjugate bases are among the strongest of all carboxylates. Finally, a series of electrophilic Hammett constants derived from ^{13}C NMR chemical shift correlations further highlight the electron-donating potential of ligated borane substituents. Taken together, the pK_a measurements and Hammett constants confirm that ligated boranes are among the strongest of all organic inductive electron-donating groups.

Moving forward, the door is open to explore the synthetic utility of ligated α -boryl acetic acids. Conversion of the carboxylic acid functional group to an isocyanate (similar to Yudin's MIDA-boryl acids) through a Curtius rearrangement would allow access to further downstream scaffold diversity. Further, hydrolysis of the boryl amino esters prepared in Chapter 3 would give arise the opportunity for solution phase coupling reactions, and allow for the boryl amino acid analogy to be extended to NHC-boryl peptides.

5.0 EXPERIMENTAL

5.1 GENERAL INFORMATION

All reactions were performed in oven-dried glassware under an argon atmosphere. Chemicals and solvents were purchased from commercial suppliers and used as received, excepting as follows. Dichloromethane was dried by passing through an activated alumina column. All flash chromatography was performed by Combiflash Rf machine with pre-packed silica gel columns purchased from Teledyne Isco Inc. Melting points (mp) were determined with a Mel-Temp II apparatus. Proton (^1H), carbon (^{13}C), boron (^{11}B), and fluorine (^{19}F) nuclear magnetic resonance spectra (NMR) were performed on a Bruker Avance III 400 or 500. Chloroform (δ 7.26 ppm) or TMS (δ 0.00 ppm) was used as an internal standard for ^1H NMR spectra and CDCl_3 (δ 77.00 ppm) was used as an internal standard for ^{13}C NMR spectra. The following abbreviations were used to describe coupling: s = singlet, d = doublet, t = triplet, q = quartet, m = multiplet, br = broad. IR spectra were recorded as thin films (CH_2Cl_2) or neat on KBr plates on an ATI Mattson Genesis Series FTIR spectrometer. Compound names were generated from ChemBioDraw (version 14.0).

The characterization of NHC-boranes and the monitoring of their reactions is conducted by ^{11}B NMR spectroscopy. The NMR solvent used for NHC-borane samples is usually CDCl_3 . ^{11}B NMR chemical shifts are relative to $\text{Et}_2\text{O}-\text{BF}_3$ ($\delta = 0.00$ ppm). The N-heterocyclic carbene

ligand does not significantly affect the upfield ^{11}B chemical shift values. For example, the ^{11}B NMR resonances of all currently known NHC– BH_3 complexes appear between –32 and –38 ppm. This is upfield compared to $\text{Me}_2\text{O–BH}_3$ ($\delta = 2.5$ ppm), $\text{Me}_3\text{N–BH}_3$ ($\delta = -8.3$ ppm), $\text{Me}_2\text{S–BH}_3$ ($\delta = -20.1$ ppm), and in a similar range to $\text{Me}_3\text{P–BH}_3$ ($\delta = -36.8$ ppm).

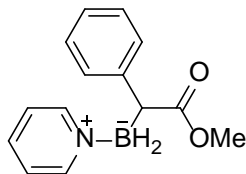
In contrast to the lack of information provided about the NHC group, the value of the ^{11}B chemical shift is often diagnostic of the nature of the atoms directly connected to boron. Downfield shifts are usually observed when the hydrogen atoms at the boron atom are substituted by alkyl groups or heteroatoms.⁶ For example, NHC– BH_2 –alkyl ^{11}B chemical shifts are between –20 and –30 ppm, which is more upfield compared to NHC– BH_2 –(N) compounds (–15 and –25 ppm) and NHC– BH_2 –(O) compounds (–5 and –15 ppm).

NHC– BH_3 resonances are split into 1:3:3:1 quartets because of spin–spin coupling of ^{11}B with the three equivalent protons with $^1J_{\text{B-H}}$ values in the range of 80–90 Hz. Similar coupling constants are observed for NHC– BH_2R (R = alkyl, aryl, CN), but when the boron atom is substituted with a more electronegative atom [NHC– BH_2X (X = O, N, halide)], the $^1J_{\text{B-H}}$ value increases to 90–110 Hz.

^{11}B NMR spectroscopy is an excellent tool for real-time monitoring of reaction progress because excellent spectra can be recorded in non-deuterated solvents and because the ^{11}B chemical shift depends strongly on the boron substituents

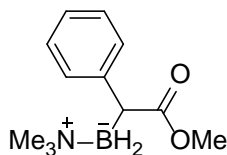
5.2 EXPERIMENTAL DATA FOR CHAPTER 1

Characterization spectra for Chapter 1 compounds can be viewed in the Supporting Information of: Allen, T. H.; Curran, D. P. *J. Org. Chem.* **2016**, *81*, 2094–2098.



(2-Methoxy-2-oxo-1-phenylethyl)(1 λ^4 -pyridin-1-yl)dihydroborate (51):

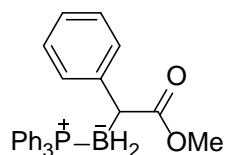
Pyridine-borane (93.0 mg, 1.00 mmol, 1.0 equiv) and Rh₂(esp)₂ (7.9 mg, 0.01mmol, 1 mol%) were dissolved in dry CH₂Cl₂ (5 mL) under argon. A solution of methyl 2-diazo-2-phenylacetate (211.0 mg, 1.20 mmol, 1.2 equiv) in dry CH₂Cl₂ (5 mL) was added via syringe pump over a period of 2 h. The solution color transitioned from light green to orange. ¹¹B NMR spectrum of the crude product showed 79% conversion to the desired single-insertion product. The reaction mixture was concentrated under vacuum and purified by flash chromatography (hexane: ethyl acetate, 1:1) to yield 189.4 mg (79%) of **51** as a colorless oil: ¹H NMR (400 MHz, CDCl₃) δ 8.21–8.20 (m, 2H), 7.95–7.91 (m, 1H), 7.43–7.39 (m, 2H), 7.17–7.11 (m, 1H), 3.60 (s, 3H), 3.40 (s, 1H); ¹³C NMR (100 MHz, CDCl₃) δ 178.1, 147.4, 142.5, 140.0, 127.8, 127.7, 124.8, 124.3, 50.8, 48.8 (weak); ¹¹B NMR (128 MHz, CDCl₃) δ -2.8 (t, J_{BH} = 101 Hz); IR (neat) 3059, 3022, 2947, 2393, 2340, 1710, 1622, 1599, 1458, 1362; HRMS (ESI) m/z (M^+ + Na) calcd for C₁₄H₁₆O₂NBNa 264.1166, found 264.1164.



(2-Methoxy-2-oxo-1-phenylethyl)(trimethyl- λ^4 -azanyl)dihydroborate (48):

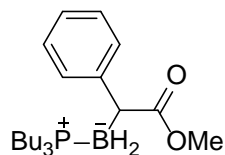
Reaction of trimethylamine-borane (75.0 mg, 1.00 mmol), Rh₂(esp)₂ (7.9 mg, 0.01mmol) and methyl 2-diazo-2-phenylacetate (211.0 mg, 1.20 mmol) according to the general procedure.

^{11}B NMR spectrum of the crude product showed 72% conversion to the desired single-insertion product. The residue was purified by flash chromatography (hexane: ethyl acetate, 1:1) to yield 95.0 mg (43%) of **48** as a white solid: ^1H NMR (400 MHz, CDCl_3) δ 7.45–7.43 (m, 2H), 7.26–7.22 (m, 2H), 7.12–7.09 (m, 1H), 3.62 (s, 3H), 3.26 (s, 1H), 2.51 (s, 9H); ^{13}C NMR (100 MHz, CDCl_3) δ 178.5, 143.4, 129.1, 127.8, 124.9, 52.4, 51.2, 46.5 (weak); ^{11}B NMR (160 MHz, CDCl_3) δ -1.5 (t, $J_{\text{BH}} = 99$ Hz); IR (film) 3022, 2946, 2367, 2309, 1715, 1480, 1451, 1353, 1171 cm^{-1} ; mp 95-97 $^\circ\text{C}$; HRMS (ESI) m/z ($\text{M}^+ + \text{Na}$) calcd for $\text{C}_{12}\text{H}_{20}\text{O}_2\text{NBNa}$ 244.1479, found 244.1476.



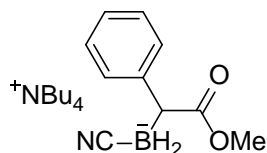
(2-Methoxy-2-oxo-1-phenylethyl)(triphenyl- λ^4 -phosphanyl)dihydroborate (33):

Reaction of triphenylphosphine-borane (285.0 mg, 1.00 mmol), $\text{Rh}_2(\text{esp})_2$ (32 mg, 0.04mmol) and methyl 2-diazo-2-phenylacetate (211.0 mg, 1.20 mmol) according to the general procedure. ^{11}B NMR spectrum of the crude product showed 71% conversion to the desired single-insertion product. The residue was purified by flash chromatography (hexane: ethyl acetate, 3:2) to yield 211.0 mg (50%) of **33** as an orange solid: ^1H NMR (400 MHz, CDCl_3) δ 7.49–7.47 (m, 9H), 7.43–7.39 (m, 6H), 7.35–7.32 (m, 2H), 7.17–7.13 (m, 2H), 7.06–7.02 (m, 1H), 3.33 (s, 1H), 3.17 (s, 3H); ^{13}C NMR (125 MHz, CDCl_3) δ 178.8, 178.7, 144.4, 133.5, 131.3, 128.9, 127.8, 127.7, 127.4, 124.8, 50.5, 41.7 (weak); ^{11}B NMR (160 MHz, CDCl_3) δ -23.4 (br); IR (film) 3058, 3023, 2946, 2375, 1720, 1484, 1436, 1136; mp 110-115 $^\circ\text{C}$; HRMS (ESI) m/z ($\text{M}^+ + \text{Na}$) calcd for $\text{C}_{27}\text{H}_{26}\text{O}_2\text{BNaP}$ 447.1656, found 447.1646.



(2-Methoxy-2-oxo-1-phenylethyl)(tributyl- λ^4 -phosphanyl)dihydroborate (50):

Reaction of tributylphosphine-borane (216.0 mg, 1.00 mmol), $\text{Rh}_2(\text{esp})_2$ (32 mg, 0.04 mmol) and methyl 2-diazo-2-phenylacetate (211.0 mg, 1.20 mmol) according to the general procedure. ^{11}B NMR spectrum of the crude product showed 86% conversion to the desired single-insertion product. The residue was purified by flash chromatography (hexane: acetone, 30:1) to yield 110.0 mg (30%, 97% purity) of **50** as an orange oil: ^1H NMR (500 MHz, CDCl_3) δ 7.43–7.41 (m, 2H), 7.23–7.20 (m, 2H), 7.32–7.35 (m, 2H), 7.10–7.07 (m, 1H), 3.62 (s, 1H), 3.21–3.16 (m, 1H), 1.43–1.29 (m, 20H), 0.88 (t, $J = 7$ Hz, 9H); ^{13}C NMR (125 MHz, CDCl_3) δ 179.3, 179.2, 144.4, 144.4, 128.7, 127.6, 124.8, 51.0, 41.9, 24.6, 24.3, 24.2, 20.7, 20.5, 13.4; ^{11}B NMR (160 MHz, CDCl_3) δ -25.8 (br); IR (film) 2957, 2932, 2871, 2356, 1719, 1494, 1276, 1014, 700; HRMS (ESI) m/z ($\text{M}^+ + 1$) calcd for $\text{C}_{21}\text{H}_{39}\text{O}_2\text{BP}$ 365.2775, found 365.2779.



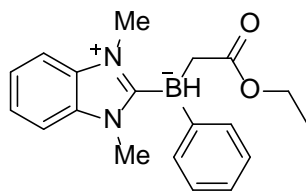
Tetrabutylammonium cyano(2-methoxy-2-oxo-1-phenylethyl)dihydroborate (55):

Tetrabutylammonium cyanoborohydride (283.0 mg, 1.00 mmol) and $\text{Rh}_2(\text{esp})_2$ (7.9 mg, 0.01 mmol) were dissolved in dry CH_2Cl_2 (2 mL), under argon. A solution of methyl 2-diazo-2-phenylacetate (211.0 mg, 1.20 mmol) in CH_2Cl_2 (2 mL) was added via syringe pump over 2h. The reaction mixture color transitioned from light blue to pink. ^{11}B NMR spectrum of the crude

product showed 86% conversion to the desired single-insertion product and 14% of the double-insertion product. Isolation of pure insertion product **55** by flash chromatography was not attempted, but crude ^1H and ^{13}C NMR spectra supported the structure: ^1H NMR (400 MHz, CDCl_3) δ 7.43–7.45 (m, 2H), 7.13–7.17 (m, 2H), 6.98–7.03 (m, 1H), 3.57 (s, 3H), 3.16 (br, 1H), 3.00–3.04 (m, 8H), 1.46–1.54 (m, 8H), 1.33–1.38 (m, 8H), 0.97 (t, $J = 7$ Hz, 12H); ^{13}C NMR (100 MHz, CDCl_3) δ 180.1, 146.4, 129.2, 128.7, 123.7, 58.4, 50.4, 44.7 (weak), 23.8, 19.6, 13.6; ^{11}B NMR (160 MHz, CDCl_3) δ -27.2 (t, $J_{\text{BH}} = 94$ Hz); HRMS (ESI) m/z (M^+) calcd for $\text{C}_{10}\text{H}_{11}\text{O}_2\text{NB}$ 188.0877, found 188.0881.

General procedure for the competitive insertions between X–BH₃ **1 with X–BH₃ **2****

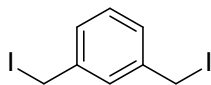
Pyridine-borane **4** (34.5.0 mg, 0.4 mmol, 2.0 equiv) and NHC-borane **5** (41.2 mg, 0.4 mmol, 2.0 equiv) were dissolved in dry CH_2Cl_2 (1 mL) under argon. A crude ^{11}B NMR spectrum of the reaction mixture was obtained prior to addition of the diazo substrate and catalyst to determine the initial ^{11}B NMR integration of both borane species. After addition of $\text{Rh}_2(\text{esp})_2$ (2.8 mg, 0.02 mol%), a solution of ethyl 2-diazo-2-phenylacetate diazoacetate **31** (38.5 mg, 0.2 mmol, 1.0 equiv) in 1mL CH_2Cl_2 was added by syringe pump to the reaction solution. After 2 h, the reaction mixture was concentrated and an ^{11}B NMR spectrum was recorded.



(1,3-Dimethyl-1*H*-benzo[*d*]imidazol-3-ium-2-yl)(2-ethoxy-2-oxoethyl)(phenyl)hydroborate

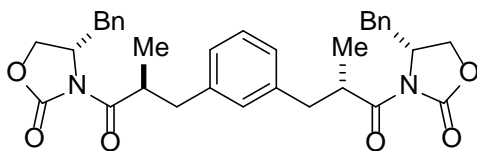
(68):

The borane adduct (1.0 equiv) and Rh₂esp₂ (3.3 mg, 0.085 mmol, 0.05 equiv) were dissolved in dry DCM (4 mL) under argon. A solution of the ethyl diazoacetate (14 mg, 0.102 mmol, 1.20 equiv) in dry DCM (5 mL) was added via syringe pump over a period of 1 h under reflux. The solution color transitioned from light green to dull green. ¹¹B NMR spectrum of the crude product showed 46% conversion to the desired single-insertion product. The mixture was concentrated and purified by flash chromatography to give the product. The reaction mixture was concentrated under vacuum and purified by flash chromatography (hexane: ethyl acetate, 4:1) to yield 10.0 mg (37%) of product **68** as a white solid. Insertion product enantiomers were resolved by HPLC using an (*S,S*)-Whelk-O1 column. Column conditions were as follows: 85% IPA/Hexanes, 1.0 mL/min flow rate, 10 μL injection volume: ¹H NMR (300 MHz, CDCl₃) δ 7.41–7.44 (m, 4H), 7.15–7.19 (m, 4H), 7.04–7.09 (m, 1H), 3.87 (s, 6H), 3.80 (q, *J* = 14, 7 Hz, 2H), 2.30 (br, 1H), 2.03 (br, 1H), 0.89 (t, *J* = 7 Hz, 3H); ¹³C NMR (100 MHz, CDCl₃) δ 180.3, 133.3, 132.6, 127.4, 124.4, 124.3, 111.0, 58.7, 32.6, 14.2; ¹¹B NMR (128 MHz, CDCl₃) δ –18.8 (d, *J*_{BH} = 88 Hz).



1,3-Bis(iodomethyl)benzene (74):

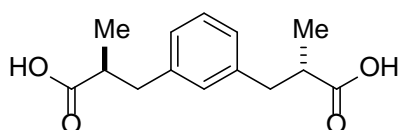
Sodium iodide (6.30 g, 42.0 mmol, 10.0 equiv) was added to a solution of 1,3-bis(bromomethyl)benzene (1.11 g, 4.20 mmol, 1.00 equiv) in acetone (100 mL). The solution was refluxed for 18 h in a dark fume hood. The solvent was removed under reduced pressure and the light yellow crude solid was dissolved in DCM/water (1:1). To remove iodine impurities, both organic and aqueous layers were washed with sat. Na₂S₂O₃. The combined organic layers were washed with brine and dried over Na₂SO₄. Concentration under vacuum afforded 1.27 g of bis(iodomethyl)benzene **74** as a light yellow solid. The compound was stored wrapped in an aluminum foil wrapped flask under argon at 0 °C until needed for alkylation: ¹³C NMR (125 MHz, CDCl₃) δ 139.9, 129.3, 128.9, 128.3, 4.8.



(4S,4'S)-3,3'-((2S,2'S)-3,3'-(1,3-Phenylene)bis(2-methylpropanoyl))bis(4-benzylloxazolidin-2-one) (71):

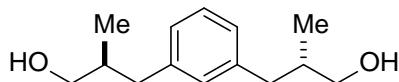
To oven dried 1L round bottom flask, added freshly distilled THF (150 mL) and (*S*)-4-benzyl-3-propionyloxazolidin-2-one (1.82 g, 7.80 mmol, 2.2 equiv). Cooled to -78 °C and added NaHMDS (4.26 mL, 2 M in THF, 8.52 mmol, 2.4 equiv) dropwise. Allowed to stir at -78 °C for 30 min. Added freshly prepared diiodomethyl benzene (1.27 g, 3.55 equiv, 1.0 equiv) in 10mL THF and stirred for 60 min while warming from -78 °C to 0 °C. After 60 min, warmed to rt and stirred for 18 h. Desired product was observed in ¹H NMR spectrum of the crude product

mixture. Quenched reaction with water, extracted with ether (x3), washed org layer with sat. $\text{Na}_2\text{S}_2\text{O}_4$ and brine. Dried over Na_2SO_4 and concentrated under reduced pressure. Purified by flash chromatography (100% EtOAc) to yield 1.00 g bis-alkylated product **71** as a light yellow, foamy solid (49%): ^1H NMR (400 MHz, CDCl_3) δ 7.07–7.30 (m, 14H), 4.63–4.65 (m, 2H), 4.08–4.18 (m, 6H), 3.10–3.16 (m, 4H), 2.61–2.67 (m, 2H), 2.51–2.57 (m, 2H), 1.16 (d, $J = 7$ Hz, 6H); ^{13}C NMR (100 MHz, CDCl_3) δ 176.5, 153.0, 139.2, 135.3, 130.5, 129.4, 128.9, 128.3, 127.4, 127.3, 65.9, 55.2, 39.7, 39.5, 37.8, 16.6.



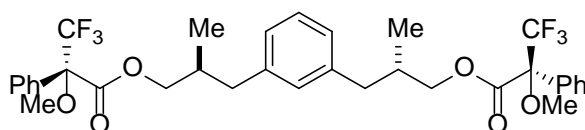
(2*S*,2'*S*)-3,3'-(1,3-Phenylene)bis(2-methylpropanoic acid) (72):

Dissolved bis-alkylated compound (98 mg, 0.17 mmol, 1.0 equiv) in 5 mL THF from SPS. Cooled to 0 °C and added 0.16 mL H_2O_2 (30 wt%, 7.8 equiv) dropwise, followed by addition of $\text{LiOH}\cdot\text{H}_2\text{O}$ in 2 mL H_2O (29 mg, 0.69 mmol, 4.0 equiv). Allowed to stir at 0 °C for 5 h. Quenched with 1.5 mL sat. NaHCO_3 and 1.5 mL sat. Na_2SO_4 . Removed solvent *in vacuo* and diluted with H_2O . Extracted aqueous layer with DCM (x3). Acidified aq. layer to ~1.5 pH with 6 M HCl. Extracted aq. layer with EtOAc (x3). Dried org. layers over Na_2SO_4 , filtered and concentrated to yield methyl diacid **72** as a colorless oil (85%): ^1H NMR (400 MHz, CDCl_3) δ 7.19–7.22 (m, 1H), 7.00–7.04 (m, 3H), 2.93–3.01 (m, 2H), 2.67–2.78 (m, 4H), 1.15 (d, $J = 7$ Hz, 6H); ^{13}C NMR (100 MHz, CDCl_3) δ 182.2, 139.0, 129.5, 128.4, 127.3, 41.3, 39.4, 16.4.



(2*S*,2'*S*)-3,3'-(1,3-Phenylene)bis(2-methylpropan-1-ol) (75):

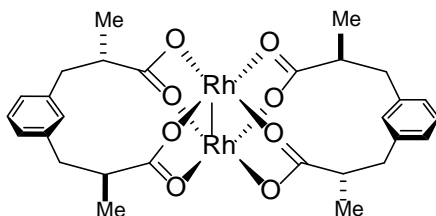
To oven dried 20 dram vial, added diacid **72** (0.49 mg, 0.20 mmol, 1.0 equiv) and freshly distilled THF (1.5 mL) under an argon atmosphere. Cooled to 0 °C and added LAH (0.6 mL, 1 M in diethyl ether, 3.0 equiv) dropwise. A white precipitate immediately formed and the reaction mixture was stirred at 0 °C for 3 h. The reaction mixture was quenched with 1 N HCl and the white precipitate was filtered. The crude product mixture was extracted with EtOAc (x3). Org layers were washed with brine and dried over Na₂SO₄, filtered and concentrated. Purified by flash chromatography (1:1, hexanes : EtOAc) to yield the dialcohol **75** (30%) as a colorless oil: ¹H NMR (300 MHz, CDCl₃) δ 7.17–7.26 (m, 1H), 6.99–7.02 (m, 3H), 3.43–3.55 (m, 4H), 2.69–2.75 (m, 2H), 2.38–2.45 (m, 2H), 1.88–1.99 (m, 2H), 0.91 (d, *J* = 7 Hz, 6H); ¹³C NMR (75 MHz, CDCl₃) δ 140.6, 130.0, 128.2, 126.7, 67.7, 39.7, 37.8, 16.5.



(2*S*,2'*S*)-1,3-Phenylenebis(2-methylpropane-3,1-diyl)(2*S*,2'*S*)-bis(3,3,3-trifluoro-2-methoxy-2-phenylpropanoate) (76):

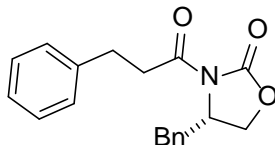
To 20 dram vial containing dialcohol **75** (13 mg, 0.06 mmol, 1.0 equiv) and 2 mL DCM, (*S*)-MTPA (85 mg, 0.36 mmol, 6.2 equiv), 1 M DCC (0.36 mL, 0.36 mmol, 6.2 equiv) and DMAP (44 mg, 0.36 mmol, 6.2 equiv) were added sequentially. White precipitate formed upon addition of DMAP. Allowed to stir for 45 h at rt and under native atmosphere. Reaction progress was monitored by TLC analysis; after 45 h, dialcohol spot (PMA stain) had disappeared. Filtered

dicyclohexyl urea and recorded ^1H NMR spectrum of crude rxn mixture showed full conversion of dialcohol to diester. Purified crude residue by flash chromatography. Ester product **76**, DCC and MTPA co-eluted at 20% EtOAc/Hex, while excess DMAP was removed: ^1H NMR (500 MHz, CDCl_3) δ 7.41–7.43 (m, 10H), 7.15–7.18 (m, 1H), 6.89–6.91 (m, 2H), 6.83 (s, 1H), 4.12–4.19 (m, 4H), 3.57 (s, 6H), 2.62–2.66 (m, 2H), 2.38–2.42 (m, 2H), 2.10–2.16 (m, 2H), 0.92 (d, $J = 7$ Hz, 6H); ^{13}C (125 MHz, CDCl_3) δ 166.5, 139.5, 132.3, 129.8, 129.6, 128.7, 128.4, 127.3, 126.9, 70.2, 55.4, 39.2, 34.9, 25.4, 25.2; ^{19}F NMR (470 MHz, CDCl_3) δ -71.4.



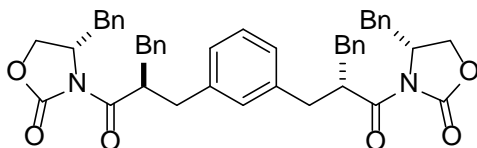
Bis[rhodium((2S,2'S)-3,3'-(1,3-phenylene)bis(2-methylpropanoic acid))] (73):

A 10 mL round bottom equipped with a reflux condenser was charged with rhodium(II) trifluoroacetate (38 mg, 0.14 mmol, 1.0 equiv), 5.0 mL DCE and methyl diacid **72** (0.022 mL, 1 M in DCE, 0.5 equiv). Heated under reflux for 1 h. Cooled reaction mixture to rt and added additional 0.5 eq of diacid solution. Repeated heating/cooling cycle for additional 2 equiv diacid total in 0.5 eq aliquots, and continued heating for 12 h. Purified the crude product mixture by flash chromatography. First eluted band at 20% EtOAc/Hexanes was monochelated rhodium **77** (66%). Fully complexed rhodium **73** eluted at 30% EtOAc/Hexanes and 11.0 mg (34%) of the bright green solid was obtained: ^1H NMR (300 MHz, CD_3CN) δ 7.08–7.13 (m, 2H), 6.87–6.90 (m, 4H), 6.83 (s, 2H), 2.76–2.82 (m, 4H), 2.48–2.82 (m, 8H), 0.87 (d, $J = 7$ Hz, 12H); ^{13}C NMR (75 MHz, CD_3CN) δ 196.1, 140.0, 131.4, 128.7, 128.0, 44.9, 40.2, 17.1; HRMS (ESI) m/z ($\text{M}^+ + 1$) calcd for $\text{C}_{28}\text{H}_{33}\text{O}_8\text{Rh}_2$ 703.0280, found 703.0240.



(S)-4-Benzyl-3-(3-phenylpropanoyl)oxazolidin-2-one (79):

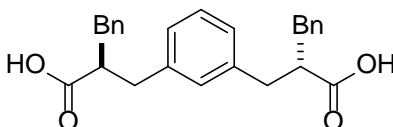
To oven dried round bottom flask flushed with argon, added 10 mL freshly distilled THF and (S)-4-benzyl-3-(3-phenylpropanoyl)oxazolidin-2-one (144 mg, 1.00 mmol, 1.0 equiv). Cooled to $-78\text{ }^{\circ}\text{C}$ and added 0.4 mL nBuLi (2.5 M, 1.0 equiv) dropwise. Allowed to stir for 15 min. Added hydrocinnamoyl chloride (0.17 mL, 1.10 mmol, 1.0 equiv) dropwise, warmed to $0\text{ }^{\circ}\text{C}$ and stirred for 30 min. Added NaHCO_3 and stirred at $0\text{ }^{\circ}\text{C}$ for 15 min. Extracted with DCM (x3). Washed org layers w/ brine and dried over Na_2SO_4 , filtered and concentrated under reduced pressure. Purification by flash chromatography gave 248 mg (80%) benzyl chiral auxiliary **79** as a white solid: ^1H NMR (400 MHz, CDCl_3) δ 7.16–7.34 (m, 10H), 4.63–4.69 (m, 1H), 4.15–4.20 (m, 2H), 3.21–3.36 (m, 3H), 3.01–3.05 (m, 2H), 2.72–2.78 (m, 1H); ^{13}C NMR (100 MHz, CDCl_3) δ 172.4, 153.4, 140.4, 135.2, 129.4, 128.9, 128.6, 128.5, 127.3, 126.3, 66.2, 55.1, 37.8, 37.1, 30.2.



(4S,4'S)-3,3'-((2S,2'S)-3,3'-(1,3-Phenylene)bis(2-benzylpropanoyl))bis(4-benzyl-3-(3-phenylpropanoyl)oxazolidin-2-one) (80):

To oven dried 300 mL round bottom flask, added freshly distilled THF (150 mL) and (S)-4-benzyl-3-(3-phenylpropanoyl)oxazolidin-2-one (2.69 g, 8.70 mmol, 2.2 equiv). Cooled to $-78\text{ }^{\circ}\text{C}$ and added NaHMDS (4.74 mL, 2 M in THF, 9.49 mmol, 2.4 equiv) dropwise. Allowed to stir at $-78\text{ }^{\circ}\text{C}$ for 30 min. Added freshly prepared diiodomethyl benzene (1.42 g, 3.95 equiv, 1.0

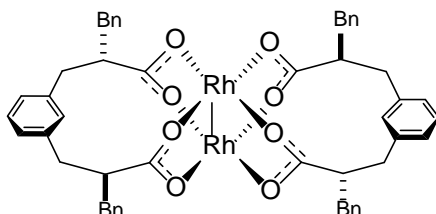
equiv) in 10 mL THF and stirred for 60 min while warming from $-78\text{ }^{\circ}\text{C}$ to $0\text{ }^{\circ}\text{C}$. After 60 min, warmed to rt and stirred for 20 h. Desired product was observed in ^1H NMR spectrum of the crude product mixture. Quenched reaction with water, extracted with ether (x3), washed org layer with sat. $\text{Na}_2\text{S}_2\text{O}_4$ and brine. Dried over Na_2SO_4 and concentrated under reduced pressure. Purified by flash chromatography (100% EtOAc) to yield 1.99 g of bis-alkylated product **80** as a colorless, foamy solid (70%): ^1H NMR (400 MHz, CDCl_3) δ 7.14–7.23 (m, 20H), 6.96–6.98 (m, 4H), 4.54–4.58 (m, 2H), 4.34–4.39 (m, 2H), 3.88–3.91 (m, 2H), 3.72–3.76 (m, 2H), 3.10–3.15 (m, 2H), 2.93–3.00 (m, 4H), 2.76–2.81 (m, 4H), 2.39–2.45 (m, 2H); ^{13}C NMR (100 MHz, CDCl_3) δ 175.2, 152.7, 139.0, 138.8, 135.2, 130.5, 129.3, 129.0, 128.8, 128.5, 128.3, 127.3, 127.1, 126.3, 65.6, 55.1, 46.2, 38.5, 38.0, 37.5; HRMS (ESI) m/z ($\text{M}^+ + 1$) calcd for $\text{C}_{46}\text{H}_{45}\text{O}_6\text{N}_2$ 721.3272, found 721.3285.



(2S,2'S)-3,3'-(1,3-Phenylene)bis(2-benzylpropanoic acid) (81):

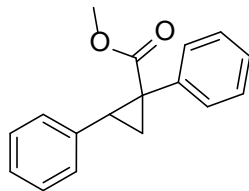
Dissolved benzyl bis-alkylated compound (1.97 g, 2.73 mmol, 1.0 equiv) in 100 mL THF from SPS. Cooled to $0\text{ }^{\circ}\text{C}$ and added 0.64 mL H_2O_2 (30 wt%, 7.8 equiv) dropwise, followed by addition of $\text{LiOH}\cdot\text{H}_2\text{O}$ in 40 mL H_2O (468 mg, 10.9 mmol, 4.0 equiv). Allowed to stir at $0\text{ }^{\circ}\text{C}$ for 5 h. Quenched with 30 mL sat. NaHCO_3 and 30 mL sat. Na_2SO_4 . Removed solvent *in vacuo* and diluted with H_2O . Extracted aqueous layer with DCM (x3). Acidified aq. layer to ~ 1.5 pH with 6 M HCl. Extracted aq. layer with EtOAc (x3). Dried org. layers over Na_2SO_4 , filtered and concentrated to yield benzyl diacid **81** as a colorless oil (83%): ^1H NMR (400 MHz, CDCl_3) δ 7.20–7.25 (m, 4H), 7.14–7.18 (m, 7H), 6.97–6.98 (m, 3H), 2.92–3.00 (m, 4H), 2.85–2.88 (m,

2H), 2.72–2.79 (m, 4H); ^{13}C NMR (100 MHz, CDCl_3) δ 180.5, 138.7, 138.7, 129.5, 128.9, 128.5, 128.5, 127.3, 126.5, 49.0, 37.8, 37.5; HRMS (ESI) m/z ($\text{M}^+ - 1$) calcd for $\text{C}_{26}\text{H}_{25}\text{O}_4$ 401.1747, found 401.1759.



Bis[rhodium(2*S*,2'*S*)-3,3'-(1,3-phenylene)bis(2-benzylpropanoic acid)] (82**):**

A 10 mL round bottom equipped with a reflux condenser was charged with rhodium(II) trifluoroacetate (202 mg, 0.29 mmol, 1.0 equiv), 20 mL DCE and benzyl diacid (0.58 mL, 1 M in DCE, 1.0 equiv). Heated under reflux for 1 h. Cooled reaction mixture to rt and added additional 1.0 equiv of diacid solution and continued heating for 18 h. Purified the crude product mixture by flash chromatography. First eluted band at 20% EtOAc/Hexanes was monochelated rhodium dimer (87%). Fully complexed rhodium **82** eluted at 30% EtOAc/Hexanes and 38.5 mg (13%) of the bright green solid was obtained: ^1H NMR (500 MHz, CD_3CN) δ 7.25–7.26 (m, 8H), 7.14–7.18 (m, 12H), 7.07–7.10 (m, 2H), 6.84 (s, 2H), 6.77–6.84 (m, 4H), 2.59–2.67 (m, 12H), 2.49–2.53 (m, 4H), 2.37–2.42 (m, 4H); ^{13}C NMR (125 MHz, CD_3CN) δ 195.4, 141.2, 140.1, 132.2, 130.5, 129.6, 129.3, 128.3, 127.4, 52.1, 38.0, 37.7; HRMS (ESI) m/z ($\text{M}^+ + 1$) calcd for $\text{C}_{52}\text{H}_{49}\text{O}_8\text{Rh}_2$ 1007.1516, found 1007.1466.



Methyl 1,2-diphenylcyclopropane-1-carboxylate (83):

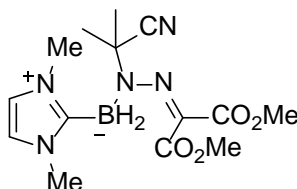
An oven dried 10 mL round bottom was charged with pentane (1 mL), styrene (0.11 mL, 1.00 mmol, 5.0 equiv) and $\text{Rh}_2(\text{S-DOSP})_4$ (3.7 mg, 1 mol%). Dissolved phenyldiazo **31** in 1 mL pentane and added via syringe pump over 1 h at rt. Concentrated crude product under reduced pressure and purified the residue by flash column chromatography (10% EtOAc/Hexanes) to give 30.4 mg (60%) cyclopropane **83** as a white solid. Column conditions were as follows: 1% IPA/Hexanes, 1.0 mL/min flow rate, 10 μL injection volume: ^1H NMR (400 MHz, CDCl_3) δ 7.13–7.14 (m, 3H), 7.02–7.07 (m, 5H), 6.76–6.79 (m, 2H), 3.67 (s, 3H), 3.10–3.15 (m, 1H), 2.13–2.17 (m, 1H), 1.87–1.91 (m, 1H); ^{13}C NMR (100 MHz, CDCl_3) δ 174.3, 136.3, 134.7, 131.9, 128.0, 127.6, 127.6, 127.0, 126.3, 52.6, 37.4, 33.1, 20.4.

General procedure for rhodium(II) catalyzed enantioselective B–H insertion

The borane adduct (1.0 equiv) and chiral rhodium(II) catalyst (0.01 equiv) were dissolved in dry DCM (5 mL) under argon. A solution of the diazo compound in dry DCM (5 mL) was added via syringe pump over a period of 2 h. The solution color transitioned from light green to orange. The reaction mixture was concentrated under vacuum and the crude ^{11}B NMR spectrum was recorded. The mixture was concentrated and purified by flash chromatography to give the product. Insertion product enantiomers were resolved by HPLC using an (*S,S*)-Whelk-O1 column. Column conditions were as follows: 30% IPA/Hexanes, 1.0 mL/min flow rate, 10 μL injection volume.

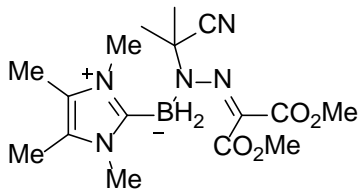
5.3 EXPERIMENTAL DATA FOR CHAPTER 2

Characterization spectra for Chapter 2 compounds can be viewed in the Supporting Information of: Allen, T. H.; Geib, S. J.; Curran, D. P. *Organometallics* **2016**, *35*, 2975–2979.



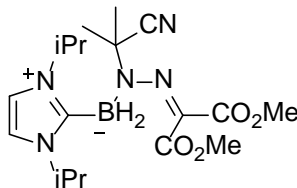
(1-(2-Cyanopropan-2-yl)-2-(1,3-dimethoxy-1,3-dioxopropan-2-ylidene)hydrazinyl)(1,3-dimethyl-1H-imidazol-3-ium-2-yl)dihydroborate (91):

In a pressure tube, (1,3-dimethyl-1H-imidazol-3-ium-2-yl)trihydroborate (301.0 mg, 2.71 mmol, 1.0 equiv) was dissolved in degassed trifluorotoluene (27 mL). Dimethyl diazomalonate (515.0 mg, 3.25 mmol, 1.2 equiv) and AIBN (545.0 mg, 3.25 mmol, 1.2 equiv) were added and the reaction was heated to 120 °C for 2 h. The crude reaction mixture turned a yellow-orange. An ^{11}B NMR spectrum of the crude product showed 95% conversion of the NHC–BH₃ starting material. The reaction mixture was concentrated under vacuum and purified by flash chromatography (ethyl acetate 100%) to yield 361.0 mg (40%) of **91** as a yellow solid: ^1H NMR (500 MHz, CDCl₃) δ 1.71 (s, 6H), 3.45 (s, 3H), 3.66 (s, 6H), 3.72 (s, 3H), 6.81 (s, 2H); ^{13}C NMR (125 MHz, CDCl₃) δ 26.6, 35.4, 51.1, 51.5, 61.8, 118.8, 121.0, 123.1, 165.0, 167.1; ^{11}B NMR (160 MHz, CDCl₃) δ -17.9 (br t); IR (film) 2949, 2368, 1720, 1534, 1436, 1316, 1234, 1169, 734 cm⁻¹; mp 113–116 °C; HRMS (ESI) m/z ($\text{M}^+ - 1$) calcd for C₁₄H₂₁BN₅O₄ 334.1687, found 334.1686.



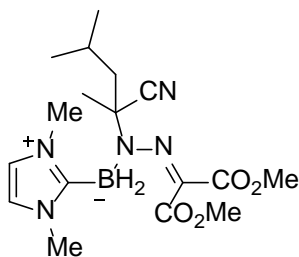
(1-(2-Cyanopropan-2-yl)-2-(1,3-dimethoxy-1,3-dioxopropan-2-ylidene)hydrazinyl)(1,3,4,5-tetramethyl-1*H*-imidazol-3-ium-2-yl)dihydroborate (93):

In a pressure tube, (1,3,4,5-tetramethyl-1*H*-imidazol-3-ium-2-yl)trihydroborate (138.0 mg, 1.00 mmol, 1.0 equiv) was dissolved in degassed trifluorotoluene (10 mL). Dimethyl diazomalonate (190.0 mg, 1.20 mmol, 1.2 equiv) and AIBN (201.0 mg, 1.20 mmol, 1.2 equiv) were added and the reaction was heated to 120 °C for 2 h. The crude reaction mixture turned a yellow-orange. An ^{11}B NMR spectrum of the crude product showed 92% conversion of the NHC– BH_3 starting material. The reaction mixture was concentrated under vacuum and purified by flash chromatography (ethyl acetate 100%) to yield 118.0 mg (33%) of **93** as a yellow solid: ^1H NMR (500 MHz, CDCl_3) δ 1.73 (s, 6H), 2.12 (s, 6H), 3.47 (s, 3H), 3.51 (s, 6H), 3.74 (s, 3H); ^{13}C NMR (125 MHz, CDCl_3) δ 8.7, 26.8, 31.6, 51.2, 51.6, 61.8, 118.8, 123.2, 123.9, 165.1, 167.3; ^{11}B NMR (160 MHz, CDCl_3) δ –17.7 (br t); mp 129–131 °C; HRMS (ESI) m/z ($\text{M}^+ - 1$) calcd for $\text{C}_{16}\text{H}_{27}\text{BN}_5\text{O}_4$ 364.2151, found 364.2141.



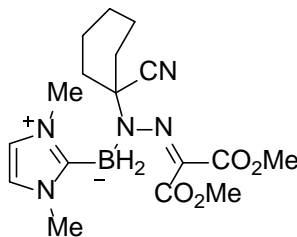
(1-(2-Cyanopropan-2-yl)-2-(1,3-dimethoxy-1,3-dioxopropan-2-ylidene)hydrazinyl)(1,3-diisopropyl-1*H*-imidazol-3-ium-2-yl)dihydroborate (95**):**

In a pressure tube, (1,3-diisopropyl-1*H*-imidazol-3-ium-2-yl)trihydroborate (166.0 mg, 0.54 mmol, 1.0 equiv) was dissolved in degassed trifluorotoluene (5 mL). Diazo dimethyl malonate (102.0 mg, 0.65 mmol, 1.2 equiv) and AIBN (106.0 mg, 0.65 mmol, 1.2 equiv) were added and the reaction was heated to 120 °C for 2 h. The crude reaction mixture turned a yellow-orange. An ¹¹B NMR spectrum of the crude product showed 78% conversion of the NHC–BH₃ starting material. The reaction mixture was concentrated under vacuum and purified by flash chromatography (ethyl acetate 100%) to yield 91.0 mg (43%) of **95** as a yellow solid: ¹H NMR (500 MHz, CDCl₃) δ 1.43 (d, *J*_{CH} = 6.5 Hz, 12H), 1.72 (s, 6H), 3.51 (s, 3H), 3.74 (s, 3H), 4.79 (septet, *J*_{CH} = 7.0 Hz, 2H), 7.01 (s, 2H); ¹³C NMR (125 MHz, CDCl₃) δ 23.0, 23.1, 26.9, 48.8, 51.1, 51.6, 61.8, 116.1, 118.8, 123.4, 165.1, 167.0; ¹¹B NMR (160 MHz, CDCl₃) δ –17.8 (br t); mp 136–139 °C; HRMS (ESI) *m/z* (*M*⁺ + 1) calcd for C₁₈H₃₁O₄N₅B 392.2464, found 392.2446.



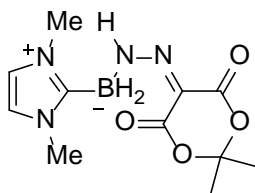
(1-(2-Cyano-4-methylpentan-2-yl)-2-(1,3-dimethoxy-1,3-dioxopropan-2-ylidene)hydrazinyl)(1,3-dimethyl-1*H*-imidazol-3-ium-2-yl)dihydroborate (96):

In a pressure tube, (1,3-dimethyl-1*H*-imidazol-3-ium-2-yl)trihydroborate (22.0 mg, 0.20 mmol, 1.0 equiv) was dissolved in degassed trifluorotoluene (2.0 mL). Diazo dimethyl malonate (43.0 mg, 0.24 mmol, 1.2 equiv) and V-65 (59.0 mg, 0.24 mmol, 1.2 equiv) were added and the reaction was heated to 120 °C for 2 h. The crude reaction mixture turned a yellow-orange. An ¹¹B NMR spectrum of the crude product showed 50% conversion of the NHC-BH₃ starting material. The reaction mixture was concentrated under vacuum and purified by flash chromatography (ethyl acetate : hexanes 3:2) to yield 13.0 mg (18%) of **96** as a yellow solid: ¹H NMR (500 MHz, CDCl₃) δ 1.01 (dd, *J*_{CH} = 6.5 Hz, 6H), 1.75 (s, 3H), 1.85 (m, 2H), 2.04 (m, 1H), 3.48 (s, 3H), 3.67 (s, 6H), 3.74 (s, 3H), 6.80 (s, 2H); ¹³C NMR (125 MHz, CDCl₃) δ 23.8, 24.1, 24.7, 25.3, 35.5, 47.5, 51.2, 51.6, 65.2, 118.3, 121.0, 122.9, 165.1, 167.4; ¹¹B NMR (160 MHz, CDCl₃) δ -18.0 (br t); mp 128–130 °C; HRMS (ESI) *m/z* (*M*⁺ + 1) calcd for C₁₇H₂₉O₄N₅B 378.2307, found 378.2295.



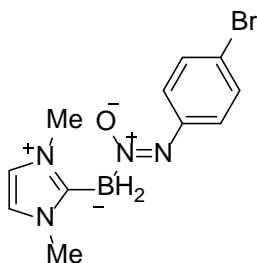
(1-(1-Cyanocyclohexyl)-2-(1,3-dimethoxy-1,3-dioxopropan-2-ylidene)hydrazinyl)(1,3-dimethyl-1H-imidazol-3-ium-2-yl)dihydroborate (97**):**

In a pressure tube, (1,3-dimethyl-1H-imidazol-3-ium-2-yl)trihydroborate (25.0 mg, 0.22 mmol, 1.0 equiv) was dissolved in degassed trifluorotoluene (2.0 mL). Diazo dimethyl malonate (43.0 mg, 0.27 mmol, 1.2 equiv) and AIBN (67.0 mg, 0.27 mmol, 1.2 equiv) were added and the reaction was heated to 120 °C for 2 h. The crude reaction mixture turned a yellow-orange. An ¹¹B NMR spectrum of the crude product showed 100% conversion of the NHC–BH₃ starting material. The reaction mixture was concentrated under vacuum and purified by flash chromatography (ethyl acetate : hexanes 3:2) to yield 361.0 mg (17%) of **97** as a yellow solid: ¹H NMR (500 MHz, CDCl₃) δ 1.26 (m, 1H), 1.65 (m, 3H), 1.86 (m, 2H), 2.05 (m, 2H), 2.19 (m, 2H), 3.47 (s, 3H), 3.67 (s, 6H), 3.74 (s, 3H), 6.80 (s, 2H); ¹³C NMR (125 MHz, CDCl₃) δ 23.6, 24.7, 34.8, 35.5, 51.2, 51.6, 68.7, 118.5, 121.0, 121.4, 165.1, 167.4; ¹¹B NMR (160 MHz, CDCl₃) δ –17.9 (br t); mp 150–152 °C; HRMS (ESI) *m/z* (*M*⁺ + 1) calcd for C₁₇H₂₇O₄N₅B 376.2151, found 376.2139.



(1,3-Dimethyl-1*H*-imidazol-3-ium-2-yl)(2-(2,2-dimethyl-4,6-dioxo-1,3-dioxan-5-ylidene)hydrazinyl)dihydroborate (101):

(1,3-Dimethyl-1*H*-imidazol-3-ium-2-yl)trihydroborate (111.0 mg, 1.00 mmol, 1.0 equiv) and diazo 2,2-dimethyl-1,3-dioxane-4,6-dione (204.0 mg, 1.20 mmol, 1.2 equiv) were dissolved in dry dichloromethane (5 mL). The reaction mixture was refluxed for 20 h, gradually turning a yellow color. An ^{11}B NMR spectrum of the crude reaction mixture showed 100% conversion of the starting NHC-borane. The reaction mixture was concentrated under vacuum and purified by flash chromatography (ethyl acetate 100%) to yield 172.0 mg (61%) of **101** as a yellow solid: ^1H NMR (500 MHz, CDCl_3) δ 1.69 (s, 6H), 3.84 (s, 6H), 6.96 (s, 2H), 12.42 (s, 1H); ^{13}C NMR (125 MHz, CDCl_3) δ 26.9, 36.5, 103.8, 110.8, 121.5, 160.9, 161.7; ^{11}B NMR (160 MHz, CDCl_3) δ -18.7 (br t); IR (film) 3144, 2407, 1722, 1669, 1519, 1375, 1268, 1204, 1111, 936, 734 cm^{-1} ; mp 193–195 $^\circ\text{C}$; HRMS (ESI) m/z ($\text{M}^+ + 1$) calcd for $\text{C}_{11}\text{H}_{18}\text{O}_4\text{N}_4\text{B}$ 281.1416, found 281.1404.



(Z)-(2-(4-Bromophenyl)-1-(λ^1 -oxidanyl)-1 λ^4 -diazenyl)(1,3-dimethyl-1*H*-imidazol-3-ium-2-yl)dihydroborate (108):

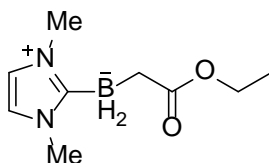
(1,3-Dimethyl-1*H*-imidazol-3-ium-2-yl)trihydroborate (111.0 mg, 1.00 mmol, 1.0 equiv) was dissolved in dry acetonitrile (5 mL) and brought to reflux under argon. A solution of 4-bromobenzenediazonium tetrafluoroborate (282.0 mg, 1.00 mmol, 1.0 equiv) in dry acetonitrile (5 mL) was added via syringe pump over a period of 2 h. An ^{11}B NMR spectrum of the crude product showed 95% conversion to the intermediate salt and NHC-BF₃ side-product. The reaction mixture was concentrated under vacuum and purified by flash chromatography (ethyl acetate 100%) to give the intermediate salt as a light yellow oil. The salt was washed with aqueous K₂CO₃ and the combined organic layers were dried over Na₂SO₄. Concentrating the organic layers yielded 33.0 mg (10%) of **108** as a purple solid: ^1H NMR (500 MHz, CDCl₃) δ 3.77 (s, 6H), 6.92 (s, 2H), 7.40 (d, $J_{\text{CH}} = 8.5$ Hz, 2H), 7.50 (d, $J_{\text{CH}} = 9.0$ Hz, 2H); ^{13}C NMR (125 MHz, CDCl₃) δ 36.2, 120.8, 122.2, 122.3, 122.8, 131.6; ^{11}B NMR (160 MHz, CDCl₃) δ -12.0 (t, $J_{\text{BH}} = 94$ Hz); IR (film) 3386, 2923, 2331, 1658, 1575, 1468, 1233, 1089, 1005, 837, 730 cm⁻¹; mp 67–70 °C; HRMS (ESI) m/z ($\text{M}^+ + 1$) calcd for C₁₁H₁₅ON₄BBr 309.0517, found 309.0521. Intermediate salt: ^1H NMR (500 MHz, CDCl₃) δ 3.83 (s, 6H), 5.55 (br s, 1H), 6.58 (br s, 2H), 6.86 (d, $J_{\text{CH}} = 9.0$ Hz, 2H), 7.00 (s, 2H), 7.37 (d, $J_{\text{CH}} = 9.0$ Hz, 2H); ^{13}C NMR δ 36.5, 115.7, 117.2, 122.6, 132.4, 144.1; ^{11}B NMR δ -20.1 (br), -1.3 (s); HRMS (ESI) m/z ($\text{M}^+ - 1$) calcd for C₁₁H₁₇N₄BBr 295.0724, found 295.0718.

5.4 EXPERIMENTAL DATA FOR CHAPTER 3

Characterization spectra for Chapter 3 compounds can be viewed in the Supporting Information of: Allen, T. H.; Kawamoto, T.; Gardner, S.; Geib, S. J.; Curran, D. P. *Org. Lett.* **2017**, *19*, 3680–3683.

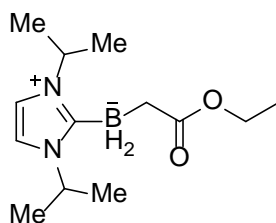
General procedure for Reactions in Tables 20 and 22:

In a 1 dram vial, NHC-BH₃ (1.0 equiv) was dissolved in dichloromethane (1.0 M). Iodine (0.1 equiv) was added and allowed to stir for 5 min as gas evolution ceased. The diazo compound (1.2 equiv) was then added, and vigorous gas evolution was initially observed. The reaction mixture was allowed to stir for 1 h. Reaction progress was monitored by a ¹¹B NMR spectrum of the crude reaction mixture. The reaction mixture was concentrated under vacuum and purified by flash chromatography (3:2 ethyl acetate:hexanes).



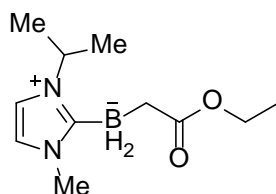
(1,3-Dimethyl-1*H*-imidazol-3-ium-2-yl)(2-ethoxy-2-oxoethyl)dihydroborate (114):

Reaction of (1,3-dimethyl-1*H*-imidazol-3-ium-2-yl)trihydroborate (**5**) (111.0 mg, 1.00 mmol), iodine (25.4 mg, 0.1 equiv), and ethyl 2-diazoacetate (**11**) (166.5 mg, 1.2 equiv) according to the general procedure afforded 104.0 mg (53%) of product **114** as a colorless oil. Compound characterization data matched literature values.



(1,3-Diisopropyl-1*H*-imidazol-3-ium-2-yl)(2-ethoxy-2-oxoethyl)dihydroborate (116):

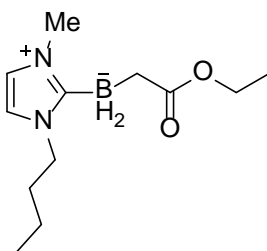
Reaction of (1,3-diisopropyl-1*H*-imidazol-3-ium-2-yl)trihydroborate (**7**) (166.0 mg, 1.00 mmol), iodine (25.4 mg, 0.1 equiv), and ethyl 2-diazoacetate (**11**) (166.5 mg, 1.2 equiv) according to the general procedure afforded 143.3 mg (57%) of product **116** as a colorless oil: ^1H NMR (500 MHz, CDCl_3) δ 6.98 (s, 2H), 5.12 (sept, $J = \text{Hz}$, 2H), 3.95 (q, $J = \text{Hz}$, 2H), 1.62 (br, 2H), 1.41 (d, $J = 7.0$ Hz, 12H), 1.14 (t, $J = 7.0$ Hz, 3H); ^{13}C NMR (125 MHz, CDCl_3) δ 180.6, 168.1 (br), 115.4, 58.5, 49.1, 25.5, 23.0, 14.4; ^{11}B NMR (160 MHz, CDCl_3) δ -28.2 (t, $J_{\text{BH}} = 90$ Hz); IR (neat) 2978, 2335, 1691, 1440, 1245, 1205, 1031 cm^{-1} ; HRMS (ESI) m/z ($\text{M}^+ + 1$) calcd for $\text{C}_{13}\text{H}_{26}\text{O}_2\text{N}_2\text{B}$ 253.2082, found 253.2083.



(2-Ethoxy-2-oxoethyl)(3-isopropyl-1-methyl-1*H*-imidazol-3-ium-2-yl)dihydroborate (118):

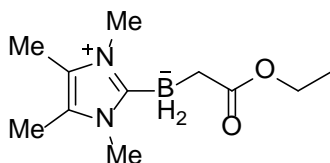
Reaction of (3-isopropyl-1-methyl-1*H*-imidazol-3-ium-2-yl)trihydroborate (**117**) (138 mg, 1.00 mmol), iodine (25.4 mg, 0.1 equiv), and ethyl 2-diazoacetate (**11**) (166.5 mg, 1.2 equiv) according to the general procedure afforded 112.7 mg (50%) of product **118** as a colorless oil: ^1H NMR (500 MHz, CDCl_3) δ 6.90 (d, $J = 2.0$ Hz, 1H), 6.83 (d, $J = 2.0$ Hz, 1H), 4.99 (sept, $J = 6.5$ Hz, 1H), 3.84–3.89 (m, 2H), 3.69 (s, 3H), 1.55 (br, 2H), 1.35 (d, $J = 7.0$ Hz, 6H), 1.05–1.07 (m, 3H); ^{13}C NMR (125 MHz, CDCl_3) δ 180.7, 169.2 (br), 120.8, 114.8, 58.5, 49.4, 35.5, 24.9 (br),

22.9, 14.3; ^{11}B NMR (160 MHz, CDCl_3) δ -28.2 (t, $J_{\text{BH}} = 88$ Hz); IR (neat) 2980, 2332, 1690, 1466, 1243, 1034 cm^{-1} ; HRMS (ESI) m/z ($\text{M}^+ + 1$) calcd for $\text{C}_{11}\text{H}_{22}\text{O}_2\text{N}_2\text{B}$ 225.1769, found 225.1771.



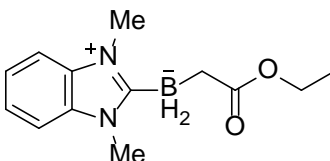
(3-Butyl-1-methyl-1H-imidazol-3-ium-2-yl)(2-ethoxy-2-oxoethyl)dihydroborate (120):

Reaction of (3-butyl-1-methyl-1H-imidazol-3-ium-2-yl)trihydroborate (**119**) (152 mg, 1.00 mmol), iodine (25.4 mg, 0.1 equiv), and ethyl 2-diazoacetate (**11**) (166.5 mg, 1.2 equiv) according to the general procedure afforded 137.5 mg (58%) of product **120** as a colorless oil: ^1H NMR (500 MHz, CDCl_3) δ 6.81–6.82 (m, 2H), 4.04 (t, $J = 8.0$ Hz, 2H), 3.86 (q, $J = 7.0$ Hz, 2H), 3.70 (s, 3H), 1.69 (quin, $J = 7.0$ Hz, 2H), 1.54 (br, 2H), 1.31 (sex, $J = 7.5$ Hz, 2H), 1.06 (t, $J = 7.5$ Hz, 3H), 0.89 (t, $J = 7.5$ Hz, 3H); ^{13}C NMR (125 MHz, CDCl_3) δ 180.7, 170.3 (br), 120.4, 118.7, 58.5, 48.2, 35.6, 32.4, 24.7 (br), 19.5, 14.3, 13.4; ^{11}B NMR (160 MHz, CDCl_3) δ -28.3 (t, $J_{\text{BH}} = 93$ Hz); IR (film) 2958, 2344, 2295, 1687, 1476, 1250, 1106 cm^{-1} ; HRMS (ESI) m/z ($\text{M}^+ + 1$) calcd for $\text{C}_{12}\text{H}_{24}\text{O}_2\text{N}_2\text{B}$ 239.1925, found 239.1928.



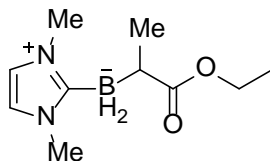
(2-Ethoxy-2-oxoethyl)(1,3,4,5-tetramethyl-1H-imidazol-3-ium-2-yl)dihydroborate (121):

Reaction of (1,3,4,5-tetramethyl-1H-imidazol-3-ium-2-yl)trihydroborate (**92**) (138 mg, 1.00 mmol), iodine (25.4 mg, 0.1 equiv), and ethyl 2-diazoacetate (**11**) (166.5 mg, 1.2 equiv) according to the general procedure afforded 82.9 mg (37%) of product **121** as a colorless oil: ^1H NMR (500 MHz, CDCl_3) δ 3.92 (q, $J = 7.0$ Hz, 2H), 3.60 (s, 6H), 2.09 (s, 6H), 1.57 (br, 2H), 1.12 (t, $J = 7.0$ Hz, 3H); ^{13}C NMR (125 MHz, CDCl_3) δ 181.1, 168.1 (br), 123.3, 58.6, 32.3, 24.7 (br), 14.4, 8.7; ^{11}B NMR (160 MHz, CDCl_3) δ -28.2 (t, $J_{\text{BH}} = 88$ Hz); IR (neat) 2952, 2310, 1691, 1441, 1252, 1096 cm^{-1} ; HRMS (ESI) m/z ($\text{M}^+ + 1$) calcd for $\text{C}_{11}\text{H}_{22}\text{BN}_2\text{O}_2$ 225.1769, found 225.1770.



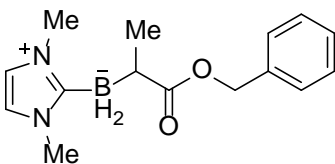
(1,3-dimethyl-1H-benzo[d]imidazol-3-ium-2-yl)(2-ethoxy-2-oxoethyl)dihydroborate (122):

Reaction of (1,3-dimethyl-1H-benzo[d]imidazol-3-ium-2-yl)trihydroborate (**8**) (160.0 mg, 1.00 mmol), iodine (25.4 mg, 0.1 equiv), and ethyl 2-diazoacetate (**11**) (166.5 mg, 1.2 equiv) according to the general procedure afforded 160.7 mg (65%) of product **122** as a white solid. Compound characterization data matched literature values.



(1,3-Dimethyl-1*H*-imidazol-3-ium-2-yl)(1-ethoxy-1-oxopropan-2-yl)dihydroborate (45):

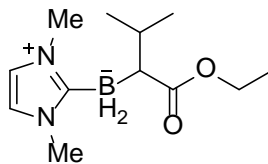
Reaction of (1,3-dimethyl-1*H*-imidazol-3-ium-2-yl)trihydroborate (**5**) (111.0 mg, 1.00 mmol), iodine (25.4 mg, 0.1 equiv), and ethyl 2-diazopropanoate (**44**) (219.7 mg, 1.2 equiv) according to the general procedure afforded 143.0 mg (68%) of product **45** as a colorless oil: ¹H NMR (500 MHz, CDCl₃) δ 6.81 (s, 2H), 3.83–3.89 (m, 1H), 3.75–3.80 (m, 1H), 3.70 (s, 6H), 1.83 (br, 1H), 1.05 (br, 3H), 1.00 (t, *J* = 7.5 Hz, 3H); ¹³C NMR (125 MHz, CDCl₃) δ 183.2, 170.1 (br), 120.2, 58.3, 35.8, 30.0 (br), 17.5, 14.2; ¹¹B NMR (160 MHz, CDCl₃) δ –24.5 (t, *J*_{BH} = 90 Hz); IR (film) 2952, 2905, 2294, 1694, 1364, 1172, 1145 cm⁻¹; HRMS (ESI) *m/z* (*M*⁺) calcd for C₁₀H₁₉O₂N₂BNa 233.1432; found 233.1424.



(1-(Benzyloxy)-1-oxopropan-2-yl)(1,3-dimethyl-1*H*-imidazol-3-ium-2-yl)dihydroborate (130):

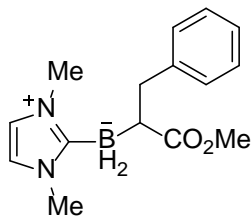
Reaction of (1,3-dimethyl-1*H*-imidazol-3-ium-2-yl)trihydroborate (**5**) (111.0 mg, 1.00 mmol), iodine (25.4 mg, 0.1 equiv), and benzyl 2-diazopropanoate (**129**) (228.3 mg, 1.2 equiv) according to the general procedure afforded 116.4 mg (43%) of product **130** as a colorless oil: ¹H NMR (500 MHz, CDCl₃) δ 7.24–7.30 (m, 5H), 6.69 (s, 2H), 4.92 (s, 2H), 3.63 (s, 6H), 1.98 (br, 1H), 1.15 (br, 3H); ¹³C NMR (125 MHz, CDCl₃) δ 182.9, 169.9 (br), 137.4, 128.1, 127.9, 127.4, 120.1, 64.5, 35.8, 30.2 (br), 17.6; ¹¹B NMR (160 MHz, CDCl₃) δ –24.5 (t, *J*_{BH} = 90 Hz); IR

(neat) 3131, 2960, 2339, 2269, 1698, 1477, 1237, 1117 cm^{-1} ; HRMS (ESI) m/z ($M^+ - 1$) calcd for $\text{C}_{15}\text{H}_{20}\text{O}_2\text{N}_2\text{B}$ 271.1612, found 271.1609.



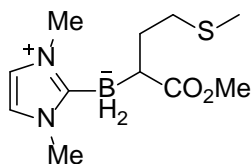
(1,3-Dimethyl-1*H*-imidazol-3-ium-2-yl)(1-ethoxy-3-methyl-1-oxobutan-2-yl)dihydroborate
(132):

Reaction of (1,3-dimethyl-1*H*-imidazol-3-ium-2-yl)trihydroborate (**5**) (111.0 mg, 1.00 mmol), iodine (25.4 mg, 0.1 equiv), and ethyl 2-diazo-3-methylbutanoate (**131**) (279.8 mg, 1.2 equiv) according to the general procedure afforded 48.0 mg (20%) of product **132** as a colorless oil: ^1H NMR (500 MHz, CDCl_3) δ 6.81 (s, 2H), 3.75–3.83 (m, 1H), 3.73 (s, 6H), 3.67–3.72 (m, 1H), 1.97 (br, 1H), 1.55 (br, 1H), 0.99–1.02 (m, 6H), 0.93 (d, $J = 6.5$ Hz, 3H); ^{13}C NMR (125 MHz, CDCl_3) δ 182.1, 171.5 (br), 120.2, 58.1, 45.9 (br), 35.9, 31.3, 23.7, 21.9, 14.3; ^{11}B NMR (160 MHz, CDCl_3) δ -24.5 (t, $J_{\text{BH}} = 90$ Hz); IR (film) 2944, 2347, 2302, 1688, 1481, 1103, 1052 cm^{-1} ; HRMS (ESI) m/z (M^+) calcd for $\text{C}_{12}\text{H}_{23}\text{O}_2\text{N}_2\text{BNa}$ 261.1745, found 261.1750.



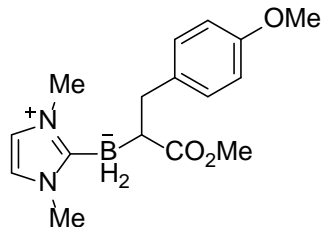
(1,3-Dimethyl-1*H*-imidazol-3-ium-2-yl)(1-methoxy-1-oxo-3-phenylpropan-2-yl)dihydroborate (134):

Reaction of (1,3-dimethyl-1*H*-imidazol-3-ium-2-yl)trihydroborate (**5**) (111.0 mg, 1.00 mmol), iodine (25.4 mg, 0.1 equiv), and methyl 2-diazo-3-phenylpropanoate (**133**) (228.3 mg, 1.2 equiv) according to the general procedure afforded 194.0 mg (71%) of product **134** as a colorless oil. Compound characterization data matched literature values.



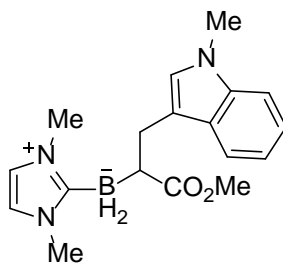
(1,3-Dimethyl-1*H*-imidazol-3-ium-2-yl)(1-methoxy-4-(methylthio)-1-oxobutan-2-yl)dihydroborate (136):

Reaction of (1,3-dimethyl-1*H*-imidazol-3-ium-2-yl)trihydroborate (**5**) (111.0 mg, 1.00 mmol), iodine (25.4 mg, 0.1 equiv), and methyl 2-diazo-4-(methylthio)butanoate (**135**) (188.2 mg, 1.1 equiv) over 18 h according to the general procedure afforded 132.5 mg (52%) of product **136** as a colorless oil: ¹H NMR (500 MHz, CDCl₃) δ 6.82 (s, 2H), 3.73 (s, 6H), 3.41 (s, 3H), 2.49–2.55 (m, 1H), 2.40–2.46 (m, 1H), 2.06 (s, 4H), 1.92 (br, 1H), 1.63 (br, 1H); ¹³C NMR (125 MHz, CDCl₃) δ 182.0, 170.0 (br), 120.3, 50.3, 36.3 (br), 35.9, 34.7, 32.5, 15.2; ¹¹B NMR (160 MHz, CDCl₃) δ -25.4 (t, *J*_{BH} = 90 Hz); IR (neat) 2945, 2296, 1690, 1481, 1431, 1233 cm⁻¹; HRMS (ESI) *m/z* (*M*⁺ - 1) calcd for C₁₁H₂₀O₂N₂BS 255.1333, found 255.1332.



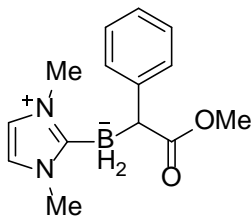
(1,3-Dimethyl-1*H*-imidazol-3-ium-2-yl)(1-methoxy-3-(4-methoxyphenyl)-1-oxopropan-2-yl)dihydroborate (140**):**

Reaction of (1,3-dimethyl-1*H*-imidazol-3-ium-2-yl)trihydroborate (**5**) (88.0 mg, 0.80 mmol), iodine (25.4 mg, 0.1 equiv), and methyl 2-diazo-3-(4-methoxyphenyl)propanoate (**139**) (209.6 mg, 1.2 equiv) according to the general procedure afforded 140.0 mg (58%) of product **140** as a colorless oil: ^1H NMR (500 MHz, CDCl_3) δ 7.10 (d, $J = 8.5$ Hz, 2H), 6.80 (s, 2H), 6.74 (d, $J = 8.5$ Hz, 2H), 3.74 (s, 3H), 3.71 (s, 6H), 3.36 (s, 3H), 3.00–3.05 (m, 1H), 2.62–2.65 (m, 1H), 2.14 (br, 1H); ^{13}C NMR (125 MHz, CDCl_3) δ 181.8, 170.0 (br), 157.1, 136.9, 129.2, 120.3, 113.3, 55.1, 50.2, 39.5 (br), 38.1, 35.9; ^{11}B NMR (160 MHz, CDCl_3) δ -25.1 (t, $J_{\text{BH}} = 90$ Hz); IR (neat) 2946, 2335, 2294, 1698, 1509, 1481, 1241, 1145 cm^{-1} ; HRMS (ESI) m/z (M^+) calcd for $\text{C}_{16}\text{H}_{23}\text{O}_3\text{N}_2\text{BNa}$ 325.1694, found 325.1698.



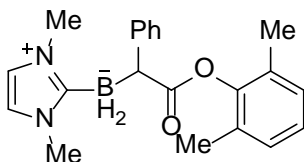
(1,3-Dimethyl-1*H*-imidazol-3-ium-2-yl)(1-methoxy-3-(1-methyl-1*H*-indol-3-yl)-1-oxopropan-2-yl)dihydroborate (144**):**

Reaction of (1,3-dimethyl-1*H*-imidazol-3-ium-2-yl)trihydroborate (**5**) (111.0 mg, 1.00 mmol), iodine (25.4 mg, 0.1 equiv), and methyl 2-diazo-3-(1-methyl-1*H*-indol-3-yl)propanoate (**143**) (292.0 mg, 1.2 equiv) according to the general procedure afforded 150.0 mg (46%) of product **144** as a light yellow solid. Crystals were grown via slow vapor diffusion of a dichloromethane / pentanes solution: ^1H NMR (500 MHz, CDCl_3) δ 7.58–7.59 (m, 1H), 7.21–7.22 (m, 1H), 7.13–7.16 (m, 1H), 7.02–7.05 (m, 1H), 6.80 (s, 3H), 3.76 (s, 6H), 3.68 (s, 3H), 3.39 (s, 3H), 3.18–3.23 (m, 1H), 2.80–2.84 (m, 1H), 2.31 (br, 1H); ^{13}C NMR (125 MHz, CDCl_3) δ 182.4, 170.2 (br), 136.8, 128.2, 125.9, 120.8, 120.2, 119.1, 118.0, 117.4, 108.7, 50.2, 38.5 (br), 35.9 (br), 32.3, 28.2; ^{11}B NMR (160 MHz, CDCl_3) δ -25.0 (t, $J_{\text{BH}} = 92$ Hz); IR (film) 2941, 2334, 1700, 1481, 1198 cm^{-1} ; mp 162–164 $^\circ\text{C}$; HRMS (ESI) m/z ($\text{M}^+ + 1$) calcd for $\text{C}_{18}\text{H}_{25}\text{O}_2\text{N}_3\text{B}$ 326.2034, found 326.2030.



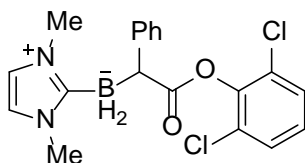
(1,3-Dimethyl-1*H*-imidazol-3-ium-2-yl)(2-methoxy-2-oxo-1-phenylethyl)dihydroborate (32):

Reaction of (1,3-dimethyl-1*H*-imidazol-3-ium-2-yl)trihydroborate (**5**) (111.0 mg, 1.00 mmol), iodine (25.4 mg, 0.1 equiv), and methyl 2-diazo-2-phenylacetate (**31**) (211.5 mg, 1.2 equiv) according to the general procedure afforded 141.2 mg (55%) of product **32** as a colorless oil. Compound characterization data matched literature values.



(1,3-Dimethyl-1*H*-imidazol-3-ium-2-yl)(2-(2,6-dimethylphenoxy)-2-oxo-1-phenylethyl)dihydroborate (61):

Reaction of (1,3-dimethyl-1*H*-imidazol-3-ium-2-yl)trihydroborate (**5**) (111.0 mg, 1.00 mmol), iodine (25.4 mg, 0.1 equiv), and 2,6-dimethylphenyl 2-diazo-2-phenylacetate (**60**) (319.6 mg, 1.2 equiv) according to the general procedure afforded 187.6 mg (54%) of product **61** as a white solid: ^1H NMR (500 MHz, CDCl_3) δ 7.25–7.27 (m, 2H), 7.10–7.13 (m, 2H), 6.95–7.03 (m, 4H), 6.65 (s, 2H), 3.49 (br, 1H), 3.39 (s, 6H), 2.16 (s, 6H); ^{13}C NMR (125 MHz, CDCl_3) δ 176.7, 167.7 (br), 148.8, 145.1, 130.8, 128.1, 127.5, 127.4, 124.8, 123.8, 120.4, 45.2 (br), 35.6, 16.5; ^{11}B NMR (160 MHz, CDCl_3) δ -22.8 (t, $J_{\text{BH}} = 91$ Hz); IR (film) 3175, 2953, 2354, 1720, 1483, 1113 cm^{-1} ; mp 152–154 $^\circ\text{C}$; HRMS (ESI) m/z ($\text{M}^+ + \text{Na}$) calcd for $\text{C}_{21}\text{H}_{25}\text{O}_2\text{N}_2\text{BNa}$ 371.1901, found 371.1905.

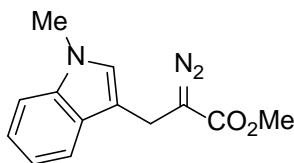


(2-(2,6-Dichlorophenoxy)-2-oxo-1-phenylethyl)(1,3-dimethyl-1*H*-imidazol-3-ium-2-yl)dihydroborate (59**):**

Reaction of (1,3-dimethyl-1*H*-imidazol-3-ium-2-yl)trihydroborate (**5**) (111.0 mg, 1.00 mmol), iodine (25.4 mg, 0.1 equiv), and 2,6-dichlorophenyl 2-diazo-2-phenylacetate (**58**) (368.7 mg, 1.2 equiv) according to the general procedure afforded 104.7 mg (27%) of product **59** as a colorless solid. The two enantiomers were resolved by chiral HPLC ((*S,S*)-Whelk-O column, hexane/*i*PrOH = 70:30): ¹H NMR (500 MHz, CDCl₃) δ 7.27–7.31 (m, 4H), 7.14–7.17 (m, 2H), 7.04–7.07 (m, 2H), 6.75 (s, 2H), 3.65 (br, 1H), 3.46 (s, 6H); ¹³C NMR δ 175.5, 167.7 (br), 145.0, 144.0, 129.5, 128.3, 127.6, 127.3, 126.1, 124.0, 120.5, 44.3 (br), 35.7; ¹¹B NMR (160 MHz, CDCl₃) δ –23.2 (t, *J*_{BH} = 99 Hz); IR (film) 3141, 3072, 2370, 1737, 1445, 1237, 1069 cm⁻¹; mp 123–126 °C; HRMS (ESI) *m/z* (*M*⁺ + Na) calcd for C₁₉H₁₉O₂N₂BCl₂Na 411.0809, found 411.0815.

Preparation of diazo compounds:

The following diazo compounds were prepared according to literature procedures: **44** and **131**,⁸⁹ **135**, **139**, and **143**,⁹⁰ **129**,¹⁰⁵ **58** and **60**.³⁶



Methyl 2-diazo-3-(1-methyl-1H-indol-3-yl)propanoate (143):

Methyl 1-methyltryptophanate (2.53 g, 10.9 mmol, 1.00 equiv), isopentyl nitrite (1.68 mL, 12.0 mmol, 1.10 equiv), and acetic acid (0.06 mL, 1.09 mmol, 0.10 equiv) were dissolved in benzene (50 mL). The reaction mixture was heated to reflux for 1 h. The yellow solution was cooled, extracted with CH₂Cl₂, and washed with NaHCO₃ (aq). The combined organic fractions were dried over Na₂SO₄, filtered and concentrated under reduced pressure. The crude residue was purified by flash chromatography (7:3 hexanes:ethyl acetate) to afford 1.49 g (56%) of **143** as a yellow oil: ¹H NMR (500 MHz, CDCl₃) δ 7.57–7.58 (m, 1H), 7.29–7.31 (m, 1H), 7.23–7.25 (m, 1H), 7.11–7.14 (m, 1H), 6.95 (s, 1H), 3.79 (s, 5H), 3.76 (s, 3H); ¹³C NMR δ 167.7, 137.2, 127.3, 121.3, 119.2, 118.9, 109.6, 109.3, 51.9, 32.7, 19.5; IR (neat) 2940, 2075, 1680, 1435, 1327, 1103 cm⁻¹; HRMS (ESI) *m/z* (*M*⁺ + 1) calcd for C₁₃H₁₄O₂N₃ 244.1081, found 244.1084.

Procedure for reaction between NHC-boryl ester 114 and iodine:

Iodine (12.7 mg, 0.05 mmol, 0.5 equiv) was added to a solution of NHC-boryl ester **114** (19.0 mg, 0.1 mmol) in CH₂Cl₂ (0.5 mL). The reaction mixture was allowed to stir for 1 h and then transferred to an NMR tube. The key intermediate NHC-boryl iodide **155** was detected as a broad doublet at –21.6 ppm by ¹¹B NMR spectroscopy.

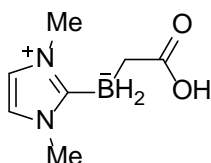
Procedure for regeneration of NHC-boryl ester 114 via reduction of 155 by NHC–BH₃ 5:

Iodine (12.7 mg, 0.05 mmol, 0.5 equiv) was added to a solution of NHC-boryl ester **114** (19.0 mg, 0.1 mmol) in CH₂Cl₂ (0.5 mL). The reaction mixture was allowed to stir for 1 h and

then transferred to an NMR tube. The key intermediate NHC-boryl iodide **155** was detected as a broad doublet at -21.6 ppm by ^{11}B NMR spectroscopy and no starting material **114** remained. DiMe-Imidazole- BH_3 **5** (110.0 mg, 1 mmol, 10 equiv) was added to the mixture and allowed to stir for 1 h. NHC-boryl ester **114** was reformed.

5.5 EXPERIMENTAL DATA FOR CHAPTER 4

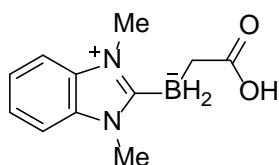
Characterization spectra for Chapter 4 compounds can be viewed in the Supporting Information of: Allen, T. H.; Horner, A. R.; Geib, S. J.; Weber, S. G.; Curran, D. P. *Chem. Eur. J.* **2018**, *24*, 822–825.



(Carboxymethyl)(1,3-dimethyl-1*H*-imidazol-3-ium-2-yl)dihydroborate (**163**):

In a 50 mL round bottom flask, (1,3-dimethyl-1*H*-imidazol-3-ium-2-yl)(2-ethoxy-2-oxoethyl)dihydroborate **114** (1.36 g, 5.79 mmol) was dissolved in methanol (11.6 mL, 0.5 M). After the addition of 1.0 M NaOH (14.5 mL, 2.5 equiv), the flask was capped and heated at 55 °C for 48 h. Reaction progress was monitored by a ^{11}B spectrum of the crude reaction mixture. The carboxylate intermediate manifested as a triplet signal approximately one ppm downfield from the starting ester signal. Full conversion was signified by the disappearance of the starting ester signal. The reaction mixture was quenched with a solution of 1.0 M formic acid, and the organic layer was then extracted with CH_2Cl_2 . The organic layers were dried over Na_2SO_4 and

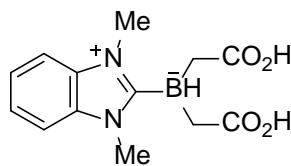
filtered. Concentrating under reduced pressure gave 436.0 mg (45%) of **163** as a white solid. Crystals were grown via slow vapor diffusion of a dichloromethane/pentanes solution: ^1H NMR (500 MHz, CDCl_3) δ 10.41 (br, 1H), 6.82 (s, 2H), 3.77 (s, 6H), 1.62 (br, 2H); ^{13}C NMR (125 MHz, CDCl_3) δ 186.5, 120.5, 35.9, 24.4 (br); ^{11}B NMR (160 MHz, CDCl_3) δ -28.0 (t, $J_{\text{BH}} = 90$ Hz); IR (neat) 3123, 2969, 2366, 2312, 1648, 1402, 1300, 1059 cm^{-1} ; mp 137–140 $^\circ\text{C}$; HRMS (ESI) m/z ($\text{M}^+ + 1$) calcd for $\text{C}_7\text{H}_{14}\text{N}_2\text{O}_2\text{B}$ 169.1143, found 169.1140.



(Carboxymethyl)(1,3-dimethyl-1H-benzo[d]imidazol-3-ium-2-yl)dihydroborate (164):

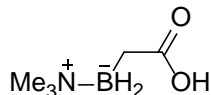
In a 20 mL scintillation vial, (1,3-dimethyl-1H-benzo[d]imidazol-3-ium-2-yl)(2-ethoxy-2-oxoethyl)dihydroborate **122** (246.0 mg, 1.00 mmol) was dissolved in methanol (2.0 mL, 0.5 M). After the addition of 1.0 M NaOH (2.5 mL, 2.5 equiv), the flask was capped and heated at 55 $^\circ\text{C}$ for 48 h. Reaction progress was monitored by a ^{11}B spectrum of the crude reaction mixture. The carboxylate intermediate manifested as a triplet signal approximately one ppm downfield from the starting ester signal. Full conversion was signified by the disappearance of the starting ester signal. The reaction mixture was quenched with a solution of 1.0 M formic acid, and the organic layer was then extracted with CH_2Cl_2 . The organic layers were dried over Na_2SO_4 and filtered. Concentrating under reduced pressure gave 170.0 mg (78%) of **164** as a white solid. Crystals were grown from via slow vapor diffusion of a dichloromethane/pentanes solution: ^1H NMR (500 MHz, CDCl_3) δ 10.65 (br, 1H), 7.40–7.46 (m, 4H), 3.97 (s, 6H), 1.71 (br, 2H); ^{13}C NMR (125 MHz, CDCl_3) δ 186.6, 133.1, 124.2, 110.9, 32.2, 24.6 (br); ^{11}B NMR

(160 MHz, CDCl₃) δ -27.8 (t, $J_{\text{BH}} = 90$ Hz); IR (neat) 2948, 2317, 1669, 1463, 1261, 1034 cm⁻¹; mp 175–177 °C; HRMS (ESI) m/z ($M^+ - 1$) calcd for C₁₁H₁₄N₂O₂B 217.1143, found 217.1148.



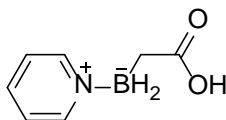
Bis(carboxymethyl)(1,3-dimethyl-1H-benzo[d]imidazol-3-ium-2-yl)hydroborate (166):

In a 20 mL scintillation vial, (1,3-dimethyl-1H-benzo[d]imidazol-3-ium-2-yl)bis(2-ethoxy-2-oxoethyl)hydroborate **165** (401.0 mg, 1.21 mmol) was dissolved in methanol-d₄ (2.4 mL, 0.5 M). After the addition of 1.0 M NaOH (6.0 mL, 5.0 equiv), the flask was capped and heated at 55 °C for 78 h. Reaction progress was monitored by a ¹H spectrum of the crude reaction mixture. Full conversion was signified by quantitative formation of free ethanol (1.19 ppm). The reaction mixture was quenched with a solution of 1.0 M formic acid, resulting in the formation of a white precipitate. The precipitate was filtered and the removal of residual solvent under reduced pressure gave 150.0 mg (45%) of **166** as a white solid. Crystals were grown from via slow vapor diffusion of an acetonitrile/methanol solution: ¹H NMR (500 MHz, CD₃OD) δ 7.67–7.68 (m, 2H), 7.47–7.49 (m, 2H), 4.03 (s, 6H), 1.82 (br, 4H); ¹³C NMR (125 MHz, CD₃OD) δ 184.7, 134.8, 125.7, 112.4, 33.1; ¹¹B NMR (160 MHz, CD₃OD) δ -19.7 (d, $J_{\text{BH}} = 89$ Hz); IR (neat) 2935, 2175, 1686, 1465, 1301, 911 cm⁻¹; mp 202–203 °C; HRMS (ESI) m/z ($M^+ - 1$) calcd for C₁₃H₁₆N₂O₄B 275.1198, found 275.1207.



(Carboxymethyl)(trimethyl- λ^4 -azaneyl)dihydroborate (167):

In a 20 mL scintillation vial, (2-ethoxy-2-oxoethyl)(trimethyl- λ^4 -azaneyl)dihydroborate **126** (136.0 mg, 0.86 mmol) was dissolved in methanol- d_4 (1.8 mL, 0.5 M). After the addition of 1.0 M NaOH (2.14 mL, 2.5 equiv), the reaction mixture was stirred at rt for 7 d. Reaction progress was monitored by a ^1H spectrum of the crude reaction mixture. Full conversion was signified by quantitative formation of free ethanol (1.19 ppm). The reaction mixture was quenched with a solution of 1.0 M formic acid, and the organic layer was then extracted with CH_2Cl_2 . The organic layers were dried over Na_2SO_4 and filtered. Concentrating under reduced pressure gave 27.0 mg (24%) of **167** as a white solid. Crystals were grown from via slow vapor diffusion of a dichloromethane/pentanes solution: ^1H NMR (500 MHz, CDCl_3) δ 11.01 (br, 1H), 2.62 (s, 9H), 1.69 (br, 2H); ^{13}C NMR (125 MHz, CDCl_3) δ 185.4, 52.1, 25.7 (br); ^{11}B NMR (160 MHz, CDCl_3) δ -3.7 (t, J_{BH} = 104 Hz); IR (neat) 2954, 2365, 1670, 1462, 1299, 1173 cm^{-1} ; mp 113–115 $^\circ\text{C}$; HRMS (ESI) m/z ($\text{M}^+ - 1$) calcd for $\text{C}_7\text{H}_{13}\text{N}_2\text{O}_2\text{B}$ 130.1034, found 130.1032.



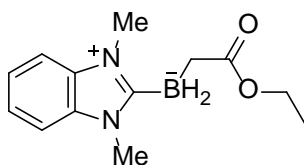
(Carboxymethyl)($1\lambda^4$ -pyridin-1-yl)dihydroborate (168):

In a 20 mL scintillation vial, (2-ethoxy-2-oxoethyl)($1\lambda^4$ -pyridin-1-yl)dihydroborate **128** (333.0 mg, 1.88 mmol) was dissolved in methanol- d_4 (3.8 mL, 0.5 M). After the addition of 1.0 M NaOH (4.70 mL, 2.5 equiv), the reaction mixture was stirred at rt for 4 d. Reaction progress was monitored by a ^1H spectrum of the crude reaction mixture. Full conversion was signified by

quantitative formation of free ethanol (1.19 ppm). The reaction mixture was quenched with a solution of 1.0 M formic acid, and the organic layer was then extracted with CH₂Cl₂. The organic layers were dried over Na₂SO₄ and filtered. Concentrating under reduced pressure gave 154.0 mg (54%) of **168** as a light yellow solid. Crystals were grown from via slow vapor diffusion of a dichloromethane/pentanes solution: ¹H NMR (500 MHz, CDCl₃) δ 11.36 (br, 1H), 8.58–8.60 (m, 2H), 7.97–8.00 (m, 1H), 7.55–7.57 (m, 2H), 1.81 (t, *J* = 5.0 Hz, 2H); ¹³C NMR (125 MHz, CDCl₃) δ 185.9, 147.2, 140.0, 125.5, 29.9 (br); ¹¹B NMR (160 MHz, CDCl₃) δ -5.7 (t, *J*_{BH} = 93 Hz); IR (neat) 2975, 2381, 2333, 1660, 1620, 1442, 1303, 1077, 755 cm⁻¹; mp 76–78 °C; HRMS (ESI) *m/z* (*M*⁺ - 1) calcd for C₇H₉N₂O₂B 150.0721, found 150.0719.

Preparation of α-boryl ester compounds:

NHC-boryl ester compounds were prepared by boryl-iodide catalyzed B–H insertion with ethyl diazoacetate.⁸⁶ Trimethylamine-, pyridine-, and tributylphosphine-boryl ester compounds were prepared by Rh-catalyzed B–H insertion with ethyl diazoacetate.⁴³

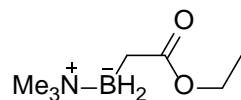


(1,3-Dimethyl-1*H*-benzo[*d*]imidazol-3-ium-2-yl)bis(2-ethoxy-2-oxoethyl)hydroborate (**122**):

In a 20 mL scintillation vial, (1,3-dimethyl-1*H*-benzo[*d*]imidazol-3-ium-2-yl)trihydroborate (978.0 mg, 6.11 mmol) was dissolved in dichloromethane (6.11 mL, 1.0 M). Iodine (155.1 mg, 0.1 equiv) was added and allowed to stir for 5 min as gas evolution ceased. Ethyl diazoacetate (1.59 g, 2.0 equiv) was then added, and vigorous gas evolution was initially observed. The reaction mixture was allowed to stir for 18 h. Reaction progress was monitored by

an ^{11}B NMR spectrum of the crude reaction mixture. The ratio between single insertion and double insertion products was 63/37. The reaction mixture was concentrated under vacuum and purified by flash chromatography (2:3 ethyl acetate:hexanes) to give (1,3-dimethyl-1*H*-benzo[*d*]imidazol-3-ium-2-yl)(2-ethoxy-2-oxoethyl)dihydroborate in 30% yield (451.1 mg) as a white solid. Compound characterization data matched literature values.

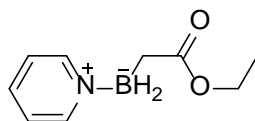
The double insertion product **165** was isolated (3:2 ethyl acetate:hexanes) in 20% yield (402.0 mg) as a colorless oil: ^1H NMR (500 MHz, CDCl_3) δ 7.44–7.46 (m, 2H), 7.40–7.42 (m, 2H), 4.00 (s, 6H), 3.81–3.86 (m, 4H), 1.85 (br, 2H), 1.79 (br, 2H), 0.94 (t, $J = 7.0$ Hz, 6H); ^{13}C NMR (125 MHz, CDCl_3) δ 179.3, 133.3, 124.4, 110.9, 58.7, 32.6, 25.5 (br), 14.3; ^{11}B NMR (160 MHz, CDCl_3) δ -20.2 (d, $J_{\text{BH}} = 93$ Hz); IR (neat) 2976, 2368, 1692, 1461, 1242, 1094, 1033, 742 cm^{-1} ; HRMS (ESI) m/z ($\text{M}^+ + 1$) calcd for $\text{C}_{17}\text{H}_{26}\text{O}_4\text{N}_2\text{B}$ 333.1980, found 333.1994.



(2-Ethoxy-2-oxoethyl)(trimethyl- λ^4 -azaneyl)dihydroborate (126):

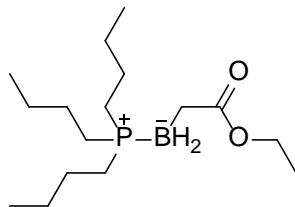
Trimethylamine-borane (165.0 mg, 2.20 mmol, 1.0 equiv) and $\text{Rh}_2(\text{esp})_2$ (17.3 mg, 0.01 mmol, 1 mol%) were dissolved in dichloromethane (9 mL) under argon. A solution of ethyl diazoacetate (569.0 mg, 2.00 mmol, 2.0 equiv) in dichloromethane (2 mL) was added via syringe pump over a period of 2 h. An ^{11}B NMR spectrum of the crude product showed 52% conversion to the desired single-insertion product. The reaction mixture was concentrated under vacuum and purified by flash chromatography (hexane: ethyl acetate, 1:1) to yield 157.0 mg (79%) of **126** as a colorless oil: ^1H NMR (500 MHz, CDCl_3) δ 4.04–4.09 (m, 2H), 2.60 (s, 9H), 1.66 (br, 2H), 1.21–1.24 (m, 3H); ^{13}C NMR (125 MHz, CDCl_3) δ 179.6, 59.1, 52.0, 26.0 (br), 14.4; ^{11}B NMR

(160 MHz, CDCl₃) δ -3.7 (t, $J_{\text{BH}} = 102$ Hz); IR (neat) 2951, 2359, 1697, 1466, 1247, 1113, 988, 842 cm⁻¹; HRMS (ESI) m/z ($M^+ - 1$) calcd for C₇H₁₇O₂NB 158.1347, found 158.1345.



(2-Ethoxy-2-oxoethyl)(1 λ ⁴-pyridin-1-yl)dihydroborate (128):

Pyridine-borane (464.0 mg, 5.00 mmol, 1.0 equiv) and Rh₂(esp)₂ (39.4 mg, 0.01 mmol, 1 mol%) were dissolved in dichloromethane (20 mL) under argon. A solution of ethyl diazoacetate (776.9 mg, 1.20 mmol, 1.2 equiv) in dichloromethane (5 mL) was added via syringe pump over a period of 2 h. An ¹¹B NMR spectrum of the crude product showed 45% conversion to the desired single-insertion product. The reaction mixture was concentrated under vacuum and purified by flash chromatography (hexane: ethyl acetate, 1:1) to yield 335.0 mg (37%) of **128** as a colorless oil: ¹H NMR (500 MHz, CDCl₃) δ 8.59–8.60 (m, 2H), 7.97–8.00 (m, 1H), 7.54–7.57 (m, 2H), 3.92–3.96 (m, 2H), 1.79–1.81 (m, 2H), 1.10 (t, $J = 7$ Hz); ¹³C NMR (125 MHz, CDCl₃) δ 179.3, 147.2, 139.8, 125.3, 58.8, 30.0 (br), 14.4; ¹¹B NMR (160 MHz, CDCl₃) δ -5.7 (t, $J_{\text{BH}} = 101$ Hz); IR (neat) 2978, 2369, 1692, 1458, 1252, 1097, 1037, 690 cm⁻¹; HRMS (ESI) m/z ($M^+ - 1$) calcd for C₉H₁₃O₂NB 178.1034, found 178.1031.



(2-Ethoxy-2-oxoethyl)(tributyl- λ^4 -phosphanyl)dihydroborate (169):

Tributylphosphine-borane (452.0 mg, 2.09 mmol, 1.0 equiv) and $\text{Rh}_2(\text{esp})_2$ (66.1 mg, 0.01 mmol, 1 mol%) were dissolved in dichloromethane (8 mL) under argon. A solution of ethyl diazoacetate (256.1 mg, 2.00 mmol, 0.95 equiv) in dichloromethane (2 mL) was added via syringe pump over a period of 2 h. An ^{11}B NMR spectrum of the crude product showed 100% conversion to the desired single-insertion product. The reaction mixture was concentrated under vacuum and purified by flash chromatography (hexane: ethyl acetate, 1:1) to give **169**: ^1H NMR (500 MHz, CDCl_3) δ 4.04 (q, 2H, $J = 7$ Hz), 1.62 (m, 6H), 1.41 (m, 12H), 1.32 (t, 2H, $J = 8$ Hz), 1.24 (t, 3H, $J = 7$ Hz), 0.95 (t, 9H, $J = 7$ Hz); ^{11}B NMR (160 MHz, CDCl_3) δ -30.1 (br).

BIBLIOGRAPHY

1. Staubitz, A.; Robertson, A. P. M.; Sloan, M. E.; Manners, I., Amine- and Phosphine-Borane Adducts: New Interest in Old Molecules. *Chem. Rev.* **2010**, *110*, 4023-4078.
2. Staubitz, A.; Robertson, A. P. M.; Manners, I., Ammonia-Borane and Related Compounds as Dihydrogen Sources. *Chem. Rev.* **2010**, *110*, 4079-4124.
3. Corey, E. J.; Bakshi, R. K.; Shibata, S., Highly enantioselective borane reduction of ketones catalyzed by chiral oxazaborolidines. Mechanism and synthetic implications. *J. Am. Chem. Soc.* **1987**, *109*, 5551-5553.
4. Busacca, C. A.; Farber, E.; DeYoung, J.; Campbell, S.; Gonnella, N. C.; Grinberg, N.; Haddad, N.; Lee, H.; Ma, S.; Reeves, D.; Shen, S.; Senanayake, C. H., Ambient Temperature Hydrophosphination of Internal, Unactivated Alkynes and Allenyl Phosphineoxides with Phosphine Borane Complexes. *Org. Lett.* **2009**, *11*, 5594-5597.
5. Andrews, G. C.; Crawford, T. C., The synthetic utility of amine borane reagents in the reduction of aldehydes and ketones. *Tetrahedron Lett.* **1980**, *21*, 693-696.
6. Curran, D. P.; Solovyev, A.; Makhlof Brahmi, M.; Fensterbank, L.; Malacria, M.; Lacôte, E., Synthesis and Reactions of N-Heterocyclic Carbene Boranes. *Angew. Chem. Int. Ed.* **2011**, *50*, 10294-10317.
7. Wang, Y.; Quillian, B.; Wei, P.; Wannere, C. S.; Xie, Y.; King, R. B.; Schaefer, H. F.; Schleyer, P. v. R.; Robinson, G. H., A Stable Neutral Diborene Containing a BB Double Bond. *J. Am. Chem. Soc.* **2007**, *129*, 12412-12413.
8. Pan, X.; Lacôte, E.; Lalevée, J.; Curran, D. P., Polarity Reversal Catalysis in Radical Reductions of Halides by N-Heterocyclic Carbene Boranes. *J. Am. Chem. Soc.* **2012**, *134*, 5669-5674.
9. Ueng, S.-H.; Fensterbank, L.; Lacôte, E.; Malacria, M.; Curran, D. P., Radical Deoxygenation of Xanthates and Related Functional Groups with New Minimalist N-Heterocyclic Carbene Boranes. *Org. Lett.* **2010**, *12*, 3002-3005.

10. Doyle, M. P.; Duffy, R.; Ratnikov, M.; Zhou, L., Catalytic Carbene Insertion into C–H Bonds. *Chem. Rev.* **2010**, *110*, 704-724.
11. Ren, T., Substituent effects in dinuclear paddlewheel compounds: electrochemical and spectroscopic investigations. *Coord. Chem. Rev.* **1998**, *175*, 43-58.
12. Demonceau, A.; Noels, A. F.; Hubert, A. J.; Teyssie, P., Transition-metal-catalysed reactions of diazoesters. Insertion into C-H bonds of paraffins by carbenoids. *J. Chem. Soc., Chem. Commun.* **1981**, 688-689.
13. Pirrung, M. C.; Morehead, A. T., Saturation Kinetics in Dirhodium(II) Carboxylate-Catalyzed Decompositions of Diazo Compounds. *J. Am. Chem. Soc.* **1996**, *118*, 8162-8163.
14. Doyle, M. P.; Westrum, L. J.; Wolthuis, W. N. E.; See, M. M.; Boone, W. P.; Bagheri, V.; Pearson, M. M., Electronic and steric control in carbon-hydrogen insertion reactions of diazoacetates catalyzed by dirhodium(II) carboxylates and carboxamides. *J. Am. Chem. Soc.* **1993**, *115*, 958-964.
15. Kornecki, K. P.; Briones, J. F.; Boyarskikh, V.; Fullilove, F.; Autschbach, J.; Schrote, K. E.; Lancaster, K. M.; Davies, H. M. L.; Berry, J. F., Direct Spectroscopic Characterization of a Transitory Dirhodium Donor-Acceptor Carbene Complex. *Science* **2013**, *342*, 351.
16. Nakamura, E.; Yoshikai, N.; Yamanaka, M., Mechanism of C–H Bond Activation/C–C Bond Formation Reaction between Diazo Compound and Alkane Catalyzed by Dirhodium Tetracarboxylate. *J. Am. Chem. Soc.* **2002**, *124*, 7181-7192.
17. Taber, D. F.; Petty, E. H.; Raman, K., Enantioselective ring construction: synthesis of (+)- α -cuparenone. *J. Am. Chem. Soc.* **1985**, *107*, 196-199.
18. Fulton, J. R.; Aggarwal, V. K.; de Vicente, J., The Use of Tosylhydrazone Salts as a Safe Alternative for Handling Diazo Compounds and Their Applications in Organic Synthesis. *Eur. J. Org. Chem.* **2005**, *2005*, 1479-1492.
19. Baum, J. S.; Shook, D. A.; Davies, H. M. L.; Smith, H. D., Diazotransfer Reactions with p-Acetamidobenzenesulfonyl Azide. *Synth. Commun.* **1987**, *17*, 1709-1716.
20. Popik, V. V.; Russell, A. E.; Wulff, W. D.; Mohammadlou, A., Ethyl Diazoacetate. In *Encyclopedia of Reagents for Organic Synthesis*, John Wiley & Sons: 2017.
21. Hosmane, R. S.; Liebman, J. F., Paradigms and Paradoxes: Diazomethane and Ethyl Diazoacetate: The Role of Substituent Effects on Stability. *Struct. Chem.* **2002**, *13*, 501-503.
22. Davies, H. M. L.; Hansen, T.; Churchill, M. R., Catalytic Asymmetric C–H Activation of Alkanes and Tetrahydrofuran. *J. Am. Chem. Soc.* **2000**, *122*, 3063-3070.

23. Davies, H. M. L.; Jin, Q.; Ren, P.; Kovalevsky, A. Y., Catalytic Asymmetric Benzylic C–H Activation by Means of Carbenoid-Induced C–H Insertions. *J. Org. Chem.* **2002**, *67*, 4165-4169.
24. Taber, D. F.; Meagley, R. P.; Louey, J. P.; Rheingold, A. L., Molecular complex design: bridging the tetrakis(carboxylato)dirhodium core. *Inorg. Chim. Acta* **1995**, *239*, 25-28.
25. Bickley, J.; Bonar-Law, R.; McGrath, T.; Singh, N.; Steiner, A., Dirhodium (II) carboxylate complexes as building blocks. cis-Chelating dicarboxylic acids designed to bridge the dinuclear core. *New J. Chem.* **2004**, *28*, 425-433.
26. Espino, C. G.; Fiori, K. W.; Kim, M.; Du Bois, J., Expanding the Scope of C–H Amination through Catalyst Design. *J. Am. Chem. Soc.* **2004**, *126*, 15378-15379.
27. Davies, H. M. L.; Panaro, S. A., Novel dirhodium tetraproline catalysts containing bridging proline ligands for asymmetric carbenoid reactions. *Tetrahedron Lett.* **1999**, *40*, 5287-5290.
28. Ramírez-López, P.; Sierra, M. A.; Gómez-Gallego, M.; Mancheño, M. J.; Gornitzka, H., New Reactivity Modes of Chromium(0) Fischer Carbene Complexes: Unprecedented Insertion of a Carbene Ligand into an Active B–H Bond. *Organometallics* **2003**, *22*, 5092-5099.
29. Zheng, G.; Jones, M., Reaction of (ethoxycarbonyl)carbene with o-carborane. *J. Am. Chem. Soc.* **1983**, *105*, 6487-6488.
30. Tsuneo, I.; Yoshinori, Y., Methylene Insertion Reactions of Samarium Carbenoids into Boron–Hydrogen and Phosphorus–Hydrogen Bonds. *Chem. Lett.* **1996**, *25*, 705-706.
31. Monnier, L.; Delcros, J.-G.; Carboni, B., Creation of New Boron–Carbon Bonds by Dichlorocarbene Insertion into the Boron–Hydrogen Bond of Amine– and Phosphine–Boranes. *Tetrahedron* **2000**, *56*, 6039-6046.
32. Li, X.; Curran, D. P., Insertion of Reactive Rhodium Carbenes into Boron–Hydrogen Bonds of Stable N-Heterocyclic Carbene Boranes. *J. Am. Chem. Soc.* **2013**, *135*, 12076-12081.
33. Mayr, H.; Ofial, A. R., Do general nucleophilicity scales exist? *J. Phys. Org. Chem.* **2008**, *21*, 584-595.
34. Mayr, H.; Patz, M., Scales of Nucleophilicity and Electrophilicity: A System for Ordering Polar Organic and Organometallic Reactions. *Angew. Chem., Int. Ed.* **1994**, *33*, 938-957.
35. Horn, M.; Mayr, H.; Lacôte, E.; Merling, E.; Deaner, J.; Wells, S.; McFadden, T.; Curran, D. P., N-Heterocyclic Carbene Boranes are Good Hydride Donors. *Org. Lett.* **2012**, *14*, 82-85.

36. Cheng, Q.-Q.; Zhu, S.-F.; Zhang, Y.-Z.; Xie, X.-L.; Zhou, Q.-L., Copper-Catalyzed B–H Bond Insertion Reaction: A Highly Efficient and Enantioselective C–B Bond-Forming Reaction with Amine–Borane and Phosphine–Borane Adducts. *J. Am. Chem. Soc.* **2013**, *135*, 14094-14097.
37. Yang, J.-M.; Li, Z.-Q.; Li, M.-L.; He, Q.; Zhu, S.-F.; Zhou, Q.-L., Catalytic B–H Bond Insertion Reactions Using Alkynes as Carbene Precursors. *J. Am. Chem. Soc.* **2017**, *139*, 3784-3789.
38. Chen, D.; Zhang, X.; Qi, W.-Y.; Xu, B.; Xu, M.-H., Rhodium(I)-Catalyzed Asymmetric Carbene Insertion into B–H Bonds: Highly Enantioselective Access to Functionalized Organoboranes. *J. Am. Chem. Soc.* **2015**, *137*, 5268-5271.
39. Loskutova, N. L.; Shvydkiy, N. V.; Nelyubina, Y. V.; Perekalin, D. S., Insertion of carbenoids into X-H bonds catalyzed by the cyclobutadiene rhodium complexes. *J. Organomet. Chem.* **2017**.
40. Kan, S. B. J.; Huang, X.; Gumulya, Y.; Chen, K.; Arnold, F. H., Genetically programmed chiral organoborane synthesis. *Nature* **2017**, *552*, 132.
41. He, Z.; Zajdlik, A.; Yudin, A. K., α -Borylcarbonyl compounds: from transient intermediates to robust building blocks. *Dalton Trans.* **2014**, *43*, 11434-11451.
42. Fiori, K. W.; Du Bois, J., Catalytic Intermolecular Amination of C–H Bonds: Method Development and Mechanistic Insights. *J. Am. Chem. Soc.* **2007**, *129*, 562-568.
43. Allen, T. H.; Curran, D. P., Relative Reactivity of Stable Ligated Boranes and a Borohydride Salt in Rhodium(II)-Catalyzed Boron–Hydrogen Insertion Reactions. *J. Org. Chem.* **2016**, *81*, 2094-2098.
44. Blackborow, J. R., Resonance line broadening due to chemical exchange and quadrupole-induced relaxation in the nuclear magnetic resonance spectra of some boron-nitrogen adducts. *Journal of the Chemical Society, Dalton Transactions* **1973**, 2139-2143.
45. Lipshutz, B. H.; Blomgren, P. A., Efficient Scavenging of Ph₃P and Ph₃PO with High-Loading Merrifield Resin. *Org. Lett.* **2001**, *3*, 1869-1871.
46. Richter, D.; Mayr, H., Hydride-Donor Abilities of 1,4-Dihydropyridines: A Comparison with π Nucleophiles and Borohydride Anions. *Angew. Chem. Int. Ed.* **2009**, *48*, 1958-1961.
47. Davies, H. M. L.; Morton, D., Guiding principles for site selective and stereoselective intermolecular C-H functionalization by donor/acceptor rhodium carbenes. *Chem. Soc. Rev.* **2011**, *40*, 1857-1869.
48. McNulty, J.; Zhou, Y., A highly efficient general synthesis of phosphine–borane complexes. *Tetrahedron Lett.* **2004**, *45*, 407-409.

49. Horn, M.; Schappele, L. H.; Lang-Wittkowski, G.; Mayr, H.; Ofial, A. R., Towards a Comprehensive Hydride Donor Ability Scale. *Chem. Eur. J.* **2013**, *19*, 249-263.
50. Rablen, P. R., Large Effect on Borane Bond Dissociation Energies Resulting from Coordination by Lewis Bases. *J. Am. Chem. Soc.* **1997**, *119*, 8350-8360.
51. Boruta, D. T.; Dmitrenko, O.; Yap, G. P. A.; Fox, J. M., Rh₂(S-PTTL)₃TPA-a mixed-ligand dirhodium(II) catalyst for enantioselective reactions of α -alkyl- α -diazoesters. *Chem. Sci.* **2012**, *3*, 1589-1593.
52. Taniguchi, T.; Curran, D. P., Hydroboration of Arynes with N-Heterocyclic Carbene Boranes. *Angew. Chem. Int. Ed.* **2014**, *53*, 13150-13154.
53. Jat, J. L.; Paudyal, M. P.; Gao, H.; Xu, Q.-L.; Yousufuddin, M.; Devarajan, D.; Ess, D. H.; Kürti, L.; Falck, J. R., Direct Stereospecific Synthesis of Unprotected N-H and N-Me Aziridines from Olefins. *Science* **2014**, *343*, 61.
54. Marimnganti, S.; Yasmeeen, S.; Fischer, D.; Maier, M. E., Synthesis of Jaspilkinolide Analogues Containing a Novel ω -Amino Acid. *Chem. Eur. J.* **2005**, *11*, 6687-6700.
55. Zhong, M.; Robins, M. J., Regiospecific N9 Alkylation of 6-(Heteroaryl)purines: Shielding of N7 by a Proximal Heteroaryl C-H¹. *J. Org. Chem.* **2006**, *71*, 8901-8906.
56. Hoye, T. R.; Jeffrey, C. S.; Shao, F., Mosher ester analysis for the determination of absolute configuration of stereogenic (chiral) carbinol carbons. *Nat. Protoc.* **2007**, *2*, 2451.
57. Chepiga, K. M.; Qin, C.; Alford, J. S.; Chennamadhavuni, S.; Gregg, T. M.; Olson, J. P.; Davies, H. M. L., Guide to enantioselective dirhodium(II)-catalyzed cyclopropanation with aryldiazoacetates. *Tetrahedron* **2013**, *69*, 5765-5771.
58. Laevee, J.; Fouassier, J.-P., In *Encyclopedia of Radicals in Chemistry, Biology and Materials*, Wiley: New York, NY, 2012; p 37-56.
59. Overberger, C. G.; O'Shaughnessy, M. T.; Shalit, H., The Preparation of Some Aliphatic Azo Nitriles and their Decomposition in Solution. *J. Am. Chem. Soc.* **1949**, *71*, 2661-2666.
60. Kita, Y.; Matsugi, M., In *Radicals in Organic Synthesis*, Wiley-VCH: Weinheim, 2001; p 1-10.
61. Brown, H. C.; Midland, M. M., Organic Syntheses via Free-Radical Displacement Reactions of Organoboranes. *Angew. Chem., Int. Ed.* **1972**, *11*, 692-700.
62. Yorimitsu, H.; Oshima, K., In *Radicals in Organic Synthesis*, Renaud, P.; Sibi, M. P., Eds. Wiley-VCH: Weinheim, Germany, 2001; Vol. 1, p 11-27.

63. Ueng, S.-H.; Solovyev, A.; Yuan, X.; Geib, S. J.; Fensterbank, L.; Lacôte, E.; Malacria, M.; Newcomb, M.; Walton, J. C.; Curran, D. P., N-Heterocyclic Carbene Boryl Radicals: A New Class of Boron-Centered Radical. *J. Am. Chem. Soc.* **2009**, *131*, 11256-11262.
64. Walton, J. C.; Brahmi, M. M.; Fensterbank, L.; Lacôte, E.; Malacria, M.; Chu, Q.; Ueng, S.-H.; Solovyev, A.; Curran, D. P., EPR Studies of the Generation, Structure, and Reactivity of N-Heterocyclic Carbene Borane Radicals. *J. Am. Chem. Soc.* **2010**, *132*, 2350-2358.
65. Tehfe, M.-A.; Makhlof Brahmi, M.; Fouassier, J.-P.; Curran, D. P.; Malacria, M.; Fensterbank, L.; Lacôte, E.; Lalevé, J., N-Heterocyclic Carbenes–Borane Complexes: A New Class of Initiators for Radical Photopolymerization. *Macromolecules* **2010**, *43*, 2261-2267.
66. Ueng, S.-H.; Makhlof Brahmi, M.; Derat, É.; Fensterbank, L.; Lacôte, E.; Malacria, M.; Curran, D. P., Complexes of Borane and N-Heterocyclic Carbenes: A New Class of Radical Hydrogen Atom Donor. *J. Am. Chem. Soc.* **2008**, *130*, 10082-10083.
67. Tehfe, M.-A.; Monot, J.; Malacria, M.; Fensterbank, L.; Fouassier, J.-P.; Curran, D. P.; Lacôte, E.; Lalevé, J., A Water-Compatible NHC-Borane: Photopolymerizations in Water and Rate Constants for Elementary Radical Reactions. *ACS Macro Letters* **2012**, *1*, 92-95.
68. Tehfe, M.-A.; Monot, J.; Brahmi, M. M.; Bonin-Dubarle, H.; Curran, D. P.; Malacria, M.; Fensterbank, L.; Lacote, E.; Lalevee, J.; Fouassier, J.-P., N-Heterocyclic carbene-borane radicals as efficient initiating species of photopolymerization reactions under air. *Polymer Chemistry* **2011**, *2*, 625-631.
69. Pan, X.; Vallet, A.-L.; Schweizer, S.; Dahbi, K.; Delpech, B.; Blanchard, N.; Graff, B.; Geib, S. J.; Curran, D. P.; Lalevé, J.; Lacôte, E., Mechanistic and Preparative Studies of Radical Chain Homolytic Substitution Reactions of N-Heterocyclic Carbene Boranes and Disulfides. *J. Am. Chem. Soc.* **2013**, *135*, 10484-10491.
70. Kawamoto, T.; Geib, S. J.; Curran, D. P., Radical Reactions of N-Heterocyclic Carbene Boranes with Organic Nitriles: Cyanation of NHC-Boranes and Reductive Decyanation of Malononitriles. *J. Am. Chem. Soc.* **2015**, *137*, 8617-8622.
71. Padwa, A., Intramolecular 1,3-Dipolar Cycloaddition Reactions. *Angew. Chem., Int. Ed.* **1976**, *15*, 123-136.
72. Kim, S.; Cho, J. R., Radical Cyclization of α -Diazocarbonyl Compounds. *Bull. Korean Chem. Soc.* **1993**, *14*, 664-665.
73. Karady, S.; Abramson, N. L.; Dolling, U.-H.; Douglas, A. W.; McManemin, G. J.; Marcune, B., Intramolecular Aromatic 1,5-Hydrogen Transfer in Free Radical Reactions 1. Unprecedented Rearrangements in Pschorr Cyclization, Sandmeyer, and Hydro-, Hydroxy-, and Iododediazoniatio n Reactions. *J. Am. Chem. Soc.* **1995**, *117*, 5425-5426.

74. Allen, T. H.; Geib, S. J.; Curran, D. P., Radical and Thermal Reactions of N-Heterocyclic Carbene Boranes with Diazo Compounds. *Organometallics* **2016**, *35*, 2975-2979.
75. de Oliveira Freitas, L. B.; Eisenberger, P.; Crudden, C. M., Mesoionic Carbene–Boranes. *Organometallics* **2013**, *32*, 6635-6638.
76. Zhao, X.; Liang, L.; Stephan, D. W., Facile synthesis of electrophilic vinyl boranes: reactions of alkynyl-borates and diazonium salts. *Chem. Commun.* **2012**, *48*, 10189-10191.
77. Solovyev, A.; Chu, Q.; Geib, S. J.; Fensterbank, L.; Malacria, M.; Lacôte, E.; Curran, D. P., Substitution Reactions at Tetracoordinate Boron: Synthesis of N-Heterocyclic Carbene Boranes with Boron–Heteroatom Bonds. *J. Am. Chem. Soc.* **2010**, *132*, 15072-15080.
78. Merling, E.; Lamm, V.; Geib, S. J.; Lacôte, E.; Curran, D. P., [3 + 2]-Dipolar Cycloaddition Reactions of an N-Heterocyclic Carbene Boryl Azide. *Org. Lett.* **2012**, *14*, 2690-2693.
79. De Vries, T. S.; Prokofjevs, A.; Vedejs, E., Cationic Tricoordinate Boron Intermediates: Borenium Chemistry from the Organic Perspective. *Chem. Rev.* **2012**, *112*, 4246-4282.
80. Karatjas, A. G.; Vedejs, E., Formation of Pinacol Boronate Esters via Pyridine Iodoborane Hydroboration. *J. Org. Chem.* **2008**, *73*, 9508-9510.
81. Pan, X.; Boussonnière, A.; Curran, D. P., Molecular Iodine Initiates Hydroborations of Alkenes with N-Heterocyclic Carbene Boranes. *J. Am. Chem. Soc.* **2013**, *135*, 14433-14437.
82. Ye, T.; McKervey, M. A., Organic Synthesis with α -Diazo Carbonyl Compounds. *Chem. Rev.* **1994**, *94*, 1091-1160.
83. Ford, A.; Miel, H.; Ring, A.; Slattery, C. N.; Maguire, A. R.; McKervey, M. A., Modern Organic Synthesis with α -Diazocarbonyl Compounds. *Chem. Rev.* **2015**, *115*, 9981-10080.
84. Bug, T.; Hartnagel, M.; Schlierf, C.; Mayr, H., How Nucleophilic Are Diazo Compounds? *Chem. Eur. J.* **2003**, *9*, 4068-4076.
85. Li, H.; Zhang, Y.; Wang, J., Reaction of Diazo Compounds with Organoboron Compounds. *Synthesis* **2013**, *45*, 3090-3098.
86. Allen, T. H.; Kawamoto, T.; Gardner, S.; Geib, S. J.; Curran, D. P., N-Heterocyclic Carbene Boryl Iodides Catalyze Insertion Reactions of N-Heterocyclic Carbene Boranes and Diazoesters. *Org. Lett.* **2017**, *19*, 3680-3683.
87. Kinder, D. H.; Katzenellenbogen, J. A., Acylamido boronic acids and difluoroborane analogs of amino acids: potent inhibitors of chymotrypsin and elastase. *J. Med. Chem.* **1985**, *28*, 1917-1925.

88. Smoum, R.; Rubinstein, A.; Dembitsky, V. M.; Srebnik, M., Boron Containing Compounds as Protease Inhibitors. *Chem. Rev.* **2012**, *112*, 4156-4220.
89. Huang, L.; Wulff, W. D., Catalytic Asymmetric Synthesis of Trisubstituted Aziridines. *J. Am. Chem. Soc.* **2011**, *133*, 8892-8895.
90. Takamura, N.; Mizoguchi, T.; Koga, K.; Yamada, S., Amino acids and peptides—XIV: A simple and convenient method for preparation of α -substituted α -diazo esters. *Tetrahedron* **1975**, *31*, 227-230.
91. Boussonnière, A.; Pan, X.; Geib, S. J.; Curran, D. P., Borenum-Catalyzed Hydroborations of Silyl-Substituted Alkenes and Alkynes with a Readily Available N-Heterocyclic Carbene–Borane. *Organometallics* **2013**, *32*, 7445-7450.
92. He, Z.; Yudin, A. K., Amphoteric α -Boryl Aldehydes. *J. Am. Chem. Soc.* **2011**, *133*, 13770-13773.
93. He, Z.; Zajdlik, A.; St. Denis, J. D.; Assem, N.; Yudin, A. K., Boroalkyl Group Migration Provides a Versatile Entry into α -Aminoboronic Acid Derivatives. *J. Am. Chem. Soc.* **2012**, *134*, 9926-9929.
94. Zakharkin, L. I.; Ol'shevskaya, V. A.; Evstigneeva, R. P.; Luzgina, V. N.; Vinogradova, L. E.; Petrovskii, P. V., Synthesis of 5,10,15,20-tetra[3-(*o*- and *m*-carboranyl)butyl]porphyrins containing the C–B σ -bond. *Russ. Chem. Bull.* **1998**, *47*, 340-342.
95. Zakharkin, L. I.; Guseva, V. V.; Petrovskii, P. V., Synthesis of (*m*-Carborane-9,10-diyl)diacetic Acids and Their Derivatives. *Russ. J. Gen. Chem.* **2003**, *73*, 868-870.
96. Allen, T. H.; Horner, A. R.; Geib, S. J.; Weber, S. G.; Curran, D. P., Synthesis, Structure, and Acidity Constants of Ligated α -Boryl Acetic Acids. *Chem. Eur. J.* **2018**, *24*, 822-825.
97. Subirats, X.; Bosch, E.; Rosés, M., Retention of ionisable compounds on high-performance liquid chromatography XVIII: pH variation in mobile phases containing formic acid, piperazine, tris, boric acid or carbonate as buffering systems and acetonitrile as organic modifier. *Journal of Chromatography A* **2009**, *1216*, 2491-2498.
98. Jencks, W. P.; Regenstein, J., In *Handbook of Biochemistry and Molecular Biology*, 4th ed.; Lundbland, R. L.; Macdonald, M. F., Eds. CRC Press: Boca Raton, 2010; p 595-619.
99. Sommer, L. H.; Gold, J. R.; Goldberg, G. M.; Marans, N. S., Polar Effects of Organosilicon Substituents in Carboxylic Acids. *J. Am. Chem. Soc.* **1949**, *71*, 1509-1509.
100. Brown, H. C.; Okamoto, Y., Electrophilic Substituent Constants. *J. Am. Chem. Soc.* **1958**, *80*, 4979-4987.

101. Spiess, H.; Schneider, W. G., Substituent Effects on the C^{13} and H^1 Chemical Shifts in Monosubstituted Benzenes. *The Journal of Chemical Physics* **1961**, *35*, 731-738.
102. Schulman, E. M.; Christensen, K. A.; Grant, D. M.; Walling, C., Substituent effects on carbon-13 chemical shifts in 4-substituted biphenyls and benzenes. Substituent effect transmitted through eight covalent bonds. *J. Org. Chem.* **1974**, *39*, 2686-2690.
103. Tolman, C. A., Steric effects of phosphorus ligands in organometallic chemistry and homogeneous catalysis. *Chem. Rev.* **1977**, *77*, 313-348.
104. Gusev, D. G., Electronic and Steric Parameters of 76 N-Heterocyclic Carbenes in $Ni(CO)_3(NHC)$. *Organometallics* **2009**, *28*, 6458-6461.
105. Tang, Y.; Chen, Q.; Liu, X.; Wang, G.; Lin, L.; Feng, X., Direct Synthesis of Chiral Allenolates from the Asymmetric $C\equiv C-H$ Insertion of α -Diazoesters into Terminal Alkynes. *Angew. Chem. Int. Ed.* **2015**, *54*, 9512-9516.